RECEP TAYYİP ERDOĞAN UNIVERSITY
INSTITUTE OF GRADUATE STUDIES
DEPARTMENT OF CIVIL ENGINEERING

PHYSICOCHEMICAL AND MICROSTRUCTURAL CHARACTERISTICS OF CEMENTED PASTE BACKFILL: EFFECTS OF DAM AND PROCESS TAILINGS

(Master's Thesis)

Tuğrul KASAP

Advisor
Assoc. Prof. Dr. Erol YILMAZ

Co-Advisor
Assoc. Prof. Dr. Shuai CAO

RİZE
2022

ACCEPTANCE AND APPROVAL

This study entitled *Physicochemical and Microstructural Characteristics of Cemented Paste Backfill: Effects of Dam and Process Tailings*, which was prepared by Tuğrul KASAP in the Department of Civil Engineering, Institute of Graduate Studies, Recep Tayyip Erdoğan University, under the supervision of Assoc. Prof. Dr. Erol YILMAZ was found to be successful by unanimity of votes as a result of the defense exam held on 18/07/2022 and was accepted as a **Master's Thesis** by our jury.

Jury Members	**Title, Name Surname**	**Signature**
President	Assoc. Prof. Dr. Erol YILMAZ	
Member	Prof. Dr. Erol ŞADOĞLU	
Member	Assoc. Prof. Dr. Shuai CAO	
Member	Assoc. Prof. Dr. Ayberk KAYA	
Member	Asst. Prof. Dr. Gaili XUE	

ETHICAL STATEMENT

My thesis entitled “Physicochemical and Microstructural Characteristics of Cemented Paste Backfill: Effects of Dam and Process Tailings”, which I submitted to graduate from the M.Sc. The program in Civil Engineering was written by me in line with the principles of science and research ethics.

In my thesis, all the information and quotations from other sources, it is clearly shown in keeping with your Institute's Thesis Writing Guidelines. All the information except the ones whose source is shown were obtained by me using the appropriate research method and reflected in the work in this way. No information, intentions, or faults that do not belong to me are shown as if they belong to me. No information has been used, including internet resources, without attribution to the owner/source. In the case of the contrary, all legal, administrative, academic, and ethical responsibilities will belong to me. At any time after the delivery of the work, in the event that a violation of scientific ethics is detected and/or situation that can be understood as plagiarism or plagiarism arises about my work; I freely accept, declare and undertake that your university and education staff will not be held responsible in any way. 18/07/2022

Tuğrul KASAP

ACKNOWLEDGMENTS

This study entitled “Physicochemical and Microstructural Characteristics of Cemented Paste Backfill: Effects of Dam and Process Tailings” was prepared for the MSc degree in Civil Engineering, Institute of Graduate Studies, Recep Tayyip Erdoğan University. Within the scope of thesis, experimental works were done in geotechnical, waste management, and filling laboratory.

I want to state my heartfelt gratefulness to my advisor Assoc. Prof. Dr. Erol YILMAZ for his guidance, inspiration, experience. endurance, and endless technical help in this MSc program. I also want to show appreciation my co-advisor Assoc. Prof. Dr. Shuai CAO for his assistance, guidance. assurance and commendation. As jury members, Prof. Dr. Erol ŞADOĞLU, Assoc. Prof. Dr. Ayberk KAYA and Assist. Prof. Dr. Gaili XUE are appreciatively recognized for their precious help. knowledge, and support throughout this thesis study.

Special acknowledgements go to Prof. Dr. Servet KARASU, the head of civil engineering department, for giving me the occasion to employ lab devices and services as well as for his constructive comments during the execution of the thesis. Moreover, I am very indebted to Res. Assist. Muhammet SARI and PhD Candidate Nihat Utku GÜNER for his constant help, humor, ingenuity, and guidance in every way.

This thesis would not have been possible without the financial support provided by Eti Bakir A.Ş., a subsidiary of Cengiz Holding. I wish to express gratitude Küre Mine Operating Manager Mr. Ünsal ARKADAŞ, Underground Mine Manager Mr. Kazım KÜÇÜKATEŞ, and Mineral Processing Manager. Mr. Fatih ENİSOĞLU for their valuable assistance and leadership through my thesis field work.

Last, but surely not least, I want to show thankfulness to my friends and family for their sincere support. Special thanks also go to my beloved mother Leyla KASAP, my father Enver KASAP, and my sister Gökçe KASAP for their endless support, motivating encouragement, and countless things in every single step of my life.

Tuğrul KASAP

2022/RİZE

TABLE OF CONTENTS

ACCEPTANCE AND APPROVAL I
ETHICAL STATEMENT II
ACKNOWLEDGMENTS III
TABLE OF CONTENTS IV
ABSTRACT VI
ÖZET VII
ABBREVIATIONS VIII
LIST OF FIGURES X
LIST OF TABLES XII
INTRODUCTION 1
1. GENERAL INFORMATION 3
1.1. Work Motivation and Problems 3
1.2. Underground Backfill Methods 5
1.3. Cementitious Filling Technologies 8
1.4. Factors Affecting Cemented Backfill Performance 12
1.4.1. Tailings 13
1.4.2. Binder Agents 19
1.4.3. Mixing Water 27
2. MATERIALS AND METHODS 28
2.1. Description of the Study Area 28
2.2. Specification of Testing Materials 29
2.2.1. Process/Dam Tailings 29
2.2.2. OPC and SCM 33
2.2.3. Mixing Water 34
2.3. Laboratory Techniques 35
2.3.1. Mine Fill's Manufacturing Stages 35
2.3.2. Mini-Slump (15 cm height) Test 37
2.3.3. Determination of Mechanical Properties 38
2.3.4. Determining Geotechnical Index Parameters 39

2.3.5. Measuring Geo/Chemical Parameters 39
2.3.6. Microstructure Investigations 40
3. RESULTS AND DISCUSSION 41
3.1. Mechanical Results 41
3.1.1. Effect of Mineral Additives on Filling Strength 41
3.1.2. Dam Tailings Effect on Filling Strength 43
3.1.3. Dam Tailings Effect on Stress-Strain and Elasticity of Filling 47
3.2. Determining the Geotechnical Index Parameters of Filling 50
3.2.1. Water Content's Evaluation 50
3.2.2. Void Ratio's Evaluation 52
3.2.3. Specific Surface's Evaluation 53
3.2.4. Saturation Degree's Evaluation 55
3.3. Chemical Analysis of Hardened Fills 56
3.4. Filling Bleed Water's Geochemical Analysis 59
3.4.1. Evaluation of pH Change of CPB Samples with Additives 59
3.4.2. Assessment of pH Change of CPB Containing Dam Tailings 63
3.4.3. Assessment of EC of CPB Containing Dam Tailings 64
3.4.4. Analysis of Redox Potential of CPB Containing Dam Tailings 65
3.5. Microstructural Results 67
3.5.1. XRD Results 67
3.5.2. TG/DTG Results 70
3.5.3. MIP Results 73
3.5.4. SEM Results 75
4. CONCLUSIONS 79
4.1. Extended Summary 79
4.2. Key Research Highlights 80
4.3. Limitations of This Thesis Work 83
4.4. Upcoming Research Directions 83
REFERENCES 85
APPENDIX 109

Recep Tayyip Erdoğan University Institute of Graduate Studies
Department **:** Civil Engineering
Thesis Type **:** Master's Thesis
Advisor **:** Assoc. Prof. Dr. Erol YILMAZ
Author **:** Tuğrul KASAP
Year **:** 2022
Pages **:** 122

ABSTRACT

PHYSICOCHEMICAL AND MICROSTRUCTURAL CHARACTERISTICS OF CEMENTED PASTE BACKFILL: EFFECTS OF DAM AND PROCESS TAILINGS

Diverse waste managements including cementitious paste backfill (CPB) are currently in use to properly dispose of hazardous process tailings. Tailings produced as a result of different chemical additives and methods during ore processing have harmful effects on the environment if no precautions are taken, so they should be explored in detail. This thesis research has been handled in three different stages. In the first step, the quality of paste backfills having low (4.9) and high (10.8) pH pyritic tailings was investigated. Significant savings are targeted by employing fly-ash (FA) and blast-furnace-slag (GBFS) in diverse substitution ratios rather than expensive Portland cement (OPC) used in the fill. The strength and structural properties of fill with a constant solids content of 72% and diverse OPC/GBFS-FA rates (i.e., 90/10, 70/30, and 50/50) were investigated through various lab experiments. From the outcomes. it was observed that fills covering 50% FA and acidic tailings had the lowest strength gaining. Irrespective of the type of tailings, one can interpret that BFS reinforced fill provides higher strength than FA reinforced backfill due to better pozzolanic properties and grain shape. Besides, the backfills made from basic tailings provided the highest strength. Cement hydration is immediately affected by acidic tailings pH and hence the performance of filling may be adversely affected. In the second step, physico-chemical properties and pore structure of CPB produced from dam tailings were investigated. Fills having 76% solids and 5% cement dosage were produced and exposed to 56 days of curing time. Later, the strength (UCS), geochemical (oxidation-reduction potential, pH, and electrical conductivity), and pore structure (TGA, XRD, and SEM) of fill were determined by many experiments. The results proved that, unlike others, there was a noticeable reduction in sulfur-rich tailings backfills' strength. The main reason behind the loss of strength can be clarified by the hydration materials resulting from the interaction of process and dam tailings with cement. From the analyses made, it was witnessed that backfill's pH amplified up to 14-day of curing and declined to 56-day of curing time attributable to acid formation and erosion. This is a cogent reason for the deterioration of the physicochemical and microstructural characteristics of filling. In the third stage, the basic strength and geotechnical properties of paste backfills created from dam tailings were investigated in detail. Fills prepared with fixed solid (72%) and cement (5%) contents were subjected to cure times shifting from 3- to 56-day, and then the quality and behavior of backfilling were examined with some experiments. The outcomes exhibited that strength augmented with time, except for 56-day cured fills with high pyrite content. The reason for the fluctuations observed in falling strength was due to basic tailings in the medium causing rapid cement hydration. The hydration products are completely filled between the cause and fine fractionated tailings grains. and the compact fill formed gives high strength. Since the high sulfate amount will decrease fill's pH, it is a critical aspect to be considered in fill's strength analysis. On other hand, during early curing age, cement may increase fill's pH, but during longer curing age, the fill's pH may be lowered by dam tailings, which are prone to acid formation and erosion. This pointedly worsens the structural properties of fill and leads to failure. In addition, as the curing age of fill rises, the ensuing water content/void ratio decreases to the same extent, but fill's strength increases as the specific surface area increases.

Keywords: Process and dam tailings, pH effect, Industrial waste, Microstructure, Paste backfill

Recep Tayyip Erdoğan Üniversitesi Lisansüstü Eğitim Enstitüsü
Ana Bilim Dalı : İnşaat Mühendisliği
Tez türü : Yüksek Lisans Tezi
Danışman : Doç. Dr. Erol YILMAZ
Hazırlayan : Tuğrul KASAP
Yıl : 2022
Sayfa Sayısı : 122

ÖZET

ÇİMENTOLU MACUN DOLGULARIN FİZİKOKİMYASAL VE MİKROYAPISAL ÖZELLİKLERİ: BARAJ VE PROSES ATIKLARININ ETKİLERİ

Tehlikeli proses atıklarını tekniğine uygun bir şekilde bertaraf etmek için çimentolu macun dolgu (CPB)'yu içeren farklı atık yönetimleri halihazırda kullanılmaktadır. Cevher zenginleştirme sırasında farklı kimyasal katkı ve yöntemler sonucu üretilen atıklar, önlem alınmazsa çevreye zararlı etkileri olup bu yüzden detaylı bir şekilde araştırılmaları gereklidir. Bu tez araştırması üç farklı aşamada ele alınmıştır. İlk aşamada, düşük (4.9) ve yüksek (10.8) pH piritik atık içeren macun dolguların kalitesi incelenmiştir. Dolgu içinde kullanılan pahalı Portland çimentosu (OPC) yerine farklı ikame oranlarında yüksek fırın cürufu (GBFS) ve uçucu kül (FA) kullanılarak önemli tasarruflar hedeflenmiştir. %72'lik sabit katı içeriği ve farklı OPC/GBFS-FA oranlarına sahip (örn., 90/10, 70/30 ve 50/50) sahip dolgunun dayanımı ve yapısal özellikleri çeşitli laboratuvar deneyler ile araştırılmıştır. Sonuçlardan %50 FA ve asidik atık içeren macun dolguların en düşük dayanım kazancına sahip olduğu gözlenmiştir. Atık tipine bakılmaksızın GBFS takviyeli dolgu daha iyi puzolanik özellik ve tane şeklinden dolayı FA takviyeli dolgudan daha yüksek dayanım sağladığı yorumlanabilir. Dahası bazik atıklardan imal edilen dolgular en yüksek mukavemet sağladı. Çimento hidratasyonu, asidik atik pH ile hemen etkilenir ve dolayısıyla dolgunun performansı da olumsuz yönde etkilenebilir. İkinci aşamada, baraj atıklarından imal edilen CPB'nin fiziko-kimyasal özellikleri ve gözenek yapısı incelenmiştir. %76 katı ve %5 çimento içerikli dolgular üretilmiş ve 56 günlük kür süresine maruz bırakılmıştır. Daha sonra dolguların basınç dayanımı (UCS), jeokimyasal (oksidasyon indirgeme potansiyeli, pH ve elektriksel iletkenlik) ve gözenek yapısı (XRD, TGA ve SEM) farklı testlerle tespit edilmiştir. Sonuçlar, diğerlerinin aksine sülfürce zengin atıklardan üretilen dolguların dayanımında hissedilir oranda bir düşüş olduğu ispatladı. Mukavemet kaybının arkasındaki temel neden proses ve baraj atıklarının çimento ile etkileşiminden meydana gelen hidratasyon ürünleri ile açıklanabilir. Yapılan analizlerden macun dolgunun pH değerleri 14 güne kadar yükseldiği asit oluşumu ve erozyon nedeniyle 56 günlük kür süresine kadar düştüğü gözlenmiştir. Bu ise dolgunun fiziko-kimyasal ve mikro-yapısal karakteristiklerinin bozulmasının temel nedenidir. Üçüncü aşamada baraj atıklarından üretilen macun dolguların temel dayanım ve jeoteknik özellikleri etraflıca aratılmıştır. Sabit katı (%72) ve çimento (%5) içeriklerinde hazırlanan dolgular 3 ila 56 gün arasında değişen kür sürelerine maruz bırakıldı ve sonrasında bazı deneylerle macun dolgunun kalite ve davranışı incelendi. Deneysel sonuçlar, yüksek pirit içeriğine sahip 56 günlük kürlenmiş dolgular hariç mukavemetin zamanla arttığını gösterdi. Dolgu dayanımında gözlenen dalgalanmaların sebebi hızlı çimento hidratasyonuna yol açan ortamdaki bazik atıklardan kaynaklanmıştır. İri ve ince fraksiyonlu atık tanelerinin arası hidratasyon ürünleri ile tamamıyla dolar ve oluşan kompakt dolgu yüksek dayanım verir. Yüksek sülfat miktar dolgunun pH'ını düşüreceğinden dayanım incelenmesinde ayrıca dikkat edilmesi gereken önemli bir etmendir. Öte yandan erken kür süresinde çimento dolgunun pH'ını arttırabilir fakat uzun kür süresinde dolgunun pH'ı, asit oluşumuna ve erozyon meyilli olan baraj aktıkları ile düşürebilir. Bu ise dolgunun yapısal özelliklerini önemli bir şekilde bozar ve yenilmeye yol açar. Ayrıca, dolgunun kür süresi arttıkça sorumlu su içeriği ve boşluk oranı aynı ölçüde azalır, fakat özgül yüzey alan arttığından dolgunun dayananımı da artar.

Anahtar Kelimeler: Proses ve baraj atıkları, pH etkisi, Endüstriyel atık, Mikro yapı, Macun dolgu

ABBREVIATIONS

AMD : Acid mine drainage
ASTM : American standard of testing materials
BET : Brunauer-emmett-teller
$Ca(OH)_2$: Portlandite
CaO : Calcium oxide
C_c : Coefficient of curvature
CH : Calcium hydroxide
CMB : Cemented mine backfill
CPB : Cemented paste backfill
CSA : Canadian standards association
C-S-H : Calcium-silicate-hydrate
C_u : Coefficient of uniformity
DTS : Dam tailings sample
E : Void ratio
E_{50} : Mean modulus
EC : Electrical conductivity
Eh : Redox potential
EM : Elastic modulus
E_{max} : Tangent modulus
E_s : Secant modulus
FA : Fly ash
GAYD : Geotechnical waste management and backfill
GBFS : Granulated blast furnace slag
G_s : Specific gravity
HPDT : High pH dam tailings
HPPT : High pH process tailings,
ICP-OES : Inductively coupled plasma optical emission spectroscopy
LPDT : Low pH process tailings
MDD : Maximum dry density

MIP : Mercury intrusion porosimeter

n : Porosity

OMC : Optimum moisture content

OPC : Ordinary portland cement

PSD : Particle size distribution

PTS : Process tailings sample

PW : Pore water

SCM : Supplementary cementitious materials

SEM : Scanning electron microscopy

SO_4^{-2} : Sulfate

Sr : Degree of saturation parameter

SSA, S_s : Specific surface area

TG/DTG : Thermogravimetry/Derivative thermogravimetry

TS-EN : Turkish standard-European norm

TW : Tap water

UCS : Uniaxial compressive strength

W : Water content

XRD : X-ray diffraction

XRF : X-Ray fluorescence spectrometer

LIST OF FIGURES

Figure 1. Schematic diagram of mining methods 6
Figure 2. Backfill types and history of evolution 6
Figure 3. Fill types: (a) rock, (b) slurry, and (c) paste 8
Figure 4. Mines using paste backfill technology in the world 9
Figure 5. A chart viewing the fill's major elements 10
Figure 6. A chart viewing the integrated paste technology 10
Figure 7. Features influencing the fill quality 13
Figure 8. Various mine tailings' grain size curves 14
Figure 9. Tailings' grain shape analysis via digital image 16
Figure 10. Tailings' mineral link: a) sulfides linked with gangues; b) chalcopyrite liberation properties; and (c-d) Cu sulfides contiguous link between major gangues 18
Figure 11. Grain size and typical SSA of various materials 21
Figure 12. OPC substitute with other binders in fill 22
Figure 13. SEM photos of fly ashes (a, b) and slags (c, d) 25
Figure 14. Types of chemical admixture in CPB materials 26
Figure 15. Location map of the study area 28
Figure 16. Sampling in tailings dam: general (a) and side (b) views 31
Figure 17. Cumulative and incremental grain size plots of the experimented dam (a, b, c, d and e) and process (f) tailings 32
Figure 18. Fill manufacturing stages 36
Figure 19. CPB sample experimental stages 37
Figure 20. Measurement of slump values by mini/standard slump cones 38
Figure 21. Fill strengths with time and OPC/GBFS (a), and OPC/FA (b) 42
Figure 22. Plots of acidic and basic dam tailings-based filling's stability with time 45
Figure 23. Plot of different fillings' strength values with curing time 47
Figure 24. Stress-strain plots of fills cured at 28 (a) and 56 (b) days 48
Figure 25. Plots of different fills' elastic modulus with curing age 49
Figure 26. Plots of different fills' water content with curing age 51
Figure 27. Plots of different fills' void ratio with curing age 53

Figure 28. Plots of different fills' specific surfaces with curing age 54

Figure 29. Plots of different fills' saturation degree with curing age 55

Figure 30. Plots of SO_4^{-2} (a) and Ca (b) values within filling with age 58

Figure 31. Plots of Fe-Al (a) and K-Si (b) values within filling with age 59

Figure 32. EM/pH in slag-based fills with age: (a) EM @ acidic tailings; (b) pH @ acidic tailings; (c) EM @ basic tailings; (d) pH @ basic tailings..... 61

Figure 33. EM/pH in fly ash based fills with age: (a) EM @ acidic tailings; (b) pH @ acidic tailings; (c) EM @ basic tailings; (d) pH @ basic tailings..... 62

Figure 34. Plots of pH values observed within filling with age..... 63

Figure 35. Plots of EC factor within filling with age..... 65

Figure 36. Plots of (a) Eh and (b) pH-Eh factors within filling with age 66

Figure 37. XRD profiles of acidic(a) and basic (b) based fills at 28 days..... 68

Figure 38. Fill's XRD profiles: (a) CPB-HPPT; (b) CPB-EPDT-2; and (c) CPB-LPDT-1 69

Figure 39. Thermogravimetric analyses TG (a) and DTG (b) of acidic and basic tailings based filling specimens at 28 days 71

Figure 40. TGA profiles of process and dam tailings based fills at 56 days: (a) CPB-HPPT vs. CPB- HPDT-2; and (b) CPB-HPPT vs. CPB- LPDT-1..... 72

Figure 41. Plots of cumulative/incremental PSD profiles of acidic (a, b, c) and basic (d, e, f) tailings based fillings specimens 74

Figure 42. SEM graphs of additive (c, d) and non-additive (a, b) based fills..... 76

Figure 43. SEM micrographs of process and dam tailings based filling specimens at 56 days: (a) CPB-HPPT, (b) CPB- HPDT-2 and (c) CPB- LPDT-1 78

LIST OF TABLES

Table 1. Fundamental filling types and their key characteristics 7
Table 2. Physical factors of tailings 13
Table 3. Tailings type based on grain size distribution 15
Table 4. Tailings bases and their chemistries 19
Table 5. Types of cement based on EN 197-1 standard 24
Table 6. Slag and fly ash chemistries 25
Table 7. Physical properties of process tailings 29
Table 8. Chemical properties of process tailings 30
Table 9. Physical properties of dam tailings 32
Table 10. Chemical properties of dam tailings 33
Table 11. Principal physical characteristics of main and supplementary binders 33
Table 12. Element characteristics of binding materials 34
Table 13. Chemical/Geochemical characteristics of PW and TW 34
Table 14. Recipe design of backfills containing acidic and basic tailings 36
Table 15. Fill types in terms of their experimental recipes 37
Table 16. Diverse blend recipes of fillings created by using dam tailings 37

INTRODUCTION

While the mining sector makes an undeniable contribution to the development and economic welfare of countries, it undeniably generates 9 billion tons of tailings annually (Adiansyah et al., 2015; Qi and Fourie, 2019). Surface colloidal properties of acidic or basic tailings, which are released due to some flotation reagents added during ore preparation and enrichment, change significantly, and may give rise to significant problems for environment (Falagan et al., 2017; Sun et al., 2020). Sulfur-containing tailings such as pyrite, which have serious reactive properties, react chemically with the oxygen and water present in the environment, leading to the formation of acids and sulfates, which have considerable potential as environmental pollutants (Koohestani et al., 2020; Menzel et al., 2021). Thanks to heavy metal/leachate concentrations, the rate of creation of acid-mine-drainage (AMD) of tailings significantly lowers pH level of the environment and causes a serious increase in Fe^{3+} concentration, which can cause problems (Qiao et al., 2020). If no action is taken earnestly, AMD may cause irreparable harm into soil, aquatic, and air by blending by underground and surface waters (Ighalo et al., 2022; Rezaie and Anderson, 2020). Pyritic tailings containing flotation chemicals are environmentally hazardous by reason of sulfur and other heavy metals they contain and may cause ecological problems that will endure for centuries even after operations in the mine site are completed (Koohestani et al., 2018). In fact, managing such tailings is problematic and may impose extra burdens on firms with a responsible and sustainable mining approach (Aldhafeeri and Fall, 2017). Mining wastes that reach huge sizes are a prospective basis of ecological problems thanks to the diverse heavy metals and chemical reagents they contain (Mohammed et al., 2002; Yan et al., 2022a; Chen et al., 2021). Hence, to protect environment and living things, tailings are contained in sheltered structures called tailings dams and/or impoundments (Xue and Yilmaz, 2022; Yan et al., 2022b).

The main objective of this M.Sc. thesis was to offer experimental bases for evaluating the quality and performance of industrial waste (e.g., slag and fly ash) based backfills considering the reduction option of cemented-related cost. More specifically, an attempt is made to examine the effect of mineral admixtures on strength/structure

evolution in CPB with low and high pH pyritic tailings. The specific objectives and scope of the thesis are as follows:

- To offer a review of the recent literature on paste backfill technique, with an emphasis on physical, chemical, mineralogical, and microstructural properties;

- To explore the mechanical and geotechnical index parameters of CPB samples made up with dam and process tailings;

- To study the effect of pH in dam tailings on physical and chemical behavior of CPB structures for underground metalliferous mines;

- To valorize dam tailings as a recycling material in CPB on their mechanical and geotechnical properties.

The research scope covers a widespread investigation of the compressive strength, industrial waste, curing time, substitution proportions, tailings type, rheology and microstructure for diverse paste backfill samples using various laboratory devices. This thesis makes an original contribution by recycling dam tailings as paste backfill materials for underground mines. Due to space limitations, the scope of this thesis project study does not allow for a study of external factors (e.g., stope geometry, wall convergence, arching effect, barricade load, dynamic loading, and stress distribution) which affect the quality of paste backfill, although such investigations are needed to further assess and apply an efficient paste backfill material for mines.

1. GENERAL INFORMATION

1.1. Work Motivation and Problems

Today, the tailings accumulated in these dams/impoundments and pose a risk to the environment are used as an important raw material source in diverse sections like underground backfilling (Archibald, 1993; Brackebusch, 1994; Amaratunga and Hmidi, 1998; Cayouette, 2003), road constructing (Amrani et al., 2019), geopolymer (Koohestani et al., 2021) and ceramic/brick making (Drif et al., 2021; Ettoumi et al., 2021), and are a potential resource that should be brought into the circular economy (Figueiredo et al., 2019a; de Lurdes Dinis et al., 2020). In comparison with low-quality ores in mining sites, these tailings within dams may hold many valuable elements such as cobalt and may have saleable value (Kinnunen et al., 2018). With the technology of that time, the tailings sent to the dams without recovering some or all the valuable minerals in ore may undergo serious changes in their physicochemical/mineralogical properties after a long age of time and may be accepted as complete waste (Figueiredo et al., 2019b). Accordingly, before dam tailings are considered as a potential/economic source, analysis and test studies are required in which tailings are fully handled in every aspect (Xue et al., 2020). It is vital to regulate the spreading of metals present in the hazardous proses/dam tailings stored at diverse points and depths of the dams in detail (Wang et al., 2017).

Along with chemical analysis, determining the pH of the tailings is critical for the re-valorization of tailings stored in dam (Ouyang et al., 2020). In an experimental work (Zhang et al., 2016), pH values measured near the surface (<0.2 m) of dam tailings differ from 3 to 6 (acid), although pH differs from 8 to 11 (base) as one descends to relatively lesser levels (up to 3 m). Although it is promising to reprocess the wastes accumulated in dams and not corroded in backfilling or in different sectors, it is not at the desired level in recent years due to the costs and the need for advanced technology, especially in the handling and re-evaluation of the tailings (Kasap et al., 2022a). On the other hand, due to the increasing environmental awareness and green agreement in recent years, it has gained importance to reduce the primary raw material resources pointedly and instead boost the use of secondary resources and bring them into the economy (Fontes et al., 2019). In recent years, dam tailings have been used as

aggregate in the making of cementitious paste or mine backfill (CPB or CMB), which is preferred for refilling underground voids. Basically, the paste backfill used to close these underground mining voids has three main functions: 100% extraction of adjacent ore, local or regional ground-support, and efficient disposal of tailings (Cao et al., 2021a; Qin et al., 2021).

Several methods are already applied to capably use sulfur-rich process or dam effluent in assorted industries (Yilmaz et al., 2010; Jiang et al., 2020a). Amongst them, filling is environmentally friendly and performs an important function for mines (Chen et al., 2018). In comparison with conservative mining waste management systems, backfill ensures the extraction of ores left as pillar underground and offers major ecological advantages by placing tailings underground (Fang et al., 2021). Typically composed of tailings, cement, and mixing water, CPB performs two key functions for mines: support and storage (El Mahboub et al., 2022). The solid content of tailings used in CPB ranges from 67wt.% to 87wt.% (Cao et al., 2020). Tailings fills have a fine fraction, a typical w/c ratio of higher than 5, and a typical cement dosage of less than 8%, since they are usually milled to provide grain liberation during ore beneficiation (Ercikdi et al., 2014; Fang et al., 2020). CPB can be stored safely in a basic medium with little penetrability (Huang et al., 2021a). Accordingly, this system is continuously used in modern mines, both economically and sustainably (Xiu et al., 2022). But the cement is the strongest item representing 75% of the cost in filling manufacturing, and cost-reducing work is essential (Cao et al., 2021b; Xiao et al., 2021a; Eker and Bascetin, 2022).

Cement, which has a great effect on CPB cost, has the greenhouse gas effect released to the environment during its making, a negative contribution to global warming and the third largest CO_2 emission source (He et al., 2019a; Cao et al., 2016). Nearly 7.5% of the total CO_2 releases fitting to Portland cement (OPC) making, and 0.9 tons of CO_2 is released to the environment during the clinker production of an average of 1 ton of OPC (Akkaya et al., 2021; Qiu et al., 2019). Thus, using diverse solid admixtures like fly ash (FA) and blast furnace slag (GBFS) can pointedly reduce CO_2 production (Li et al., 2020a). CPB may be also subjected to interior/exterior SO_4^{2-} outbreaks because of the establishment of acid and/or sulfate depending on pyritic tailings' oxidation (Dong et al., 2019a; Li et al., 2022). Acids/sulfates react with

portlandite, which is a cement hydration product, and ettringite is released, which reduces the strength of fill (Koohestani et al., 2018). Some scholars (Wu et al., 2015; Wang et al., 2020a) have found that paste filling's strength property is significantly influenced through cement type/ratio, external sulfate ingress, and early temperature, proving that these factors are leading factors to consider in the fill's structural design. Consequently, employing substitute industrial waste materials (i.e., FA/GBFS) should become strongly attracted to significantly diminish the CO_2 emissions released to the environment during Portland cement manufacturing and to powerfully increase the structural resistance of paste filling against both internal and external sulfate attacks (Yan et al., 2021; Zhao, 2021).

1.2. Underground Backfill Methods

Underground openings formed during ore production are re-filled by a suitable CPB material to (i) run the support for neighboring mining constructions, (ii) ensure secure work platform for employees and/or tools; (iii) establish a disposal area for processing tailings created right after ore enrichment, and (iv) prevent or minimize possible collapses on surface formations (Alp et al., 2009; Singh et al., 2015). CPB is a crucial process to fill the voids shaped owing to underground ore production by employing a proper product (Zhengfu et al., 2010; Bascetin et al., 2021). A certain amount of dewatered (through thickener and filter) tailings, sand, coarse rock fragments gained from quarries, and aggregate are used as a filling material (Dudeney et al., 2013; Belem et al., 2016). In addition, the placement of fill in the underground cavities is usually carried out by adding a certain amount of binder and mixing water to the tailings. Figure 1 demonstrates a chart diagram of an exemplary mining method applied today (Wang et al., 2019).

The filling process was used for the first time in 1864 to prevent the collapse of a church in Pennsylvania, North America, because of surface collapses. The first cementitious filling application was successfully applied in the Sudbury Falconbridge Nickel Mine in 1957 and Portland Cement was preferred as cement due to its easy availability and cheapness. By the 1970s, the process of placing tailings underground as a backfilling with cement has become an industrial practice. Figure 2 shows the backfilling types and their historical development (Qi and Fourie, 2019).

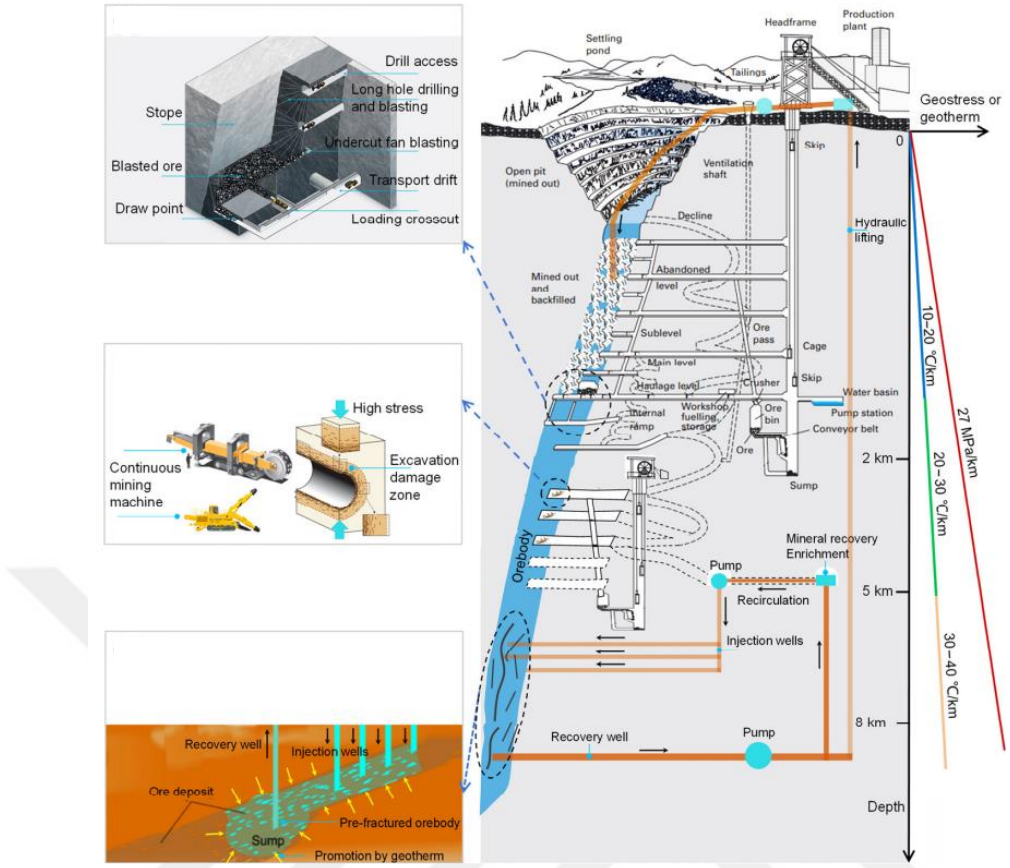


Figure 1. Schematic diagram of mining methods

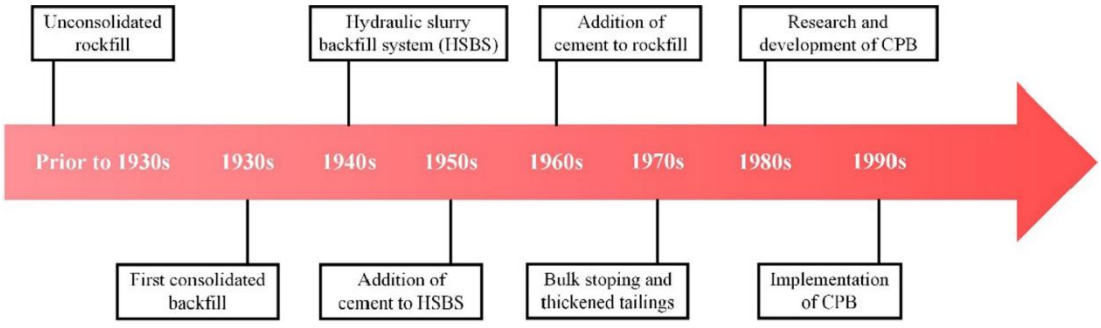


Figure 2. Backfill types and history of evolution

From the past to the present, mine backfills are divided into three according to the types of materials they contain, their mining methods and their final functionality. These are i) rock fill, ii) hydraulic fill, and iii) paste fill (Rankine et al., 2006; Stone, 2007; Nasir and Fall, 2010; Sivakugan et al., 2015). Each fill type has diverse characteristics and today, considering both unit costs and maximum benefits, paste filling has found the opportunity to be used in more mine sites compared to other methods (Table 1; Yilmaz, 2015).

Table 1. Fundamental filling types and their key characteristics

Properties	Rock-filling	Hydraulic-filling	Paste-filling
Solid ratio (wt.%)	100	60-75	75-85
Binders	Cementitious or non-cemented	Cementitious or non-cemented	Only cementitious
Strength	High	Low	Medium
Durability	High	Low	Low or high
Barricade design	None	Expensive	Cheap
Drainage	Insignificant	High	Very low
Transport	Transport pit and mobile equipment	Borehole and pipeline	Borehole and pipeline
Particle dia.	Higher than 20cm	>20μm (higher than 90%)	|>20μm(higher than 15%)
Placement speed	100-400 ton/hour	100-200 ton/hour	50-200 ton/hour
Segregation	High	High	None
Initial asset cost	High	Low	High
Operating costs	High (9.70 $/ton)	Medium (8.20 $/ton)	Low (5.10 $/ton)

Rock filling consists of crushed waste rock pieces, generally, up to 40 mm in size, obtained from surface or underground to fill the cavities that have been removed from ore, and mix the aggregate with cement and water under appropriate conditions (Figure 3a; Yilmaz et al., 2011a) (Hane et al., 2017). The main advantages of rock filling can be listed as increasing the tonnage of the filling by three times and its volume by two times, increasing the strength, and reducing the binder (cement) consumption below 2%. If the material to be used in the rock filling application is to be obtained from places such as quarries, the cost may increase significantly (Wu et al., 2018; Jiang et al., 2019a).

Hydraulic filling is established on the opinion of transporting tailings material with water, re-filling the space produced, separating the excess water from solid filling material, and hardening it (Figure 3b; Yilmaz et al., 2011a). The hydraulic filling is usually prepared at a solids rate of up to 70% by weight, and the amount of tailings material below 10μm is not required to be more than 10 wt.% to suitably provide the required permeability. Ideally, the hydraulic fill should have a free drainage feature so that the water in it can be removed as quickly as possible and not excessive pore water pressure (Sivakugan et al., 2013). Consequently, it is habitually favored to employ categorized tailings materials within hydraulic filling applications (Pirapakaran and Sivakugan, 2007). The most important advantages of hydraulic filling for most mines are that it is easy to apply and reflects a responsibly low cost.

Cementitious paste backfilling (CPB) comprises a dehydrated tailings material, water, and binder, with a large amount of less than 20μm (usually more than 15% <20

μm), from ore dressing (Figure 3c; Yilmaz et al., 2011a). Binder content is between 3-9% and the solid ratio is between 70-85% (Simms and Grabinsky, 2009; Yilmaz et al., 2009; Cui and Fall, 2016; Jiang et al., 2019a). These components are blended above ground, mixed, and sent underground by using the elevation difference or by pumping.



Figure 3. Fill types: (a) rock, (b) slurry, and (c) paste

1.3. Cementitious Filling Technologies

The cemented mine/paste backfill (CMB/CPB) way, which is widely employed as a substitute waste managing process for sheltered storage of wastes created during ore dressing, was primarily employed in Germany's Grund mine in 1981 and has grown-up and developed all over the world in last 30 years (Figure 4) (Yi et al., 2015; Qi and Fourie, 2019). It is known that the paste filling method, which was applied in only one enterprise in 1980, has been actively used in approximately 100 paste plants with capacities ranging from 12-200 m^3/h around the world in the last few years, and around 30 plants are in the design and installation phase for this aim (Figure 4; Behera et al, 2021) (le Roux et al., 2005; Yilmaz and Yilmaz, 2018). It has been reported that fill material used in Canadian underground mining consists of 64% waste rock (36% cemented, 28% non-cement), 32% facility waste (27% cemented, 5% non-cement), and the remaining 4% non-cement sand and gravel (Yilmaz, 2011).

CPB technology was started to be applied in the Çayeli Cu Mine for the first time in Türkiye in 1999 and it continues successfully (Yumlu and Guresci, 2007). Çayeli paste plant has a solids ratio of 82% by weight and has the capacity to produce 45 m^3 of backfill per hour. 75% of nearly 250,000 m^3 of filling placed in underground production voids per year are successfully carried out by the paste backfill method and the remaining part (25%) is productively carried out with cemented/non-cemented waste filling (Thompson et al., 2012).

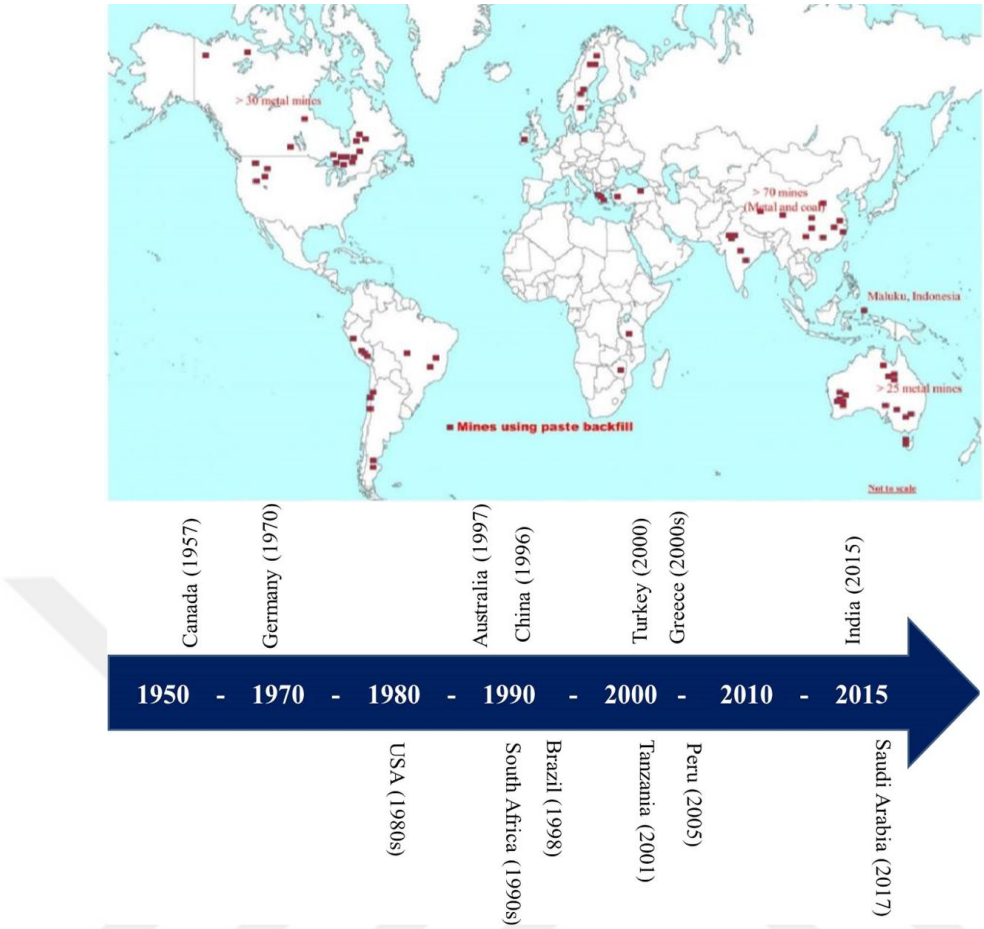


Figure 4. Mines using paste backfill technology in the world

The tailings of underground Cu mine in Kure are stored into the tailings dam, and the support of underground cavities is delivered by cemented rock fill way and CPB. In Efemcukuru Au mine, 50% of tailings are stored above ground after dewatering (10% moisture), and the remaining part is used in the support of underground production openings by paste filling. In addition, recently, cementitious paste filling has started to be applied in the Siirt Cu mine owned by Cengiz Holding.

CPB is formed by mixing the dewatered process tailings material, usually more than 15% of which is smaller than 20 μm, resulting from ore dressing, with generally 3-9% binder, and 15-25% mixing water (Yang et al., 2018; Yilmaz et al., 2022). The solid ratio of mixture is classically between 70-85% (Figure 5; Belem and Benzaazoua, 2008; Yin et al., 2012; Yilmaz, 2018; Cao et al., 2019a). These components are blended at fill facility above ground and sent underground by using the elevation difference or by pumping (Robionson et al., 2021; Xue et al., 2021a). Figure 6 shows the production stage of CPB and underground filling (Yilmaz et al., 2014a).

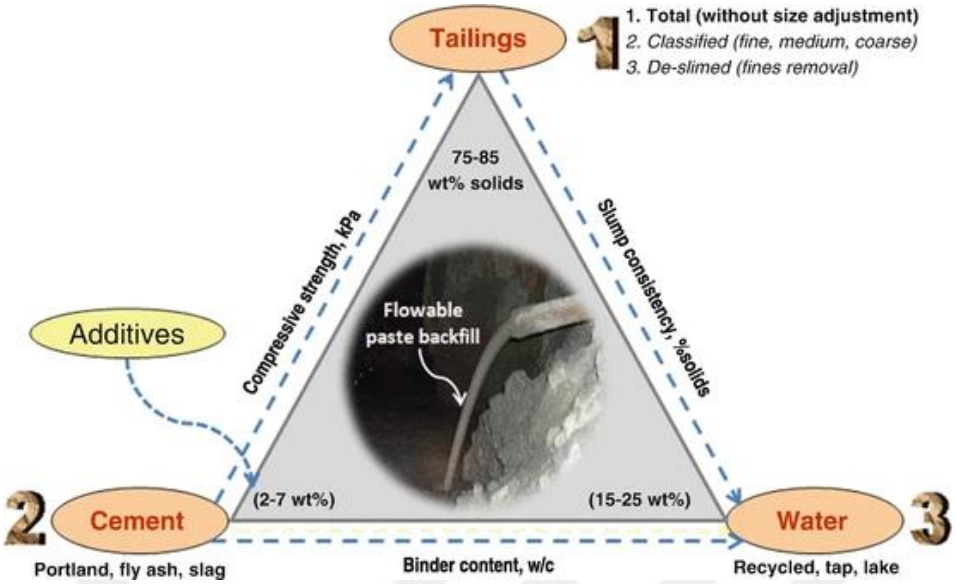


Figure 5. A chart viewing the fill's major elements

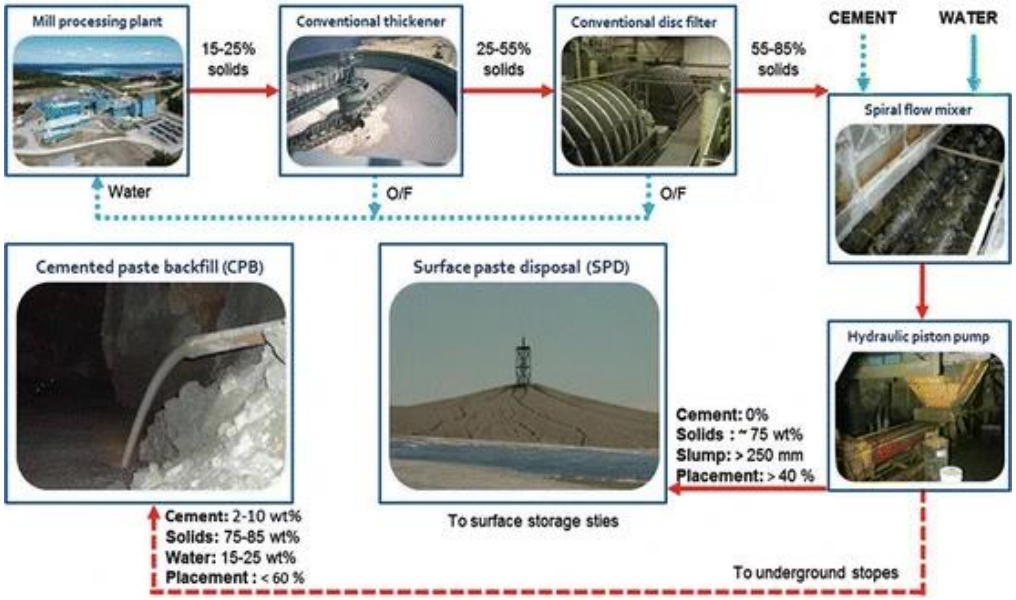


Figure 6. A chart viewing the integrated paste technology

The essential factors to be made allowance for cementitious filling projects are strength, durability, rheological properties, and operating costs (Yilmaz et al., 2003; Xue et al., 2019a). In underground mines where intermediate excavation and cut & fill method is applied as the production method, the CPB placed in ore extraction area should provide its own stability during the production of side chamber and then until it is filled with backfilling (Yilmaz et al., 2007; Lu et al., 2018). Backfill placed should

offer no less than 1000 kPa strength after a cure age of 28-day and maintain its durability during the 180-day curing age (Huang et al., 2011; Chen et al., 2019).

Tailings generated through ore preparation/enrichment processes are mixed with water and binders in certain proportions to produce paste-filling mix after getting dewatered through the thickening and filtrating units as part of dewatering processes (Yilmaz et al., 2011b; Zhang et al., 2022). The prepared CPB materials are nonstop pumped through pipelines and transported underground (Cui and Fall, 2015; Cao et al., 2019b). CPB, which will be carried underground by pipeline, should contain at least 15% or more by weight of fine-grained tailings material with a size of <20 μm to carry it in a certain fluid consistency, to prevent abrasion problems caused by friction, and to ensure water retention in the blend (Dikonda et al., 2021; Qin et al., 2021). In addition, binder is added to paste filling to complete its hardening process. To deliver the backfill mixture underground with a certain fluid consistency, the water to be added should be between 17% and 27% by weight (Yilmaz, 2018).

The advantages of the CPB method, which is used especially in underground cavities where ore production methods such as intermediate excavation and cut fill are applied, are as follows (Aldhafeeri et al., 2016; Lu et al., 2020; Huang et al., 2021b);

- It ensures that 65-70% of the milling tailings are stored underground. Thus, it reduces the above-ground tailings storage and rehabilitation costs.
- Compared to rock and hydraulic filling, the structure of non-segregation during the transportation and placement of CPB allows the underground production cavities to be fully filled (pore/void formation is prevented) and accordingly, settlements are stopped, and safe working conditions are provided.
- Nearly 90% of the process water, to which various chemicals are added during the enrichment processes, is recovered during the dewatering processes.
- Filling's low penetrability and high saturation degree prevent both the leakage of water in filling to outside and the passage of groundwater through filling. The risk of AMD formation is also reduced due to diffusion of oxygen into filling and the oxidation of sulfide minerals in the environment.
- Transporting it underground by pipeline reduces difficulties (i.e., harm to the support) caused by orthodox carriage ways like conveyor/moveable tools.

- The fact that fill is fast and runs a higher strength gain compared to hydraulic fill at identical cement ratio offer a shortening of the mining operations.
- Cement added to CPB increases the impermeability and neutralization potential of fill, as well as increases the strength and reduces the formation of AMD.
- It increases efficiency by gaining heels, functions as a support, and creates a working platform for employees and equipment.

Some disadvantages of CPB application are as follows.

- Pumping/dewatering are costly due to high capital costs and solids densities.
- High pump pressure is required to transport CPB underground. This increases pump maintenance and energy costs.
- Oxidation of tailings containing sulfide minerals (pyrite, pyrrhotite) takes place in the water/oxygen presence, causing CPB to lose its long-age stability.

1.4. Factors Affecting Cemented Backfill Performance

Studies have shown that a filling mixture design that offers high strength and stability in CPB application cannot be generalized for all mining firms (Hassani et al., 2001; 2007; Fahey et al., 2009; Jafari and Grabinsky, 2021; Jia et al., 2021). Thus, the most suitable mix design for each filling application should be determined separately by considering each specific filling elements and test conditions in mines (Khudyakov and Vashchenko, 2020). To determine the most suitable CPB blends, it is necessary to know and thoroughly examine parameters influencing paste fillings strength/stability (Figure 7; Yilmaz et al., 2015a). They can be gathered around two main collections, of which internal parameters are the materials that make up the filling itself (Helinski et al., 2007a; 2007b; Jiang et al., 2020b; Ait-Mokhtar et al., 2002). The performance of filling is important, especially because of these materials and their interaction with each other during curing (Benkendorff, 2006; Dirige and de Souza, 2007; Deschamps et al., 2008). Another key factor of influence is the external parameters such as fill-rock interaction, curing conditions, consolidation, drainage, ground water, dynamic or active loads, which determine the performance of the backfilling after it is placed underground. (Yilmaz et al, 2015; Mbonimpa et al., 2019; Libos et al., 2021).

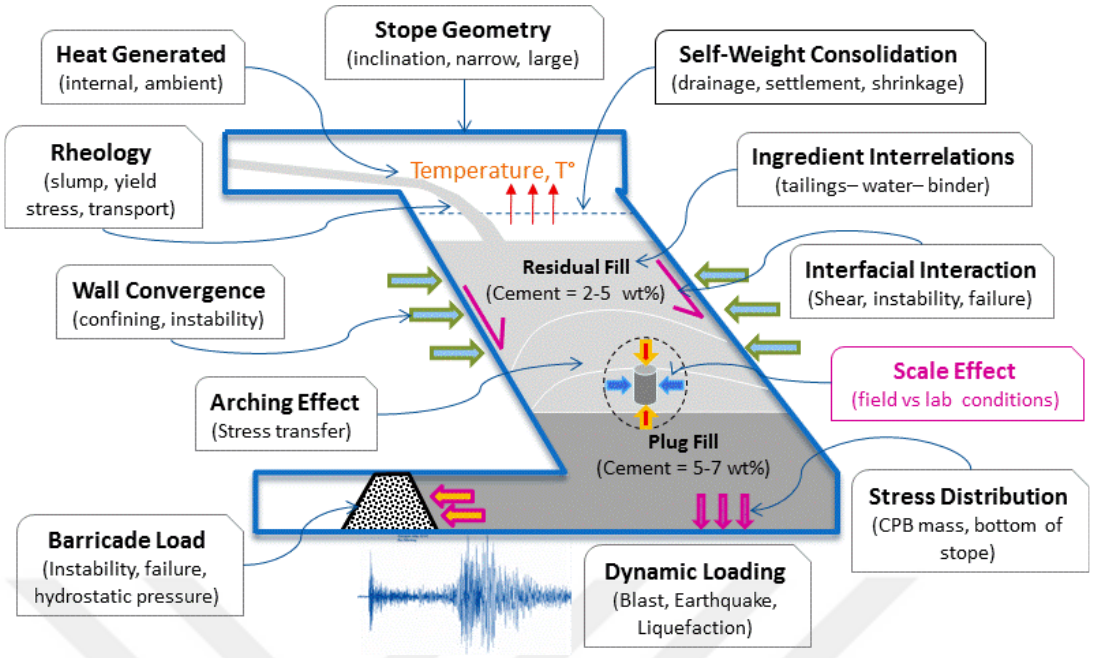


Figure 7. Features influencing the fill quality

1.4.1. Tailings

Physico-mineralogical property of tailings, which is considered one of the top elements that determine filling's characteristics, affect many factors of filling, mainly strengths. Thus, they need to be studied broadly (Aubertin et al., 1996; Consoli et al., 2006; 2007; Kiventera et al., 2020; Simonsen et al., 2020; Xiaolong et al., 2021).

1.4.1.1. Physical Factors

Among tailings' physical factors, there are many factors like size distribution, particle shape, density, specific surface, and porosity (Table 2; He et al., 2022). They determine the compatibility with cement and water and have an effect on CPB quality (Fourie et al., 2006; 2007; Qi et al., 2018a; Pan et al., 2021; Qin et al., 2022)

Table 2. Physical factors of tailings

Characteristic type	Minimum value	Maximum value
Specific gravity	2.61	2.95
Dry density	1.82	1.95
Thickened tailings	46	75
Tailings slurry	15	36
Dewatered tailings	67	92
Paste tailings	72	86
Specific surface area (m^2/g)	0.5	7.2
Apparent porosity (%)	35	45

The most important feature of tailings employed within filling is grains' size and its shape (Nasharuddin et al., 2021; Qin et al., 2021; Wang et al., 2022a) Figure 8 shows the size distributions of diverse tailings. Usually, as fine grain content in filling increases, the flow of water in paste fill becomes more difficult (Kesimal et al., 2002; Xue et al., 2019b). Additionally, the amount of fine grain is very important for fill to be transported comfortably in the pipe system to the heels underground (Cooke, 2007; Koupoli et al., 2016; McLean et al., 2021). Since the fine grain content influences paste filling consistency, it also influences fill transmission inside the pipe and causes damage to the pipes (Qi et al., 2018b; Wang et al., 2022b). Mining wastes employed within CPB must hold no less than 20 μm fine grains at a rate of 15wt% to create fling mass and retain sufficient water (Kesimal et al., 2005; Cheng et al, 2020). As well, the wastes employed in fill are classified as fine, moderate, and coarse tailings in keeping with their fine grain content and solid dosage under 20 μm (Table 3; Clayton et al., 2003; Fall and Benzaazoua, 2005; Liu et al., 2019a; Zhang et al., 2021a).

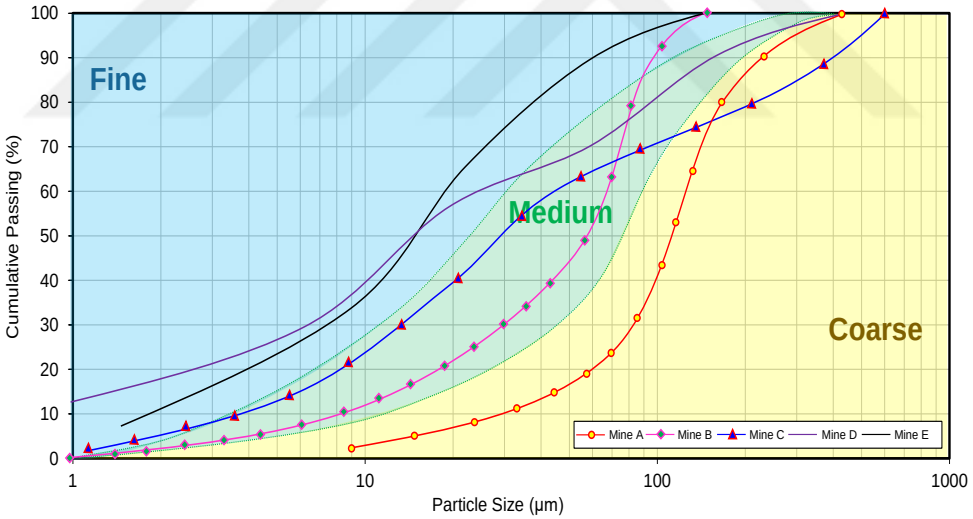


Figure 8. Various mine tailings' grain size curves

It fills the gaps between larger particles in backfill with well-dispersed fine particles (Yilmaz et al., 2013). Thus, it reduces the volume and leads to stronger bond formation with binder. Fine particles flow in pipe together with coarse particles without collapsing as a slurry. The number of fine grains is also vital for cohesion of filling during the transport in pipes (Fall et al., 2007; Cao et al., 2021a).

Table 3. Tailings type based on grain size distribution

Tailings type	Fine grains less than ≤ 20 μm (wt.%)	Solids (wt.%) at 18 cm slump values	Description (based on water/cement ratio)
Coarse	15-35	78-85	High UCS value
Medium	35-60	70-78	Low UCS value
Fine	60-90	55-70	Low UCS value

Uniformity (C_u) and curvature (C_c) coefficients were employed to govern the filling's particle sizes (Zheng et al., 2016; Xue et al, 2018). Accordingly, they stated that high fine-grained content ensures that mining wastes have a more uniform grain size distribution. Equation 1 gives the formulation of C_u and C_c. A few studies have shown that a C_u value between 4 and 6 will show that the paste filler samples will have high strength (CaO et al., 2018; Chen et al., 2022).

$$C_u = D_{60}/D_{10} \;\; ; \;\; C_C = (D_{30})^2/(D_{60} \times D_{10}) \tag{1}$$

Removing fine particles from tailings changes their fluidity, mineralogical, chemical, and physical properties. As fines content increases, tailings' specific surface surges, and the surface sections of tailings is covered with cement and become wetted. Accordingly, relatively high savings are achieved in binder consumption. It is thought that sludge removal does not always affect the strength clearly if the material content below 20 μm is not at the optimum level (Kesimal et al., 2003a; Jiang et al., 2020b).

Tailings' particle size is important in terms of fill's microstructural properties, such as the total porosity and void ratio. In previous studies, it has been revealed that the total porosity of the fill decreases with augmenting tailings' fine grain content. The tailings' packaging density is reduced when it has a fine grain content of not more than 45%. Low packing concentration is connected to greater voids between tailings grains and this area can be employed for cement hydration's development (Yilmaz et al., 2015b; Siddique and Jang, 2020). The permeability of paste filling is determined by the grain size distribution. CPB with high fine particle content has low permeability (Niroshan et al., 2018). The moisture contained in CPB generally rises as the tailings grain size gets thinner. Besides, as grain size fineness of tailings increases, it also drops the fluidity (Ke et al., 2016).

Tailings' grain shape/specific gravity may greatly influence fill's behavior and characteristics (Kesimal et al., 2003b). As a result of blasting, crushing, and grinding

processes that the ore is exposed to during extraction and processing, the tailings particle shape has a polygonal and rough texture (Figure 9; Yang et al., 2019). Flat shaped mineral particles mostly settle extra gently than round grains having equivalent specific gravity. This prominently affects the fill's setting, consolidation, and drainage period (Henderson and Revell, 2005). Besides, grain shape influences the dimension of spaces that enables fluid to be delivered and held. Filling's strength is proportional to its specific gravity property. Cement is usually put in paste filling according to tailings' solids content in the mixture. Hence, higher specific gravity will require more binders. However, the increased amount of binder will increase the operating cost of CPB (Panchal et al. 2018). Additionally, with the escalation in filling's cost, the economy of the paste filling plant finally decreases (Nasir and Fall, 2010). The fineness and density of tailings also significantly affects the hardening process and new water request, which are among CPB's properties.

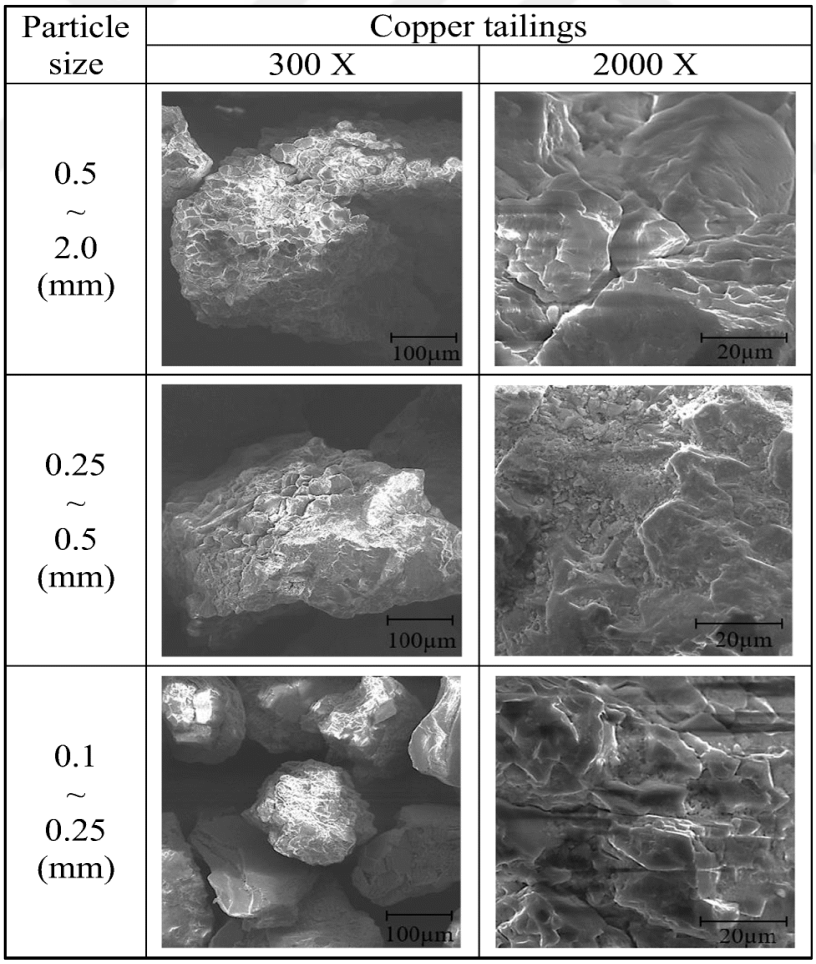


Figure 9. Tailings' grain shape analysis via digital image

1.4.1.2. Mineralogical and Chemical Composition

Mineralogical/chemical property of tailings directly affects performance and quality of filling blends. In addition, these properties could change the properties of paste filling samples like water release, stability, fresh fill characteristics, and abrasive (Lindsay et al., 2015; Kasap et al., 2022b). Figure 10 displays flotation tailings' mineral composition. Clay, mica, and muscovite minerals help to better retain the water within cementitious tailings backfill (Qi et al., 2018c; Yao et al., 2019; Zhang et al., 2021b). Silicate minerals such as quartz are very abrasive and cause damage to the piping system. Therefore, the ideal situation is a homogeneous mineral distribution in the waste (Krishna et al., 2021). In addition, sulfide minerals such as pyrite in the tailings materials unfavorably affect CPB mixture's strength and stability. Sulfate reaction depending on sulfate type and sulfidic reactivity; pyrrhotite > arsenopyrite > pyrite > chalcopyrite > sphalerite > galena > chalcocite. Additionally, as specific-surface-area within tailings grains equally rises, sulfur oxide increases in the incidence of suitable temperature and oxygen (Yilmaz et al., 2004; Toubri et al., 2022). Oxidation of the tailings used within cementitious backfill can be neglected, since the tailings, after mixing with a binder, prevents oxygen diffusion in the paste due to its high saturation degrees. Additionally, the basis of sulfate within paste filling materials may be air and sulfur dioxide, which is employed to remove the cyanide within gold mining, except for sulfur-rich tailings (Xiapeng et al., 2019).

Sulfate influence on paste filling strength/durability property is reliant on cure time, sulfate concentration, cement composition, and content (Cui and Fall, 2020). In addition, the sulfate present within the paste material may also be caused by the presence of pre-oxidized wastes. In addition, in the early period (less than 28 days), precipitates formed at some sulfate concentration (<2000 ppm) because of precipitation of minor cement hydration materials can increase filling's strength owing to filling void spaces within CPB (Zheng et al., 2019). Sulfate concentrations of up to 24000 ppm have been determined in the process water of tailings consisting typically of 80% pyrite (Benzaazoua et al., 2008).

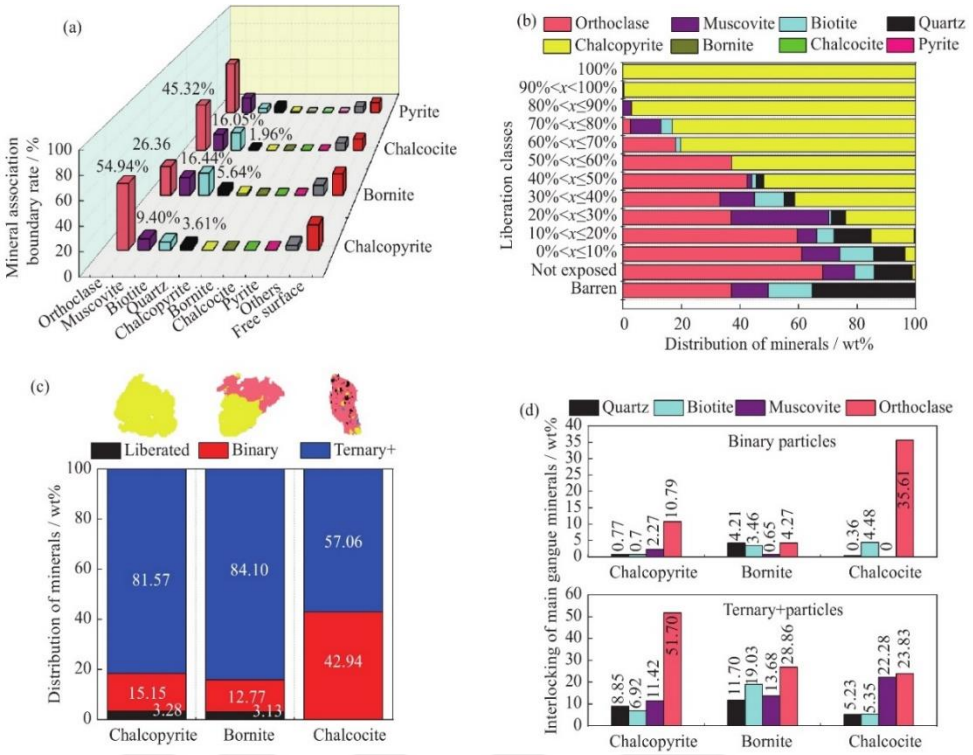


Figure 10. Tailings' mineral link: a) sulfides linked with gangues; b) chalcopyrite liberation properties; and (c-d) Cu sulfides contiguous link between major gangues

Pyrite is oxidized in water/oxygen existing to form acid/sulfate (Equation 2). Acid attacks occur owing to sulfide tailings' oxidation and configuration of CSH links is broken down (Kesimal et al., 2004). Hence, the acid released owing to oxidation causes cement hydration materials (CSH/$Ca(OH)_2$ to lose their binding properties (pH ≤ 9), reducing the fill's strength/durability (Coussy et al., 2011; Yilmaz et al., 2014b). Table 4 displays oxides formed in tailings and their amounts (Akinyemi et. al., 2022).

$$4FeS_2 + 15O_2 + 8H_2O \rightarrow Fe_2O_3 + 8SO_4^{-2} + 16H^+ \quad (2)$$

Gypsum ($CaSO_4 \cdot 2H_2O$) and anhydrite ($CaSO_4$) in the content of cement type within CPB mass can contain sulfate. These materials are added to control the cement setting in the clinker and therefore there is a small amount of sulfate transition into the mixture. The most important source of sulfate is pyrite, relying on the sort of tailings and mineral removal (Sari et al., 2022). Acid may form in the CPB samples when the pH decreases, and a rise in the cement quantity reduces acidity's development. Benefit of growing cement quantity; a rise in the hydration products' quantity occurs in the

rise in the fill's cement composition and shielding volume against acid attacks. In addition, rise in cement quantity ensures that waste surface is completely covered with hydration products, thus reducing the tailings surface required for reaction/oxidation (Koohestani et al., 2020). Sulfate produced from sulfate-rich tailings water and pyrite's oxidation reacts with free Ca ions created by dissolving insecure sulfate portlandite and calcium aluminate. Thus, as seen in equation 3 and 4, secondary gypsum/ettringite formation takes place (Jafari et al., 2019; Liu et al., 2019b; Yang et al., 2020a)

$$Ca(OH)_2 + SO_4^{-2} + 2H_2O \rightarrow Ca_2SO_4.H_2O + OH^- \text{ (Gypsum)} \quad (3)$$

$$CaO.Al_2O_3 + 3CaSO_4.2H_2O + 30H_2O \rightarrow 3CaO.Al_2O_3.3CaSO_4.32H_2O \text{ (Ettringite)} \quad (4)$$

Table 4. Tailings bases and their chemistries

Tailings bases	Chemical composites				
	SiO_2	Al_2O_3	Fe_2O_3	CaO	MgO
Phosphate mines	8.68	0.31	0.33	31.94	0.08
Sulfidic mines	51.20	10.70	11.70	12.60	6.80
Bauxite/aluminum mines	8.52	18.94	26.41	21.84	–
Tungsten mine	82.43	5.76	1.80	0.44	1.11
Copper mines	21.50	13.10	8.09	0.57	1.49
Gold mines	56.00	11.90	10.20	8.40	8.60
Iron ore mine	39.40	1.36	55.61	0.12	–
Platinum mines	11.09	0.58	22.06	2.02	8.67
Chromite ore	6.46	8.15	19.72	34.27	13.64
Vanadium mine	21.10	5.99	1.09	28.47	0.88
Molybdenum mine	40.00	10.90	9.06	27.40	2.96

1.4.2. Binder Agents

Binder properties, binder type and ratio, mineral additives and chemical additives affecting the CPB.

1.4.2.1. Binder Types and Ratio

Binder ratio and type are chief for filling's strength/stability. Portland cement type I is generally employed within CPB mixtures (Fall and Pokharel, 2010; Wu et al., 2015). Cement types/compositions, in keeping with EN 197-1, are given in Table 5. The main drive of using binders in CPB is to advance the strength characteristics like compression and shear forces governed by cohesion/the angle of internal friction. In addition, hardness contrary to static/dynamic loadings and control of permeability to

reduce contaminant transmission in tailings' ecological management can be said as other purposes (Yang et al., 2020b; Ma et al., 2021). Quantity of the cement employed in paste filling varies between 2 and 13% by weight. In addition, cement expenses are the most important cost in fill facility expenses. Thus, the determination of the binder type and ratio is of vital importance for the economy of the CPB plant. There is another type of Ordinary Portland Cement (OPC) identified as type V that is sulfate resistant. It is largely created by growing the iron content in raw mechanisms treated to produce OPC. OPC-V is generally employed as a cement in fillings created from sulfide tailings (Zheng et al., 2019; Cui and Fall, 2017). Sulfates may augment fill's early stability by connecting, reducing, or changing the pore structure with sulfate products formed and precipitating in hydration process (Koohestani et al., 2018; Grabinsky et al., 2021). This positive effect leads to negative effects due to sulfate attacks (Li and Fall, 2016). Sulfates present in CPB mixture or sulfates produced from sulfur-rich constituents may lead and degrade interior sulfate attacks in tough mortars/concretes/cementitious fillings (Cui et al., 2020; Kasap et al., 2022a). The binder composition used in filling is also vital. CPB's intrinsic degradation is regularly linked with great concentrations of C_3A. The low value of C_3A in expensive sulfate-resistant cement PC-V reduces likelihood of ettringite creation. Being an expanding mineral, ettringite lessens the weakening triggered by sulfates present in mortars (Li et al., 2019a).

1.4.2.2. Supplementary Cementitious Materials

In recent years, various pozzolanic materials and by-products of the industrial sector have been used to reduce OPC consumption and improve product performance of fills in the mining sector. Pozzolans exemplify siliceous/aluminosilicate amorphous products, which are shapeless other than glassy in nature and lack adequate greatness. To create unsolvable cementitious materials, they rejoin by lime in the aquatic medium (Hossain et al., 2016). Pozzolans are demarcated as siliceous or siliceous-aluminous substance that reacts chemically with calcium hydroxide at normal temperatures and in the incidence of moistness to create products escorted with binding characteristics (CSH gel) when ground very finely. Figure 11 shows particle sizes and specific surface area (SSA) of supplementary cementitious materials (pozzolanic materials) (Ghasemi et. al., 2019).

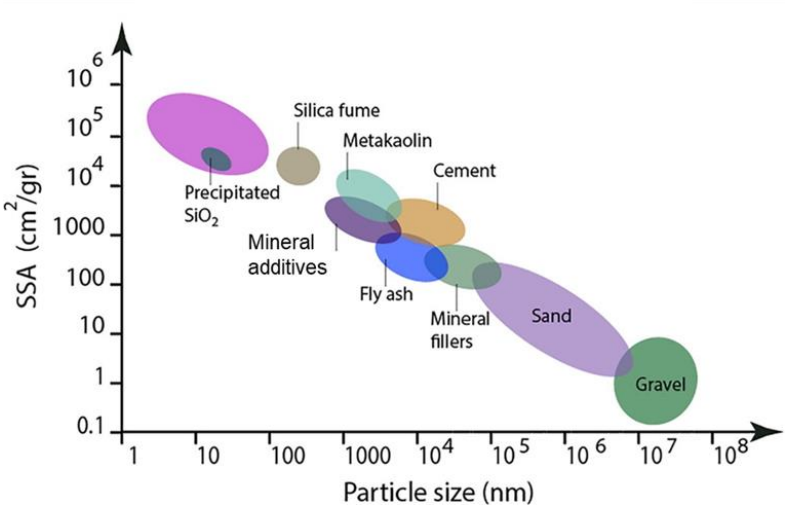


Figure 11. Grain size and typical SSA of various materials

Pozzolanic materials possess a useful influence on durability-strength property of cementitious filling materials (Kulekci et al., 2016). It notably contributes to the depletion of portlandite, which is released throughout cement's hydration. The worsening caused by sulfate outbreak can be governed by detaining/removing mono-sulfate and calcium-aluminate hydrate in binder (Zhang et al., 2021c). This limits C_3A content in OPC or can be by substituting cement fraction with proper mixing products like artificial/natural pozzolans (Tuylu, 2019). Carbon emissions also decrease with the decrease in cement use, increase in product performance and technical benefits are provided. Therefore, sustainable development is supported. Pozzolans are divided into natural and artificial pozzolans. Volcanic tuff/ash, calcined clays, and shales, and natural pozzolans such as pumice can be reflected as alternative and cost-effective products for CPB in blended cement production (Tariq and Yanful, 2013; Qi et al., 2019). The principal reasons for employing pozzolans in cementitious mixes are to improve workability, reduce porosity/void ratio and permeability, reduce cement cost/consumption, obtain more durable products, and increase resistance to sulfate effect. (Orejarena and Fall, 2010; Xiao et al., 2021b). The addition of natural pozzolans reduces C-H in mortars by delaying/preventing gypsum creation in OPC with low C_3A content, increasing sulfate resistance (Tariq and Yanful, 2013). Mortars with pozzolan reveal less growth and great durability in sulfate-rich locations (Li et al., 2021a). Pozzolanic movement of regular products is closely related to the silica content. The use of 10-30% by weight of natural pozzolans slows down fill's strength development

proportion. It is known that use of pumice at higher doses (over 30%) reduces stability of CPB samples in long-term aging (Qi and Fourie, 2019). Figure 12 shows alternative binders that can be used in CPB in the literature (Behera et al., 2021).

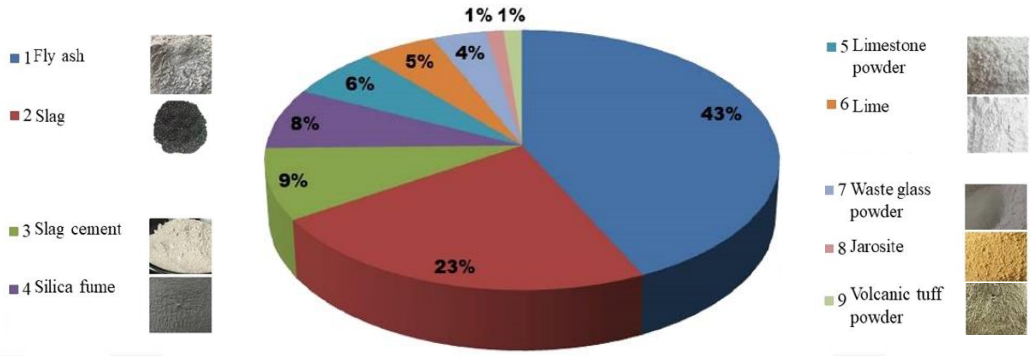


Figure 12. OPC substitute with other binders in fill

Being a thermal power plant waste, fly ash consists commonly of round, silt-sized, and shapeless ferroaluminosilicates (Blissett and Rowson, 2012). According to CSA A3001, ash is categorized to be little lime form F fly ash (a CaO content of below 8%), medium lime form CI (a CaO content of 8-20%) and high lime form CH (a CaO content of higher than 20%). According to ASTM C 618, it is classified as form C and form F fly ash depending on the burned coal type's chemistry. Form C and F fly ashes should cover a total oxide (SiO_2+Al_2O_3+Fe_2O_3) content of no less than 50% and 70%, respectively. According to TS EN 197-1, there are two kinds of fly ash: silica (V) and calcareous (W) fly ashes. V type ash is a silty powder involving of round grains with pozzolanic characteristics and has a reactive calcium oxide of no less than 10wt.%, a reactive silicon dioxide of no less than 25wt.%, aluminum oxide, iron oxide, and other compounds. W type ash is a fine powder with hydraulic/pozzolanic characteristics and has a reactive calcium oxide of no less than 10wt.%, a reactive silicon dioxide of no less than 25wt.%, aluminum oxide, iron oxide, and other compounds. Form C fly ash has cement/pozzolanic characteristics and can resist the tailings' acidity because of its great Ca content (Giergiczny, 2019) while form F fly ash has a calcium oxide of <10% and is made up of anthracite/bituminous coals (Yazici and Arel, 2012).

A slight replacement of OPC with form C fly ash is economical in producing CPB, but not suitable for strength gaining (Ali et al., 2021, Cavusoglu et al., 2021a). However, because of its use, there is a tendency to protect the backfill from the effect

of sulfate in the long-term. Through chemical and mineralogical analyses, the presence of sulfides in the wastes causes the cement hydrate phases to melt and swell, causing CPBs to deteriorate (Jafari et al., 2021; Huang et al., 2021b). OPC without help is not a right cement to afford long age durability for a high sulfate fill owing to the C_3A composite's creation. Nevertheless, strength gaining is better in long-term curing time when cement is used together with form C fly ash (Cavusoglu et al., 2021b).

Being a non-metallic by-product of iron making, BFS is made of silicates. They are basically cement-thin or finer materials that are melted concurrently with Fe in a blast furnace, cooled in liquid through rapid soaking in aquatic for creating amorphous granulated grains. In a slag composition with OPC, OPC plus form C start to hydrate and then react with the slag releasing Ca/Al ions in the solution. Slag then responds to alkali hydroxide and $Ca(OH)_2$ to form more CSH gel (Ustabas et al., 2021).

Alkali/hydroxyl ion release during cement hydration increases pore solution's pH by generating hydration responses for cement/slag systems. Silica specs convert to solvable in basic solution and the capillary porous spaces left by the hydration products of OPC are filled with secondary CSH. In keeping with OPC, if the cement properties are not triggered by adding Ca during hydration stage, the slag develops so slowly that it is not practical (Jiang et al., 2020c).

CPB mixtures containing GBFS give better results in strength parameters than mixtures prepared with other binders. CPB's hydraulic conductivity decreases because of the thinning of the pore size in backfill mixtures containing slag (Kou et al., 2020; He at al., 2021). In addition, paste fill samples prepared with slag-containing cement have the highest fine pores and reach high UCS values (Ouellet et al. 2007). A partial replacement of OPC with GBFS increases the backfill resistance at advanced wet and cure heat of 2-20°C, and adversely affects the resistance at a cure heat of ≥35 °C (Jiang et al., 2019b). In high sulfide tailings fill with alkali active slag binder, UCS amplified with augmenting cement ratio. A decrease of up to 20% in total porosity also occurred simultaneously (Xue et al., 2018; Dai et al., 2022; Sari et al., 2022).

GBFS plus FA additives enhance sulfur-rich tailings fill's long-term strength gaining and can be used suitably to lessen the cement costs in a filling facility. Figure 13 displays SEM images of slags and fly ashes while Table 6 shows their chemistry (Behera et al., 2021).

Table 5. Types of cement based on EN 197-1 standard

Cement's name		Code	Clinker	Blast furnace slag	Silica fume	Pozzolana		Fly ash		Burnt shale	Limestone	Minor additional constituents
			K	S	D	natural P	calcined Q	siliceous V	calcareous W	T	L	
I	Portland cement	I	95–100	-	-	-	-	-	-	-	-	0-5
	Portland-slag cement	II/A-S	80–94	6-20	-	-	-	-	-	-	-	0-5
		II/B-S	65–79	21-35	-	-	-	-	-	-	-	0-5
	Portland-silica fume cement	II/A-D	90-94	-	6-10	-	-	-	-	-	-	0-5
	Portland-pozzolana cement	II/A-P	80–94	-	-	6-20	-	-	-	-	-	0-5
		II/B-P	65–79	-	-	21-35	-	-	-	-	-	0-5
		II/A-Q	80–94	-	-	-	6-20	-	-	-	-	0-5
		II/B-Q	65–79	-	-	-	21-35	-	-	-	-	0-5
	Portland-fly ash cement	II/A-V	80–94					6-20	-	-	-	0-5
		II/B-V	65–79	-	-	-	-	21-35		-	-	0-5
		II/A-W	80–94	-	-	-	-	-	6-20	-	-	0-5
		II/B-W	65–79	-	-	-	-	-	21-35	-	-	0-5
II	Portland-burnt shale cement	II/A-T	80–94	-	-	-	-	-	-	6-20	-	0-5
		II/B-T	65–79	-	-	-	-	-	-	21-35	-	0-5
	Portland-limestone cement	II/A-L	80–94	-	-	-	-	-	-	-	6-20	0-5
		II/B-L	65–79	-	-	-	-	-	-	-	21-35	0-5
	Portland-composite cement	II/A-M	80–94	-	-	-	6	20	-	-	-	0-5
		II/B-M	65–79	-	-	-	21	35	-	-	-	0-5
III	Blast furnace cement	III/A	35–64	35-65	-	-	-	-	-	-	-	0-5
		III/B	20–34	66-80	-	-	-	-	-	-	-	0-5
		III/C	05–19	81-95	-	-	-	-	-	-	-	0-5
IV	Pozzolanic cement	IV/A	65–89	-	-	-	11-35	-	-	-	-	0-5
		IV/B	45–64		-	-	36-55	-	-	-	-	0-5
V	Composite cement	V/A	40–64	18-30	-	-	18-30	-	-	-	-	0-5
		V/B	30–39	31-50	-	-	31-50	-	-	-	-	0-5

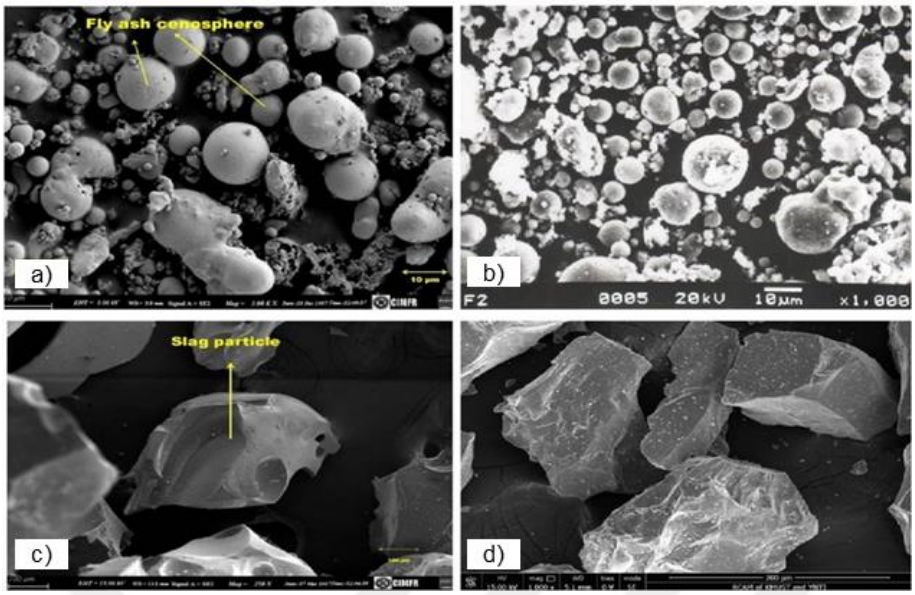


Figure 13. SEM photos of fly ashes (a, b) and slags (c, d)

Table 6. Slag and fly ash chemistries

Country	SiO_2	Al_2O_3	Fe_2O_3	TiO_2	CaO	MgO	P_2O_5	SO_3	Na_2O	K_2O	MnO
Lead-zinc fuming furnace slag, India	37.91	12.72	28.02	0.48	14.66	2.75	0.52	0.36	1.14	1.43	–
Blast furnace slag, Spain	35.50	13.60	0.40	–	41.00	4.10	–	0.10	0.01	–	–
Indian steel slag	34.40	21.50	0.20	–	33.20	9.50	0.54	0.66	–	–	–
Chinese steel slag	20.25	5.32	29.63	0.71	34.37	5.72	0.62	–	–	–	1.63
Iron blast-furnace slag, Egypt	36.95	10.01	1.48	0.52	33.07	6.43	0.10	3.52	1.39	0.74	0.52
Blast furnace slag, Turkey	39.68	15.07	–	0.96	33.37	7.84	<0.01	1.87	–	–	0.97
Lead slag, Australia	27.50	7.40	33.38	–	19.40	2.10	–	–	–	–	–
Slag, UK	34.94	11.69	3.32	0.49	40.49	7.42	0.01	1.19	0.16	0.34	0.27
Slag, China	24.36	8.06	0.49	–	57.70	4.79	–	2.61	0.25	0.63	–
Slag, Canada	35.57	10.59	0.62	0.467	39.21	11.78	–	–	0.28	0.48	0.30
Chinese nickel slag	52.31	6.22	4.20	0.10	8.81	26.88	–	–	0.11	0.16	–
Chinese Li slag	56.77	20.63	2.53	–	4.73	0.67	–	–	–	–	0.28
China	50.89	18.83	16.45	0.21	6.97	0.84	1.49	2.86	0.62	0.87	–
Europe	40.33	21.59	8.11	1.34	12.53	4.1	0.71	8.09	0.30	2.25	–
India	60.23	31.15	4.29	2.42	0.76	0.1	0.09	–	–	–	–
China	52.94	30.91	2.38	–	6.53	0.92	–	–	–	–	–
Canada	37.64	18.61	5.72	0.98	20.65	4.99	–	–	4.82	0.68	0.02
India	60.71	27.27	4.61	1.67	2.08	0.56	0.79	0.86	0.39	1.05	–

1.4.2.3. Chemical Additives

Chemical additives are typically supplemented to concrete mortar before or throughout blending. 80% of the concrete created in the construction industry in North America contains one or more types of chemical additive. Additives mend concrete's performance. CPB contains much less cement in the backfilling in comparison with concrete (Mangane et al., 2018; Saedi et al., 2021). However, it is thought that the use of cement additives can increase the performance of backfilling and reduce the costs regarding the cement usage (Haruna and Fall, 2020; Jin et al., 2022). Figure 14 shows the types of chemical additives used within filling materials (Saedi et. al., 2021). Most potential problems with CPB occur during backfill preparation, transport, and placement.

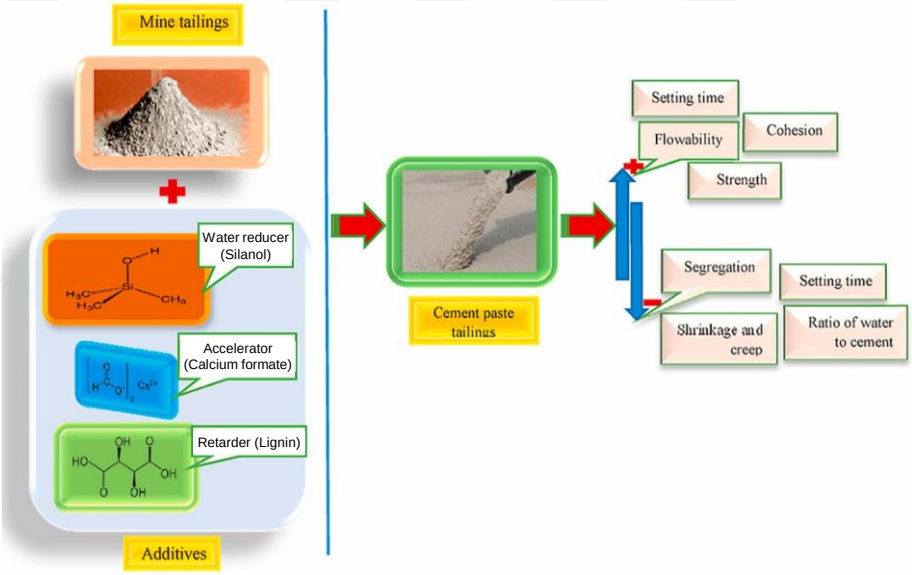


Figure 14. Types of chemical admixture in CPB materials

The mixing of additives helps to create an optimal mix design. The use of additives in cementitious CPB contributes to the following issues:

- It provides high strength to be produced in the early and final period.
- It increases compressive and flexural strength, and cohesion.
- It reduces water content and segregation in hydraulic and paste fills.
- It increases pumpability, machinability, consistency, and fluidity.
- It reduces shrinkage, creep cracking, and abrasiveness (Jiang et al., 2020d).

Studies show that the additives used for cementitious rock filling, cementitious hydraulic filling, and cementitious paste filling have a positive effect on their strength. In addition, according to the mixture designs, approximately 50% better strength was achieved compared to the backfill without additives. The use of additives reduced the water content, increased the pumpability and delayed the curing time (Quattara et al., 2018; Ouffa et al., 2022). Outcomes declared that chemical additives could aptly add to rise sulfur-rich tailings fill's strength/stability at short/long-term and fill making costs regarding cement usage. The benefits of incorporating chemical additives into fill designs in mines are frequent, and reductions in energy and cement consumption, dewatering costs, downtime and pipe blockages, and plant maintenance costs. The addition of additives directly affects the quality of fill and many operating costs.

1.4.3. Mixing Water

Process, underground and lake/river water are used in the cement paste filling mixture. Tap water can be also used in laboratory studies. The chemical compositions of these waters also differ. This difference affects cement's hydration process and fill's agglomeration and strength properties. Tailings pore water generally creates 75-80% of total mixing water, and it is rich in sulfate (SO_4^{-2}) concentration due to the use of air and chemicals rich in sulfate concentration, especially in the enrichment of sulfide ores by the flotation method. Tap water added to the mixture later dilutes the sulfate concentration in the mixing water (Wu et al., 2015; Li et al., 2020b). Using process water resulted in lower stability of filling compared to using city/lake water (Ouellet et al., 2007). The use of water with sulfate concentrations of 4613 and 7549 mg L^{1-} reduced the porosity of fill and increased its strength (Ouellet et al. 2007). In addition, fill's strength property is influenced by water's quality. Since paste fill's strength is mainly governed by cement's hydration. Consequently, water quality is an imperative consideration when designing fill's design and operation phases (Yan et al., 2019; Cao et al., 2021c).

2. MATERIALS AND METHODS

2.1. Description of the Study Area

The study area is located within the borders of Kure town, which is 312 km from Ankara and 60 km from Kastamonu city center (Figure 1). The mining site was commissioned by Etibank in 1959 as a copper pyrite facility. In 1988, the concentrator facilities were commissioned, and copper and pyrite concentrates began to be produced. The mining enterprise, which continued its activities as a public enterprise until 2004, has been continuing its activities by a private organization since that date.



Figure 15. Location map of the study area

The mine continues to invest to ensure a more efficient production process. As of the end of 2013, 546,400 meters of drilling was completed, and R&D investments reached USD 50 million. With other investments, total amount reached USD 60 million. Kure plant produces 1,350,000 tons of raw copper ore, 170,000 tons of copper concentrate and 400,000 tons of pyrite concentrate every year. Almost 20% of the generated process tailings is re-sent to underground mined-out stopes as CPB, and the remaining tailings (80%) is stored in the tailings dam.

2.2. Specification of Testing Materials

2.2.1. Process/Dam Tailings

In the present study, two different types of process tailings were used, one with a low pH (acidic: 4.9) and the other with a high pH (basic: 10.8). These process tailings are the tailings released during the processing of ores (flotation processes). Process tailings with different pH values were obtained from an active mine in Turkey. To determine some characteristic features (physico-chemical) of the process/dam tailings supplied from the mine under investigation, the tailings brought to the laboratory was first dehydrated in an oven and subjected to a series of lab tests. Table 7 shows the particle sizes determined by employing the Malvern Mastersizer 2000 device and other physical parameters of the tailings

As lab outcomes were carefully investigated, one could interpret those tailings (with different pH) showed different characteristics. An example of this is that half of the acidic tailings are larger than 42 μm, whereas demi of basic tailings are larger than 52 μm. In addition, the percentage of particle size smaller than 20 μm was determined as 29.21% and 25.93% for tailings with low/high pH values, respectively. Therefore, it can be said that the process tailings handled within the scope of the study are large and suitable for backfill. Other physical test parameters, specific gravity/(G_S) and surface area/(S_S), were found to be 3.79 and 2.82 m^2/g, respectively for low pH tailings, whereas the declared values were found to be 3.51 and 2.60 m^2/g respectively, for high pH tailings.

Table 7. Physical properties of process tailings

Physical characteristics	G_s (-)	S_s (m^2/g)	Fine content (%)	D10 (μm)	D30 (μm)	D50 (μm)	D60 (μm)	C_u (-)	C_c (-)
Low pH (4.89) tailings	3.79	2.82	29.21	4.59	23.77	41.39	60.24	13.12	2.04
High Ph (10.8) tailings	3.51	2.60	25.93	7.11	27.14	51.19	69.91	9.83	1.48

XRF (X-ray fluorescence) method was employed in the element analysis of the tailings, and Table 8 shows the analysis results. From the analysis, it was observed that iron oxide (Fe_2O_3) and silicon dioxide (SiO_2) were the main components in all tailings, regardless of the pH value.

Table 8. Chemical properties of process tailings

Chemical characteristics	CaO	Fe_2O_3	SiO_2	Al_2O_3	MgO	Na_2O	K_2O	SO_3	Others
Acidic Tailings	3.96	42.66	23.98	6.91	1.75	0.11	0.29	0.44	19.90
Basic Tailings	2.67	45.01	20.82	7.17	2.09	0.16	0.33	0.39	21.36

Copper (16-20 wt.%) and pyrite (45-50 wt.%) are produced in the mining facility where the tailings are supplied. This plant, which is actively producing, stores approximately 75% of the tailings generated after concentrate production in tailings dam, while the continuing portions are stored under-ground as filling. Excess sulfuric tailings stored in tailings dam was used as an important material in CPB production. Five different tailings (LPDT-1, LPDT-2, LPDT-3, HPDT-1, and HPDT-2) were taken from diverse locations of tailings dam (approximately 25 cm deep on the shoreline) to examine the dam tailings effect on fill performance. In addition, to make comparisons, tailings called HPPT was taken from the filter discharge. In addition, tailings from three diverse sections of tailings dam (DTS1, DTS2 and DTS3) were collected by the aid of mini digging machine at a space of 3-5 m from the shore and an average of 20 cm depth to be used to determine the geotechnical parameters of the backfill. In addition, process tailings (PTS) were used as a control sample. The tailings dam where the tailings are collected is given in Figure 15.

When examined physically and chemically, several variances between dam and process tailings could observe. For example, the particle/grain size distribution (PSD) of process tailings shows a more homogeneous distribution compared to the tailings taken from diverse sections of dam. Although the slimes zone of dam has fine-grained tailings, intermediate/beach zones have coarser-grained tailings. Moreover, chemical structure (depending on whether there is oxidation or not) of the tailings coming out of the ore production facility and sent to the tailings dam may change depending on the weather and storage conditions. It is known that the pH value of corroded mining tailings is lesser than that of non-oxidized ones. Tailings specimens were dehydrated in an industrial furnace (100°C) for 1 day to determine the characteristics of the tailings (oxidized or unoxidized) supplied from the dam.

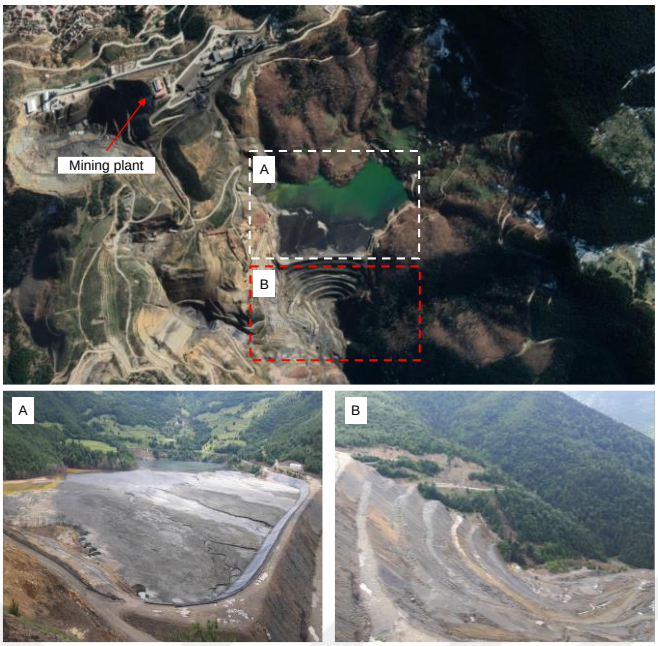


Figure 16. Sampling in tailings dam: general (a) and side (b) views

While dam tailings' fundamental physical properties are presented in Table 9, the particle size distributions (cumulative/incremental) of these tailings are presented in Figure 16. It has been observed that the fine tailings content smaller than 20 μm varies between 20.6-61.2%. While the Gs values of dam tailings vary between 3.56-3.92, the Ss values vary between 2.63-2.99 m^2/g. While the Cu value (D_{60}/D_{10}) of some dam tailings gathered for employing in this thesis study has a value between 5.28-15.6, the Cc value [$D_{30}^2/(D_{60}\times D_{10})$] has a value between 1.04-1.38. Moreover, the element properties of collected samples were measured with the Panalytical/epsilon 5 XRF device, and the results obtained are listed in Table 10. The most dominant compounds of tailings were found to be SiO_2, Fe_2O_3, Al_2O_3 and CaO and their contents were found as 31.5-44.7%, 22.7-30.9%, 6.08-8.01% and 3.66-4.92%, respectively. Some studies (Kou et al., 2020) have stated that the SiO_2 composite contained in tailings may cause adverse effects on backfilling in terms of stability, however, it may also improve some of backfills properties (settlement/permeability) (Wang et al., 2017). Also, Al_2O_3 and CaO are imperative components due to the coagulation of CPB and its contribution to strength. Sulfur (S^{-2}) and pyrite (FeS_2) dosages were designated as in the slight range of 18.4%-19.6% and 31.9-44.3%, respectively, using the ICP-OES device (Perkin Elmeroptima 7000 DV) for mineralogical analysis. Table 10 shows that the sulfur content of the tailings taken from the dam is high.

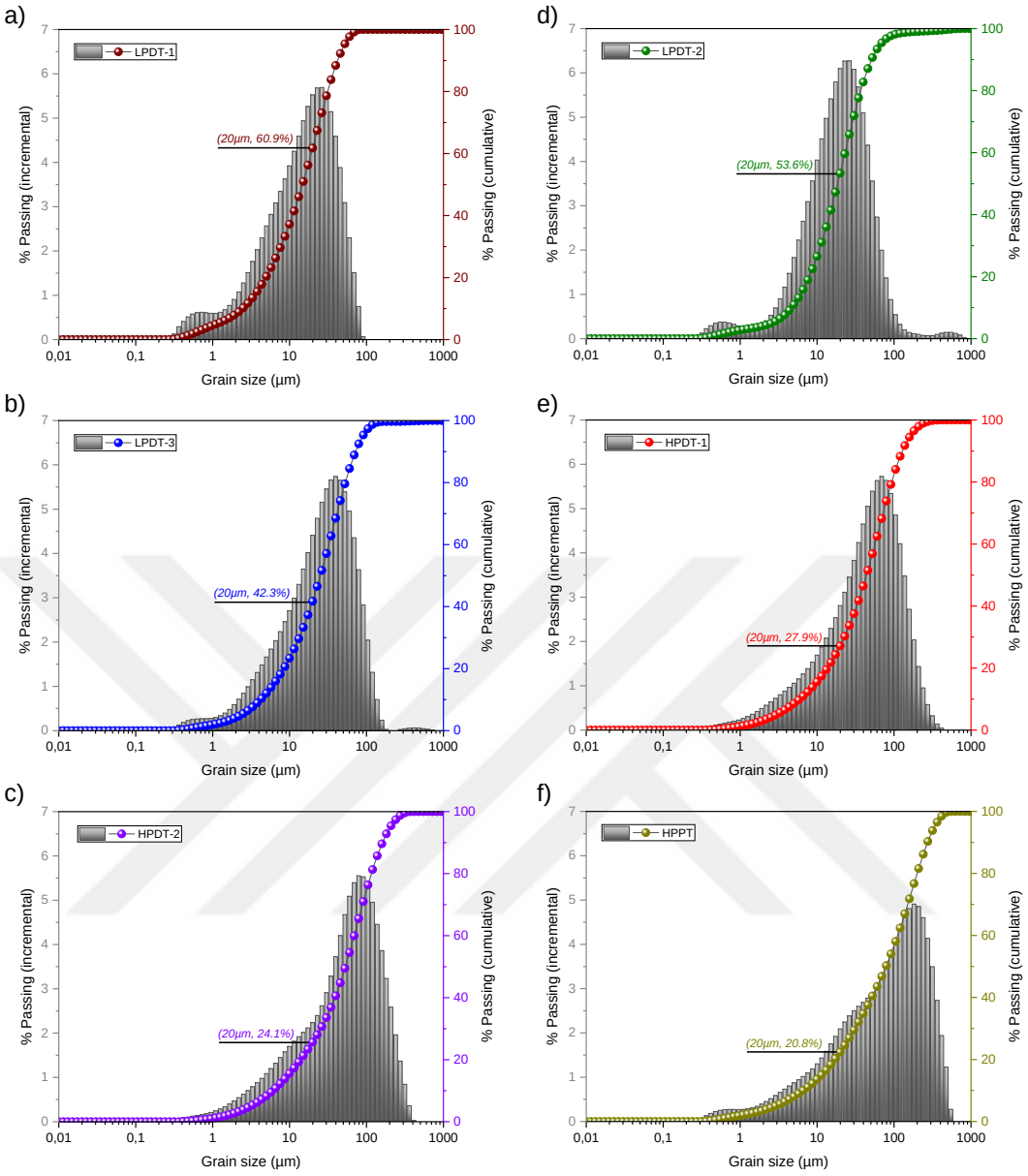


Figure 17. Cumulative and incremental grain size plots of the experimented dam (a, b, c, d and e) and process (f) tailings

Table 9. Physical properties of dam tailings

Physical features	**LPDT-1**	**LPDT-2**	**LPDT-3**	**HPDT-1**	**HPDT-2**	**HPPT**	**DTS1**	**DTS2**	**DTS3**	**PTS**
Specific gravity G_s	3.92	3.84	3.75	3.71	3.65	3.56	3.81	3.75	3.67	3.57
Specific surface area S_s (m^2/g)	2.99	2.89	2.83	2.77	2.72	2.63	2.89	2.83	2.77	2.68
Max. dry density MDD (kg/m^3)	2.65	2.54	2.49	2.46	2.44	2.35	2.55	2.49	2.42	2.37
Opt. moisture content OMC (%)	14.6	13.7	12.9	12.6	12.5	12.3	13.4	12.9	12.4	12.3
D_{10} (µm)	2.86	4.47	4.61	6.71	6.56	7.03	-	-	-	-
D_{30} (µm)	8.13	10.5	13.4	22.8	25.0	31.2	-	-	-	-
D_{50} (µm)	14.5	18.6	24.1	44.3	50.8	78.6	-	-	-	-
D_{60} (µm)	18.3	23.6	32.9	56.4	69.6	109	-	-	-	-
Uniformity coefficient C_u	6.41	5.28	7.15	8.41	10.6	15.6	-	-	-	-
Curvature coefficient C_c	1.26	1.04	1.19	1.38	1.37	1.26	-	-	-	-

Table 10. Chemical properties of dam tailings

Chemical composition (%)	LPDT-1	LPDT-2	LPDT-3	HPDT-1	HPDT-2	HPPT	DTS1	DTS2	DTS3	PTS
Silicon dioxide SiO_2	44.7	42.7	40.4	38.8	35.6	31.5	34.31	30.11	25.44	23.16
Iron oxide Fe_2O_3	22.7	24.1	25.4	26.8	28.5	30.9	33.45	37.11	40.75	43.06
Aluminum oxide Al_2O_3	6.08	6.38	6.63	7.03	7.56	8.01	6.13	6.99	7.07	7.78
Calcium oxide CaO	4.92	4.66	4.26	4.01	3.89	3.66	4.81	4.01	3.99	2.60
Magnesium oxide MgO	1.66	1.71	1.77	1.83	1.94	2.17	1.66	1.88	1.82	2.46
Potassium oxide K_2O	0.46	0.42	0.39	0.33	0.29	0.25	0.45	0.44	0.32	0.26
Sulfur oxide SO_3	0.36	0.32	0.30	0.27	0.26	0.23	0.38	0.33	0.34	0.34
Titanium oxide TiO_2	0.19	0.21	0.22	0.22	0.24	0.29	0.20	0.19	0.25	0.31
Phosphorus oxide P_2O_5	0.08	0.06	0.05	0.04	0.03	0.03	0.09	0.07	0.07	0.05
Sodium oxide Na_2O	0.06	0.05	0.04	0.05	0.07	0.08	0.06	0.05	0.06	0.11
Strontium oxide SrO	0.01	0.02	0.02	0.02	0.01	0.01	0.01	0.01	0.01	0.01
Barium oxide BaO	0.02	0.01	0.02	0.02	0.02	0.01	0.01	0.01	0.01	0.01
Loss on ignition LOI	18.3	19.0	19.7	20.2	21.2	22.1	18.32	20.11	20.17	20.23
Total sulfur S^{-2}	29.6	26.8	24.5	21.9	20.8	18.4	-	-	-	-
Total pyrite FeS_2	44.3	40.9	38.2	36.7	34.4	31.9	-	-	-	-

2.2.2. OPC and SCM

In this thesis, ordinary Portland cement (CEM I 42.5R) and accompanying supplementary products such as GBFS and FA switched for this principal binder at different rates (0%, 10%, 20%, 30% and 50%) were used. Tables 11 and 12 present the physical/chemical properties of these materials, respectively. From Table 11, one can witness that the mean grain size (D50) of GBFS is smaller than the other binders (14.19 μm), while the largest D50 size (25.84 μm) belongs to OPC. From the physical properties of the binders, G_S has values of 3.09, 2.94 and 2.72 for OPC, GBFS and FA, respectively, while the S_S values have 0.37, 0.79 and 0.46 m^2/g, respectively. Additionally, the elements of these products used as binders were measured by XRF method and presented in Table 12.

Table 11. Principal physical characteristics of main and supplementary binders

Physical parameters	G_s (-)	S_s (m^2/g)	Fine content (%)	D10 (μm)	D30 (μm)	D50 (μm)	D60 (μm)	C_u (-)	C_c (-)
OPC	3.09	0.37	42.85	4.78	13.41	25.84	31.89	6.67	1.18
GBFS	2.94	0.79	64.16	2.88	8.22	14.19	19.11	6.64	1.23
FA	2.72	0.46	58.44	4.21	10.94	18.66	23.01	5.71	1.24

In all binders used in the study, the dominant compounds were determined as CaO, SiO_2 and Al_2O_3. For OPC, GBFS and FA, the CaO content was 65.22%, 34.39%

and 6.21%, respectively, the SiO_2 content was 16.98%, 38.21% and 44.38%, and the Al_2O_3 content was 5.67%, 12.17% and 19.33%, respectively.

Table 12. Element characteristics of binding materials

Chemical characteristics	CaO	Fe_2O_3	SiO_2	Al_2O_3	MgO	Na_2O	K_2O	SO_3	Others
OPC	65.22	3.19	16.98	5.67	1.30	0.25	0.79	3.51	3.09
GBFS	34.39	1.29	38.21	12.17	5.98	0.36	0.78	2.44	4.38
FA	6.21	8.66	44.38	19.33	1.23	0.71	0.99	2.01	16.48

2.2.3. Mixing Water

The geochemistry and characterization of the waters (leaking from the surface) in the natural state of the tailings obtained from the mine site to be used in the study are important in the evaluation of the results obtained. Therefore, pore (PW) and tap water (TW) were used in this study and their chemical analyzes were determined by ICP-OES device. The geochemical analysis results of PW and TW are given in Table 13. It has been observed that the most important contents of the waters belong to sulfate and calcium. The sulfate (SO4-2) content has a value in the broad array of 4699-7597 ppm for PW and 5.02 ppm for TW. Calcium (Ca) concentration also has a value in the range of 401-603 ppm for PW, while it has a value of 39.2 ppm for TW.

Table 13. Chemical/Geochemical characteristics of PW and TW

Elements	Pore water (PW)						Tap water (TW)
	LPDT-1	LPDT-2	LPDT-3	HPDT-1	HPDT-2	HPPT	
Geo-chemical factors							
pH	3.94	4.78	5.83	7.11	7.93	10.2	7.71
EC (μS/cm)	5431	5227	4998	4623	4437	4016	0.11
Eh (V)	0.35	0.40	0.43	0.49	0.54	0.57	0.41
Chemical composition							
SO_4^{-2} (mg L^{-1})	7597	7331	6579	5988	5697	4699	5.02
Ca (mg L^{-1})	401	433	491	537	566	603	39.2
K (mg L^{-1})	19.4	23.7	26.9	29.3	31.3	35.7	0.58
Cl (mg L^{-1})	1.44	1.55	1.57	1.61	1.62	1.75	0.34
Mg (mg L^{-1})	1.56	1.66	1.79	1.86	1.92	2.08	2.16
Si (mg L^{-1})	69.1	65.7	58.3	53.2	49.1	44.8	0.84
Al (mg L^{-1})	0.64	0.65	0.58	0.59	0.57	0.54	0.01
Cu (mg L^{-1})	0.18	0.16	0.21	0.19	0.19	0.16	0.91
Fe (mg L^{-1})	3.99	3.75	3.44	3.12	3.05	2.88	0.053

Some studies (Wang et al., 2017) in the literature have stated that excess SO_4^{-2} concentration will be formed from the contact of dam tailings with O_2 and H_2O, with

the oxidation of sulfur and tailings treatment processes. Also note that the SO_4^{-2} value is computed by employing a stoichiometric transformation ($SO_4^{-2} = 2.9956 \times S$) based on sulfur ($S^{-2}$) value determined using the ICP-OES technique. The high amount of Ca concentration is related to the lime added to provide pH control during the grinding processes in the mine (Aldhafeeri and Fall, 2017). SevenCompact pH/Cond S213 test equipment was employed to determine the pH, electrical conductivity (EC), redox potential (Eh) values of the pore and tap water. While pH values vary between 3.92-10.2 for different tailings, Eh and EC values vary between 4016-5431 μS/cm and 0.35-0.57 V, respectively. pH, EC and Eh of tap water (TW) were respectively, determined as the values of 7.71, 0.11 μS/cm and 0.41 V.

2.3. Laboratory Techniques

2.3.1. Mine Fill's Manufacturing Stages

GAYD (geotechnics, tailings management and filling) lab in the university was used for the experimental studies carried out within the scope of this thesis. To produce backfill, process tailings with diverse pH (acidic_4.9 and basic_10.8) and dam tailings were manufactured at a solid content of 72% and 76% by weight and a fixed cement content (5 wt.%). In the study, in which different curing times (up to 56 days) were considered, GBFS and FA were used at different rates (0% as control sample, 10%, 30% and 50%) instead of OPC in binder. Tables 14-16 show the necessary recipes to produce backfills used in experimental studies. The materials (tailings, cement, GBFS, FA and water) whose quantities were determined with the help of the prepared recipes were mixed homogeneously in a 10-liter capacity laboratory mixer (approximately 10-12 minutes). After mingling, the fill's consistency was measured as 21 and 25 cm by slump tests. The filling with the desired consistency was placed in a rod-shaped plastic sample holder (d x h: 50 x 100 mm) with holes at the bottom. The plastic molds, which were filled in a total of three stages, were skewered (25 times for each filling step) using an iron rod to remove air bubbles in the fill. After fills are cast into molds, the mold's top section is enclosed by caps to avoid the contact of filling with air and to avoid oxidizing. CPBs, whose filling processes were completed, were then placed in the curing cabinet to be kept for the curing periods specified in their recipes. A

specially designed 1400-liter cabin was used for the curing processes. This cabin, whose temperature/humidity settings can be adjusted according to curing requirements, was modified to 20±3 °C heat and 90±5% moisture. Figures 17 and 18 show experimental studies carried out in a laboratory setting.

Table 14. Recipe design of backfills containing acidic and basic tailings

Notation	Solid content (wt.%)	Binder content (wt.%)	Blend ratio (%)			Slump (cm)	Curing time (days)
			OPC	GBFS	FA		
OPC100@H [a]	72	5	100	-	-	25	3, 14, 28, 56
OPC100@L [b]	72	5	100	-	-	25	3, 14, 28, 56
OPC90@S[c]10@H	72	5	90	10	-	25	3, 14, 28, 56
OPC90@S10@L	72	5	90	10	-	25	3, 14, 28, 56
OPC70@S30@H	72	5	70	30	-	25	3, 14, 28, 56
OPC70@S30@L	72	5	70	30	-	25	3, 14, 28, 56
OPC50@S50@H	72	5	50	50	-	25	3, 14, 28, 56
OPC50@S50@L	72	5	50	50	-	25	3, 14, 28, 56
OPC90@F[d]10@H	72	5	90	-	10	25	3, 14, 28, 56
OPC90@F10@L	72	5	90	-	10	25	3, 14, 28, 56
OPC70@F30@H	72	5	70	-	30	25	3, 14, 28, 56
OPC70@F30@L	72	5	70	-	30	25	3, 14, 28, 56
OPC50@F50@H	72	5	50	-	50	25	3, 14, 28, 56
OPC50@F50@L	72	5	50	-	50	25	3, 14, 28, 56

[a] H presents basic tailings with a pH value of 10.8; [b] L presents acidic tailings with a pH value of 4.9

[c] S presents granulated blast-furnace slag; [d] F presents pulverized fly ash (class C)

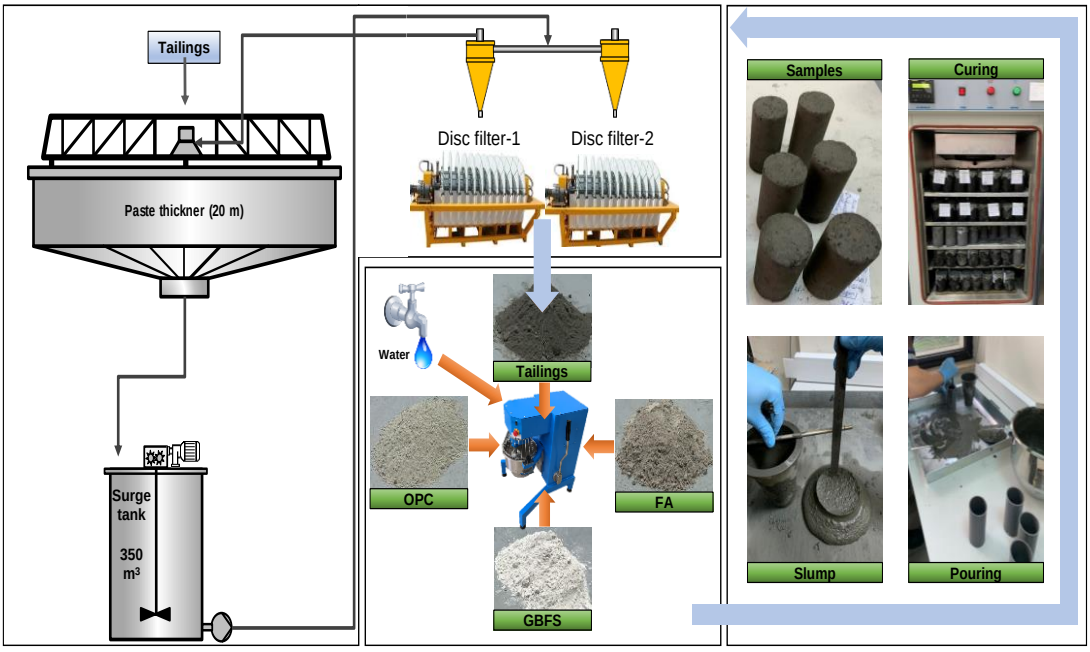


Figure 18. Fill manufacturing stages

Table 15. Fill types in terms of their experimental recipes

Mixture ID	Tailings		Solid content (wt.%)	Binder dosage (wt.%)	Slump (cm)	Curing time (days)
	Type	pH value				
CPB-LPDT-1	LPDT-1	3.94	76	5	21	3, 14, 28, 56
CPB-LPDT-2	LPDT-2	4.78	76	5	21	3, 14, 28, 56
CPB-LPDT-3	LPDT-3	5.83	76	5	21	3, 14, 28, 56
CPB-HPDT-1	HPDT-1	7.11	76	5	21	3, 14, 28, 56
CPB-HPDT-2	HPDT-2	7.93	76	5	21	3, 14, 28, 56
CPB-HPPT	HPPT	10.2	76	5	21	3, 14, 28, 56

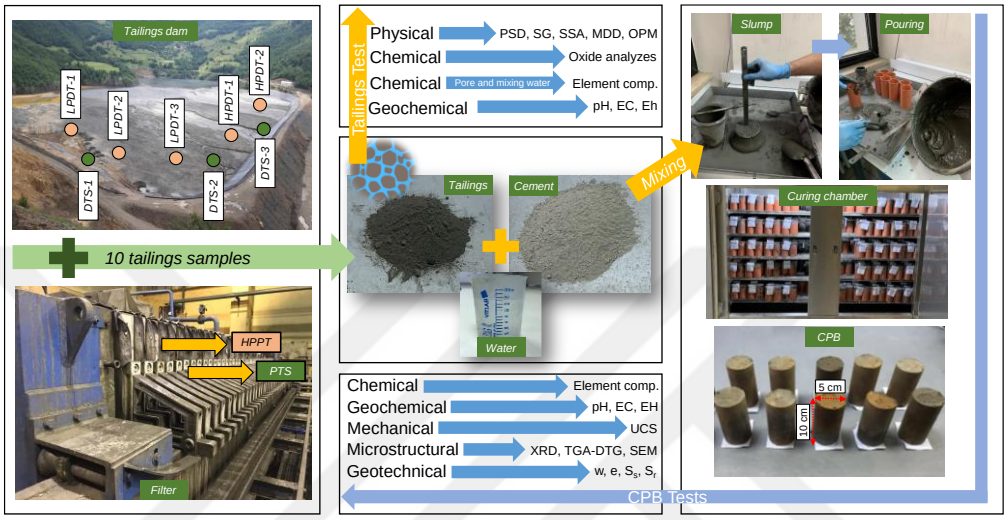


Figure 19. CPB sample experimental stages

Table 16. Diverse blend recipes of fillings created by using dam tailings

CPB ID	Tailings type	Binder content (%)	Solid content (wt.%)	Pyrite/Sulfide content (%)	pH value	Slump (cm)	Curing time (days)
CPB-D1	DTS1	5	72	46/34	4.2	25	3, 14, 28, 56
CPB-D2	DTS2	5	72	39/25	5.9	25	3, 14, 28, 56
CPB-D3	DTS3	5	72	35/21	6.8	25	3, 14, 28, 56
CPB-P	PTS	5	72	32/16	10.5	25	3, 14, 28, 56

2.3.2. Mini-Slump (15 cm height) Test

The slump value, which is frequently used in the concrete and CPB industry and which determines the consistency of the material, is determined according to ASTM standard C143. This value, which is measured with the help of a cone with a height of 30 cm and shows the decrease of the CPB under its own weight, is especially important for the applicability of the backfill in the field. Although it is reasonable and appropriate to use the standard-slump cone in the field, its use in the lab environment is not convenient and practical due to the need for more time and tailings. Therefore, the mini-slump cone test was applied instead of the standard one. This mini cone test is a quick and reasonable system of determining CPB consistency and uses merely

16% of filling used in a standard-slump cone. Thanks to these advantages, more tests could be done in a short time. The mini slump cone is a truncated cone-shaped piece of equipment with a bottom and upper diameter of 100 and 50 mm, respectively, and a tallness of 150 mm. This cone was occupied in keeping with ASTM C143 standard and while determining the slump values of the mixtures, it was filled in 3 stages and skewered 25 times, just like filling the backfill into plastic containers. There is a good correlation between the results obtained from this mini slump test and the results determined by the standard cone test. Figure 19 shows the slump values determined by both cones of CPB with different solid contents. In the thesis study, the link between the slump cones (mini/standard) was determined statistically as 2. For example, while the slump value of the backfill mixture prepared solid content of 72 wt.% is 12.5 cm for the mini-slump test, this is 25 cm for the standard slump test.

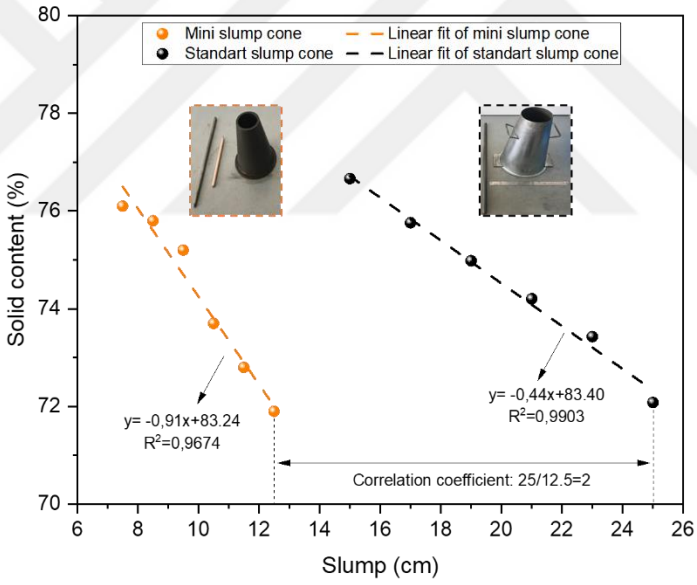


Figure 20. Measurement of slump values by mini/standard slump cones

2.3.3. Determination of Mechanical Properties

Properties such as uniaxial compressive strength_UCS, stress-strain behavior and elastic modulus_E50 of the backfill samples that completed the curing period were determined experimentally. UTEST Multiplex brand servo-controlled device with a capability of 5 tons and a movement of 1 mm per mi. was employed to determine the mechanical properties of filling. Before determining fill's strength factors, the fills to be tested were detached from plastic molds engaged in cure cabinet and measured with

the help of caliper/assay balance devices. Afterwards, the upper/lower surfaces were flattened with a sharp tool and placed between the infill plates. Cylindrical fill samples (D×H: 5×10 cm) were exposed to UCS tests, as stated by the ASTM C39 standard.

2.3.4. Determining Geotechnical Index Parameters

Following the strength tests, parameters such as specific-surface-area_Ss, water-content_w, specific-gravity_Gs, void-ratio_e and saturation-degree_Sr of the backfill samples were determined by various methods. Ss values of CPB were found using BET device (Micromeritics Gemini 2375). To determine the w values, fills were dehydrated in an industrial furnace (at 50 °C) for 2-day. Gs values of CPB were found using helium pycnometer device (Micromeritics Accupyc 1330). The pore structure of backfill samples was determined using Micromeritics Autopore III 9420 Hg intrusion porosimeter. The factor e was computed by employing the porosity value determined by the test equipment Among the determined or calculated w, Gs and e values, the unknown Sr was found by Equation (6).

$$e = \frac{n}{1-n}; \quad S_r = \frac{wGs}{e} \tag{5}$$

Where, n is the porosity (%), Gs is the specific gravity; w is the water content (wt.%), e is the void ratio; and Sr is saturation degree (%).

2.3.5. Measuring Geo/Chemical Parameters

Fill's chemical/geochemical parameters are directly linked with the water held in the pores in the backfill. It is often tough to measure the chemical factors of cured specimens after prolonged curing of CPB. The reason for this is that the excess water in the backfill is discharged through drainage at the beginning of curing (within the first 4 days). To find fill's chemical-geochemical factors, some backfill was taken and the processes were applied according to the method specified by Cihangir et al. (2012). For these processes, the backfill samples were crushed into small pieces and handed over a 2.36 mm sieve. Then, sample was homogeneously blended by using 0.1 L of purified water, with a solid/liquid fraction of 1. The mixture was shaken well for 5 minutes and left for 1 hour to settle the solid particles. A Whatman filter was used to separate the solution from solid particles after standing. Chemical/geochemical

analyzes were performed on filtered water. ICP-OES device (PerkinElmer Optima 7000 DV) was used to measure fill solutions' chemistry. pH, EC and Eh factors of the solution were measured with the SevenCompact pH/Cond S213 device. With this device, pHs were measured between -2 and 20 with a precision of 0.002, EC with a 0.05 precision shifting from 0.001 to 1000 mS/cm, and Eh with a 0.1 precision shifting from 0.1 to 1 mV. A different solution was used for each analysis.

2.3.6. Microstructure Investigations

X-ray diffraction (XRD) method was used to determine the hydration products and crystalline structure of filling samples subjected to different curing times. Rigaku SmartLab XRD device was used for this. With this device, CuKα radiation was applied to the CPB samples at an operating voltage of 40 kV, an emission current of 40 mA, and a 2θ value shifting from 5° to 60° in increments of 0.02.

Thermal gravimetric analysis (TGA) was used to indirectly determine change in mass of the backfills with temperature at an expiration of different cure times and the type of hydration products formed. For this, 10-12 mg sample (powder) was carried out using Linseis/STA TG-DSC/DTA PT1600 device at a cooking ratio of 10 °C/min between 25 and 1000 °C beneath the N_2 atmosphere.

After fill's strength tests, *SEM (scanning electron microscope)* tests on the sample pieces (broken) were performed using the JEOL JSM-6610 device. Sample pieces from the center of the broken CPB were dehydrated in an industrial furnace (at 50°C) for 24 hours. Then, the dehydrated samples were protected by Au conductive film and subjected to SEM tests. SEM analyzes were performed at an acceleration voltage of 10-20 keV at a current emission of 0.9 nA, with a maximum magnification and resolution of 2000 times and 10 μm, respectively. Working distances of 35 mm or less were applied during the measurements.

The pore size distributions of the CPB samples at the end of different curing times were determined using the *MIP (mercury intrusion porosimetry)* method. Before the measurements performed using the Quantachrome Poremaster PM60 instrument, a preliminary preparation like the preparations in the SEM test was made. The MIP tests of filling were based on the 414 MPa pressure and 0.003 μm pore diameter, and tests were carried out by making at least three tests.

3. RESULTS AND DISCUSSION

3.1. Mechanical Results

3.1.1. Effect of Mineral Additives on Filling Strength

Figure 20 shows strength development of mineral additive (e.g., GBFS and FA) substituted paste backfills prepared at different replacement ratios (see Table 14) and curing times. Progress of curing age augmented the hydration materials of specimens and decreased the void ratio. This is the foremost motive for the strength development of backfills during curing period. The strength values of control samples (OPC100@L and OPC100@H) containing low pH (acidic) and high pH (basic) process tailings vary between 0.21 and 0.63 MPa. In comparison with the OPC100@L (containing acidic tailings) sample cured for 28 days, the strength values of the samples with diverse GBFS replacements (10-30-50%) for identical curing time were 24.9%, 33.1%, and 38.8% less, respectively. Similarly, the strength values of GBFS substituted backfills were found to be 19.9%, 33.2%, and 47.6% decrease compared to the OPC100@H (containing basic waste) sample. The strength values of GBFS added CPB mixtures made with acidic/basic process tailings were at a maximum of 10% and a minimum of 50% replacement rates. The strengths of the backfills (OPC90@S10@ H/L and OPC50@S50@H/L) prepared at these substitution proportions were between 0.21 and 0.55 MPa at all curing times. Consistent with previous studies, the strength of CPBs decreased significantly with increasing GBFS substitution rate (Jiang et al., 2020a; Chowdary and Asadi, 2021). This is due to the slow hydration rate and low binding property of the GBFS additive (compared to cement). The slow hydration reactions cause high long-term strengths and low early age strengths. In addition, the finer grain size of GBFS compared to OPC is a factor that reduces strength. Compared to the 28-day OPC100@L sample, the strengths of FA added fillers prepared at 10%, 30% and 50% replacement rates for the same curing time were 40.9%, 52.2%, and 66.9% less, respectively. The highest and lowest strengths of FA substituted CPB mixtures prepared with acidic and basic process tailings were found at the same replacement rates (10 and 50%) as GBFS. The strength values (for all curing times) of 10% and 50% FA substituted backfills (OPC90@F10@H/L and OPC50@F50@H/L) were

between 0.09 and 0.44 MPa. When the results are examined, it is clearly seen that the strengths drop with the escalation of FA substitution in the backfill. This phenomenon can be explained by the inability of FA to react with portlandite (Ca(OH)2) formed by means of hydration. The chemical composition of acidic tailings (e.g., high sulfate content) disrupts the hydration environment and prevents additives such as FA from exhibiting pozzolanic properties (Li et al., 2020c; Liu et al., 2019a). Previous studies highlight the necessity of long curing times to increase the FA-based CPB's strength. Besides, the strength increases in backfills prepared with different replacement ratios are directly related to the basic properties of the tailings. Therefore, backfill containing high pH waste have greater strength development than backfills containing low pH tailings.

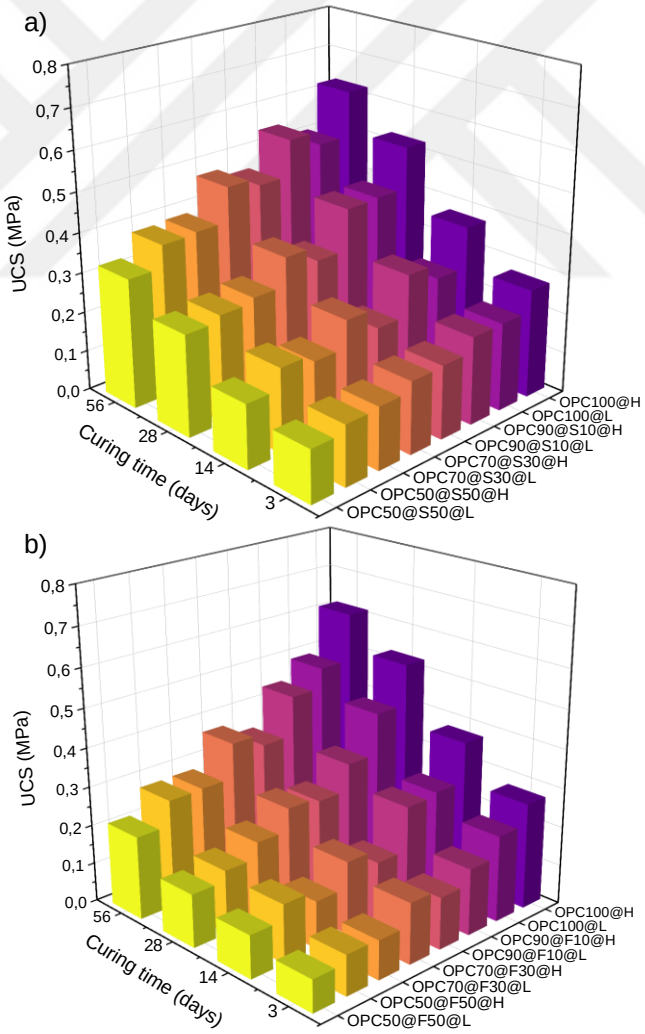


Figure 21. Fill strengths with time and OPC/GBFS (a), and OPC/FA (b)

The strength of cementitious materials (e.g., CPB/concrete) rises depending on the binder ratio. In addition, additives like slag/fly ash significantly reduce the strength of early aged backfills (Li et al., 2021b). These decreases in strength are related to the decrease in the amount of cement thanks to the additive usage instead of OPC in the fill, and corresponding growth in the rate of w/c. Compared to OPC, lower pozzolanic properties of mineral additives also reduce the strengths (Behera et al., 2021). In addition, the decrease in the strength of the backfills may be due to the creation of smaller volumes of hydration material by mineral additives containing lower CaO (calcium oxide) compared to OPC. Within the scope of the study, the lowest strength values were observed from CPB samples containing FA. This is related to the low water adsorbing property of fly ash. Because this feature increases the w/c content and delays hydration reactions (Cavusoglu et al., 2021a). In addition, the smaller particle size of fly ash compared to OPC (Table 11) supports this result. The use of bigger granulated additives (e.g., sand) in the backfill positively affects strength development (Zhou et al., 2020; Xue et al., 2021b). The alkalinity environment of filling samples with acidic and basic process tailings is the main reason for the strength differences. Basic tailings increase the pH of the backfill medium, support cement hydration reactions, and cause more hydration products to form (He et al., 2021). Especially in long curing times, both GBFS and FA additives increase the sulfate resistance of the backfills and support strength development. Aldhafeeri et al (2017) quantified that the engagement of sulfate (SO_4^{-2}) by C-S-H gels has reduced fill quality and performance. In addition, it has been emphasized completely in previous studies that the early age strength values decrease with the increase in the replacement rates of mineral additives used in cement-based mixtures such as CPB specimens (Li et al., 2019a; Huang et al., 2021a; Li et al., 2022).

3.1.2. Dam Tailings Effect on Filling Strength

Figure 21 shows stability evolution of CPB samples prepared and cured based on Table 15. The strength of the CPB samples reached high values in the first 28 days. This is an indication that cement promotes hydration reactions by growing the basicity of CPB environment (Li et al., 2021a; Xue et al., 2022). The high formation of portlandite ($Ca(OH)_2$), especially at early ages, is an important reason for the growth

in backfill stability. Furthermore, increasing amount of CaO (depending on the curing time) nullified the acid environs instigated by dam tailings and increased fills' strength. The strength of the CPB-HPPT (control) sample was 73.1% higher at the 28-day cure age compared to the 3-day cure age. For samples containing dam tailings (CPB-LPDT-1, CPB-LPDT-2, CPB-LPDT-3, CPB-HPDT-1, and CPB-HPDT-2), these values vary between 29.9% and 66.1%. However, the strengths of the samples containing dam tailings were between 20.2% and 73.1% compared to the control sample. Based on the 28-day curing time, the maximum strength (0.43 MPa) was found in the CPB-LPDT-1 sample and the minimum strength (0.17) in the CPB-HPDT-2 sample (excluding the control sample).

Strength gains were observed in all backfill samples after 28-day curing age. However, the stabilities of CPB-LPDT-1 and CPB-LPDT-2 specimens started to drop after 28-day of curing. The strengths of the 56 days cured CPB-LPDT-1 and CPB-LPDT-2 specimens were reduced by 20.1% and 13.2%, respectively, compared to the 28-day curing age. This can be enlightened by the detail that the high amount of pyrite in dam tailings undergoes oxidation and increases acid formation. The hydration evolution of CPB-LPDT-1 and CPB-LPDT-2 specimens containing a high percentage of low pH (acidic) dam effluent is complex. Especially in the long term, the decrease in the pH values of the fill medium (rise in the sulfate concentration) slows down the rate of cement hydration reactions, causing acid production and spoiling the hydration products. In addition, the decrease in pH values causes the suspension of portlandite ($Ca(OH)_2$) and the destruction of C-S-H gels (Dong et al., 2019a). This situation increases the porosity in the backfill and causes a corrosive structure (Galvão et al., 2018; Dashti et al., 2020). The suspension of portlandite minerals increases the permeability and adversely affects the quality and performance of the fillings (Li et al., 2020d). Durability of CPB-HPPT (control) sample was 19.1% higher at the 56-day curing age in comparison with the 28-day curing age. Additionally, the strengths of CPB-LPH-1, CPB-LPH-2, CPB-LPH-3, CPB-HPH-1, and CPB-HPH-2 samples were 20.9% to 73.1% lower at the same curing time compared to the CPB-HPPT specimen being cured for 56 days. CPB-HPH-2 entailed the maximum strength (0.53 MPa) after the CPB-HPPT specimen, although CPB-LPH-1 entailed the minimum strength (0.13 MPa).

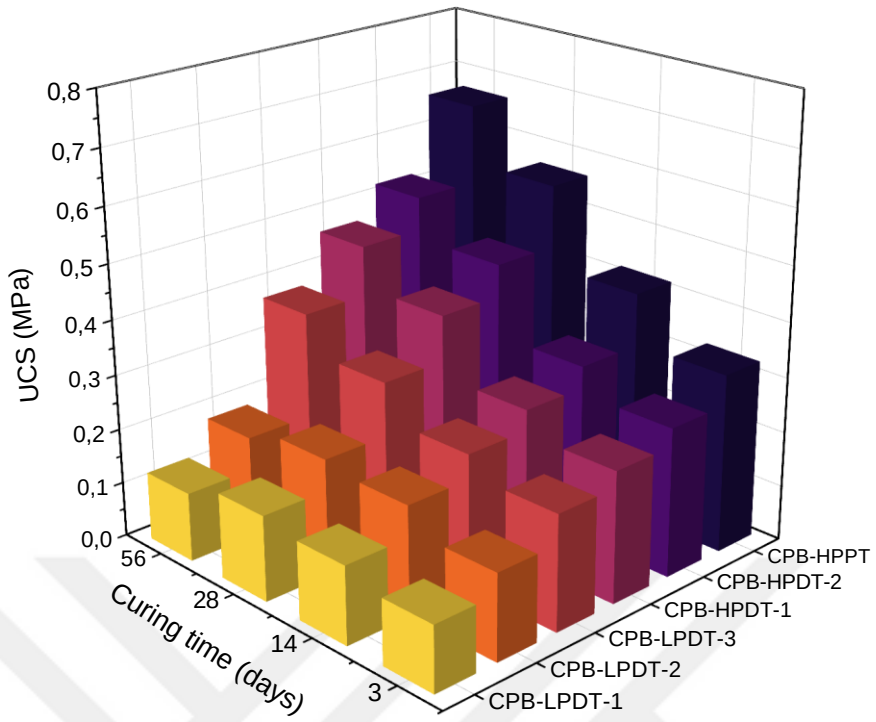


Figure 22. Plots of acidic and basic dam tailings-based filling's stability with time

Durability of CPB-LPDT-3, CPB-HPDT-1, CPB-HPDT-2, and CPB-HPPT samples cured for 56-day was not influenced much, although fills' pH value decreased due to high pH (basic) tailings content. Moreover, lessening in durability within CPB-LPH-1 and CPB-LPH-2 specimens cured for 56-day is directly due to the low pH (pH: 5.4 and 6.2, respectively) nature of dam tailings. This is the reason for the acidification of the backfill medium and the formation of a corrosive structure. In addition, acidic dam tailings accelerate the formation of erosion by decreasing the alkalinity of the samples during long curing periods. Decrease in fills' pH creates harmful environs for hydration reactions, causing the worsening of fill's main products. Also, it can be predicted that as the curing time progresses, the hydration rate will gradually slow down, the hydration materials will be depleted and the backfills will experience serious strength losses. Previous studies have shown that differences in pH values of tailings significantly affect the strength of backfills (Li and Fall, 2016; Dashti et al., 2020; Jiang et al., 2020c; Yang et al., 2020c).

Sulfate (SO_4^{-2}) reactions trigger the creation of expanding minerals such as ettringite/gypsum. Two different SO_4^{-2} reactions have been mentioned in the literature. The first one is that SO_4^{-2} ions react with C_3A to create ettringite crystals, and the other

is that they react with portlandite ($Ca(OH)_2$) to support gypsum's formation (Li and Fall, 2016; Fall and Pokharel, 2010). The ettringite and gypsum formed because of these reactions directly affect the CPB strength. The increase in CPB strength occurs because of filling the empty pores with expanding minerals. Decreased CPB strength is associated with the formation of microcracks because of mineral overgrowth and filling of capillaries (Pokharel and Fall, 2013; Li et al., 2022). Benzaazoua et al. (2004) emphasized that expanding minerals reduce the filling performance at low sulfate concentrations (<8000 ppm) but increase the filling power (especially at early ages) at high sulfate concentrations (>8000 ppm).

Figure 22 shows the durability of filling samples prepared using the values given in Table 16. Strengths of all CPBs (CPB-D1, CPB-D2, CPB-D3, and CPB-P) amplified in the initial 28 days. However, the strength of the 56-day CPB-D1 sample was 4.1% lower compared to the 28-day curing time. Similarly, CPB-D3, CPB-P, and CPB-D2 samples were 20.1%, 10.9%, and 5.3% higher, respectively. Among all samples, CPB-P had a maximum strength value (0.591 MPa), while CPB-D1 had a minimum strength value (0.231 MPa). Compared to the control sample (CPB-P), the CPB-D1 sample had lower strength values between 54.9% and 61.7% at all curing times. These values range from 41.8% to 48.4% for CPB-D2. Differences in the strength of fill specimens can be enlightened by the influence of dam tailings on hydration reactions. The increase in CaO (calcium oxide) concentration because of the development of hydration in the early curing times neutralized the dam tailings and increased the CPB strength. As mentioned before, the properties of acidic and basic dam tailings are extremely important factors affecting CPB strength. This issue has been discussed in many studies with its different aspects (Yilmaz et al., 2012; Dong et al., 2019b; Li et al., 2019b).

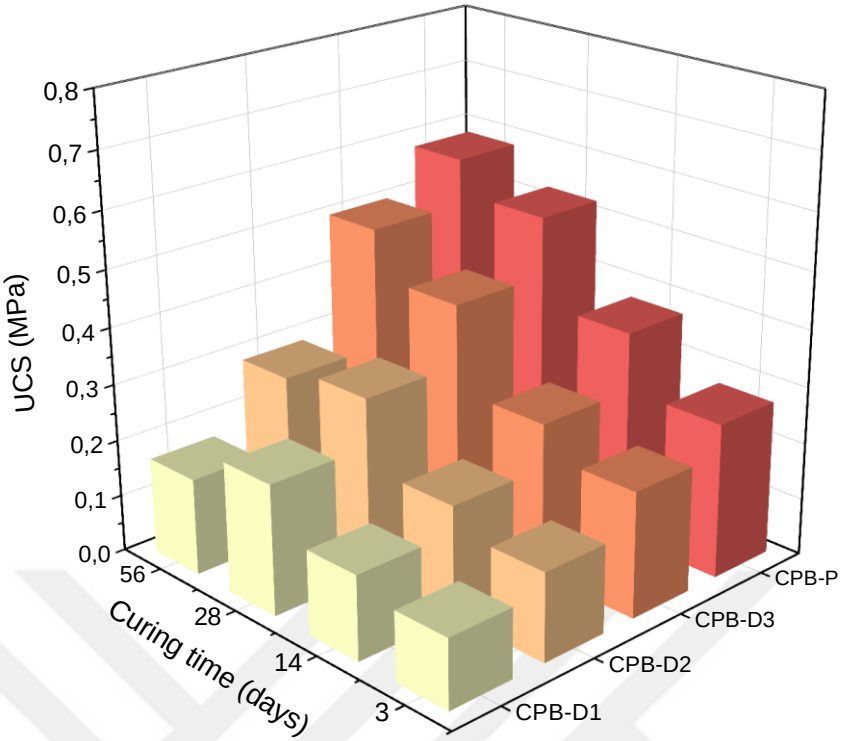


Figure 23. Plot of different fillings' strength values with curing time

3.1.3. Dam Tailings Effect on Stress-Strain and Elasticity of Filling

Figure 23 shows relationship between stress and strain for 28-/56-day cured backfills prepared using the values given in Table 16. In general, stress and strain curves are evaluated at 4 diverse stages: i) pore compression, ii) elastic-deformation, iii) plastic deformation/flow, and iv) rupture/fracture. In stage one (pore compaction), the voids of the backfill samples started to close with the first application of load. The result was a bowl-shaped curve. In the elastic deformation stage (second stage), the compressive stresses spread evenly over the surface area of the sample and the curve proceeded in a straight line, forming micro-sized cracks. In the third stage (plastic deformation/flow), the elastic deformations that the sample was exposed to turned into plastic ones and widened the gaps and cracks. Besides, at this stage, the plot extended peak (extreme) forces. The peak strengths/slopes were observed in CPB-P (control) sample compared to the other samples. Similarly, these values were the smallest in CPB-D1 specimen. In the last stage (rupturing), stresses lasted to be implemented to sample and the stress began to decrease. All fill specimens entailed the strengths lasted after rupturing had occurred. The greatest brittleness (low strain) was observed in the CPB-P (control) and CPB-D3 sample. In addition, CPB-D1 and CPB-D2 specimens

displayed more ductile property (high strain) compared to other samples. This phenomenon could be enlightened by acidic (low pH) environment of the CPB-D1 and CPB-D2 specimens. Similar stress and strain curves were also established in many preceding works (Xue et al., 2022; Yan et al., 2020a). It can be seen from Figure 23 that 56-day fillings reach higher peak values compared to 28-day cured backfills and also have higher residual resistances.

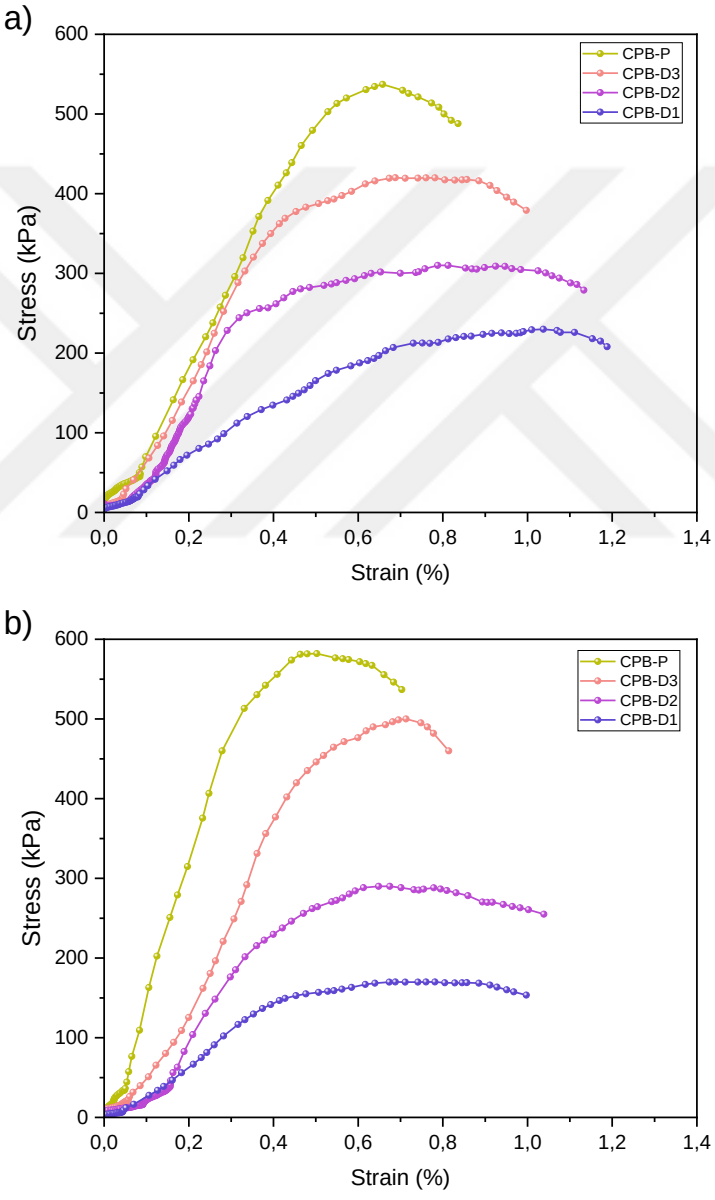


Figure 24. Stress-strain plots of fills cured at 28 (a) and 56 (b) days

Elastic modulus is very critical factor in determining fill's elastic deformation resistance. This parameter is used to determine the strength and bearing capacity of the embankments placed underground. The ASTM D3148 standard proposes three different methods for determining the elastic modulus. These are E50 (mean modulus), Emax (tangent modulus), and Es (secant modulus). The E50 value (corresponding to 50% of the shear stress) is generally used for the smooth completion of the service life of geotechnical structures such as backfills (Wu et al., 2016). The mean modulus (E50) found from the stress-strain curves was used. Figure 24 displays the link between E50 values and curing age for different filling specimens. Generally, the E50 values of the backfills vary between 10 and 80 MPa in early curing times and between 20 and 110 MPa in advanced curing times. The values found are consistent with previous studies (Yan et al., 2020a; Liu and Fall, 2022).

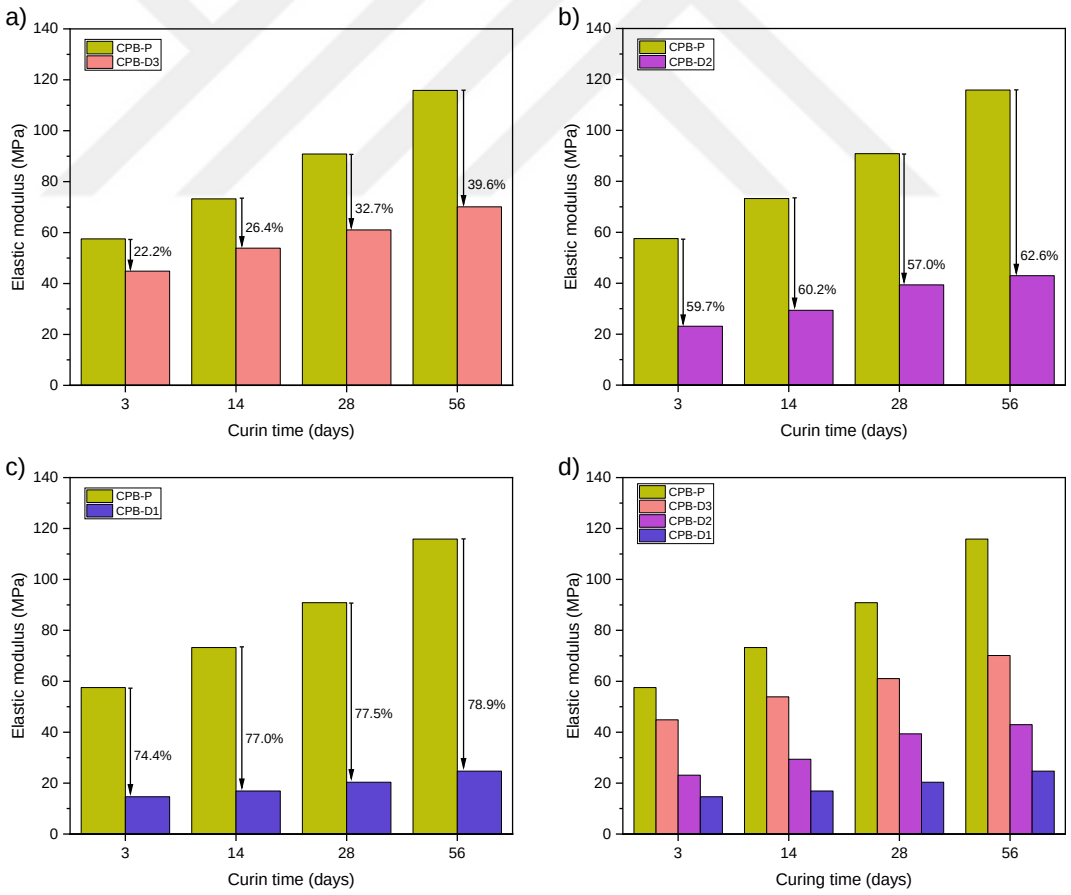


Figure 25. Plots of different fills' elastic modulus with curing age

The modulus of the elasticity obtained from filling specimens fluctuates with curing age, depending on the hydration reactions of the cement involved. Especially with the progress of curing age, increase in hydration materials filling the pores of the backfill increases the elastic modulus (Zhou et al., 2021). This situation hardens the backfill samples, triggering a more brittle material formation. This is the main motive why CPB-P (witness) specimen achieved high E50 values in comparison with other specimens. E50 values of the CPB-D1, CPB-D2, and CPB-D3 specimens containing acidic dam tailings were between 21.9% and 79.1% lower than the control sample. The reason behind these strength decreases can be explained by the effect of corrosion on the samples after 28 days of curing. Corrosion (decrease in pH values) in CPB samples significantly affects the elastic modulus (Wang et al., 2020b). In addition, this increases the amount of corrosive ions (which affect CPB hardness) by damaging the hydration products. Additionally, the acidification of the backfilling medium (low pH values/high sulfate concentration) increases the presence of expanding minerals such as ettringite, leading to crack formation. This is a factor that significantly reduces the elastic modulus of backfilling. As mentioned before, the damage to the structural integrity of the backfills in the long term is completely related to the acidic properties of the tailings. Acidic dam tailings damage the hydration products of the backfills, causing sulfate attacks and corrosion. As a result, dam tailings significantly affect the performance of paste backfills, especially the elastic modulus.

3.2. Determining the Geotechnical Index Parameters of Filling

3.2.1. Water Content's Evaluation

Factors such as water content_w, specific surface_Ss, saturation degree_Sr, and void ratio_e govern fills' characteristic properties. Both cement ratio and water content of cementitious mixtures (e.g., CPB) significantly affect the curing time (Skrzypkowski, 2021). Especially in backfills, water content is an important parameter and generally decreases with increasing curing age. Figure 25 displays the variation in fills' water content with curing age. Fills' water content (based on Table 16) varies between 7.04% and 21.1%. The highest water content was witnessed within 3-day cured CPB-D1 specimen, and the lowest water content was witnessed within 56-day

cured CPB-P (control) specimen. In addition, w values of CPB samples cured for 56 days decreased between 21.1% and 51.9% compared to those cured for 3 days. The w values of CPB-D1 and CPB-D2 specimens cured for 56 days increased between 2.21% and 5.01% compared to those cured for 28 days. Generally, drops in w values are the proof that the fill's hydration process is healthy. This is one of the main reasons for the strength gains in CPB samples. In addition, the amount of free water required for the hydration reactions taking place in the backfills is a factor that directly governs the final water amount (Saedi, 2021).

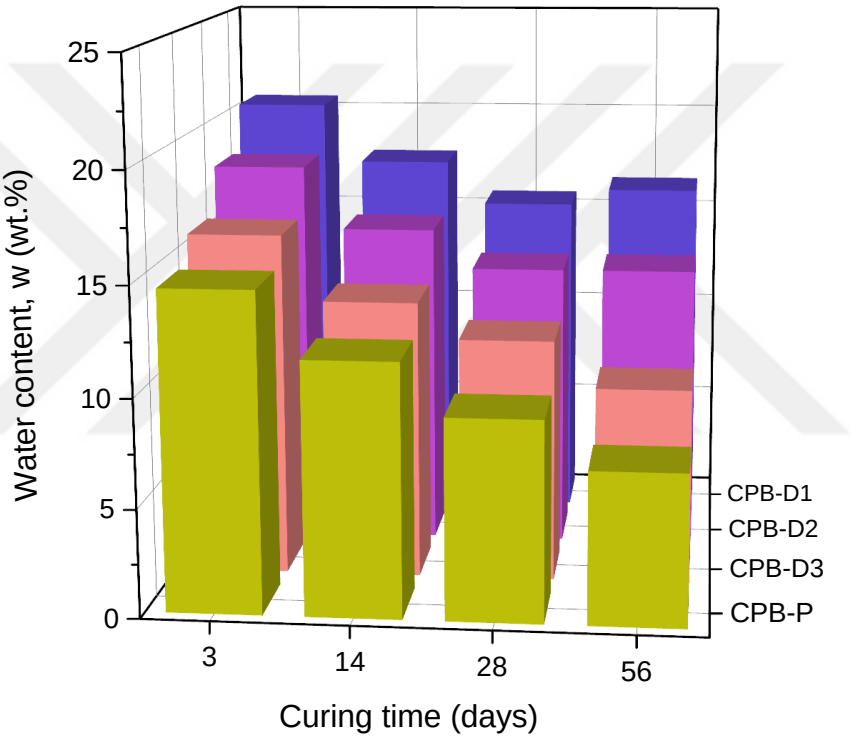


Figure 26. Plots of different fills' water content with curing age

The water employed in filling mixtures has 2 purposes: initiating the hydration reactions and increasing the workability. The drainage of pore waters in the CPB over time increases the strengths by decreasing the void ratio (Cao et al., 2019c). In addition, drainage of water in pore waters supports hydration reactions (Zhao et al., 2020). This ensures that the CPB pores are filled with hydration products and contributes to the hardening process (Akkaya et al., 2021). In general, it is estimated that water can be dropped by increasing curing time, but the opposite occurred in the 56-day CPB-D1 and CPB-D2 specimens. The reason behind this phenomenon could

be elucidated by acidic (low pH) environment formed in comparison with other specimens (Cao et al., 2019b). In CPB-D1 and CPB-D2 specimens containing acidic dam tailings, the pH decrease that occurs depending on time creates an acidic environment and damages the hydration reactions in the backfill. This causes extra water that is not involved in contributing to the hydration reactions to fill the backfill gaps. Excess water evaporates in the filling over time, increasing the formation of voids and suggestively dropping the backfill strength. Consequently, although water content is an important parameter for CPB samples, it should be kept under control.

3.2.2. Void Ratio's Evaluation

Figure 26 shows the void ratio_e as a function of time. The e values decreased significantly with growing curing age. The e values of CPB specimens ranged from 0.50 to 0.88. In addition, the e values of the 56-day CPB specimens reduced between 2.29% and 26.1% in comparison with the 3-day cure age. The highest e value (0.88) was viewed within CPB-D1 specimen, although the lowest e value (0.50) was viewed within CPB-P (control) specimen. One of most important parameters affecting the hardening process in backfills is the total void ratio. The reduction in void ratios can result in significant increases in water drainage and CPB density. This supports the development of the hydration-reaction and causes the products to cover the CPB pores, significantly reducing e values (Yan et al., 2021). CPB-D1 and CPB-D2 samples were the opposite, but e values were significantly decreased in other samples. Compared to the generally 56 days curing time, e values for the 3-day CPB-D3 and control samples were reduced by 21.1% and 26.2%, respectively. Similarly, e-values of CPB-D1 and CPB-D2 specimens diminished by 2.29% and 5.91%, respectively.

Void ratio is prominently enlarged by the vaporization of surplus mixing water that does not enter the hydration reaction (Ke et al., 2016). This is especially common in CPB samples with an acidic (low pH) environment. The reduction in pHs of CPB-D1 and CPB-D2 specimens containing acidic dam tailings with the progression of the curing time increases the e values by preventing the formation of hydration products (Qiu et al., 2020). In addition, there is an important relationship between the particle size of the materials that make up the backfill mixture and the void ratio.

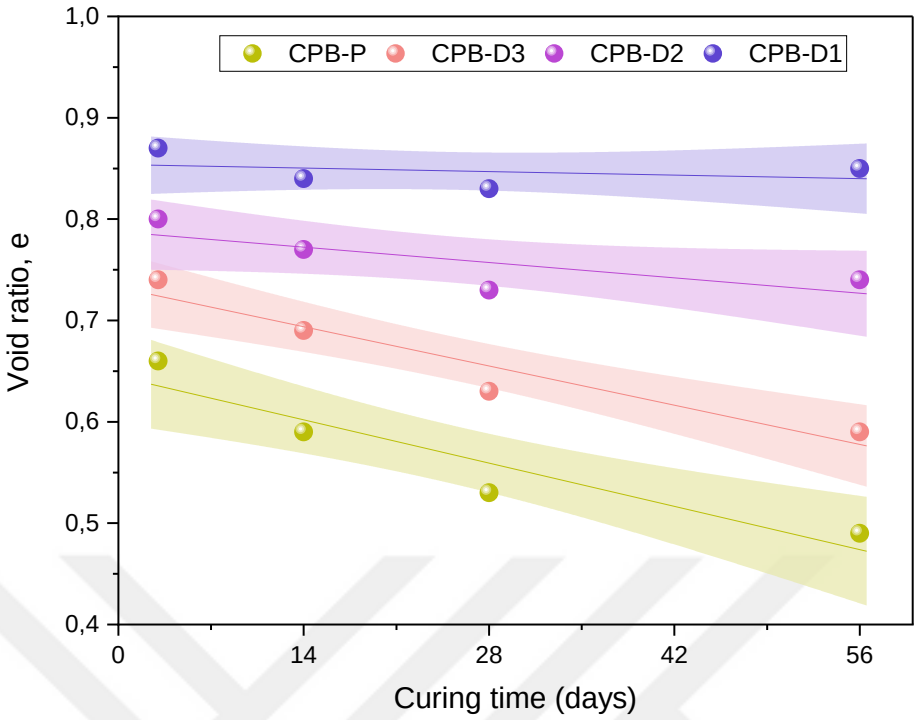


Figure 27. Plots of different fills' void ratio with curing age

The excess of fine particles in CPB will push the coarse particles and increase the need for mixing water to fill the inter-granular spaces. As a result, lack of necessary water for the hydration-reactions and/or the incidence of acidic-water in the backfill will rise the void ratios involved (Huang et al., 2021b; Zheng et al., 2016). Especially since dam tailings with low pH are corrosive, the thinning of grain sizes triggers this situation. The e values of the 56-day cured CPB-D1 and CPB-D2 specimens increased by 2.39% and 1.30%, respectively, compared to 28 days, reaching the highest void ratios. In addition, the basic nature of CPB-P (control) and CPB-D3 samples supported hydration reactions, causing a decrease in e values.

3.2.3. Specific Surface's Evaluation

Specific surface Ss is one of the central factors influencing fills' performance. Figure 27 shows the Ss values of fills changing with curing age. Specific surface areas of fills increase in proportion to curing age. Fills' Ss values ranged from 4.12 to 12.2 m^2/g. The highest Ss value was viewed in the 56-day cured CPB-P (control) sample, while the lowest Ss value was viewed in the 3-day cured CPB-D1 sample. In addition, while fills' Ss values increased in the first 28 days, only the Ss value of the CPB-D1

sample decreased by 1.31%. Ss is generally connected to fills' grain size and micro-structure, but it also has the function of determining the reactivity of the samples (Ke et al., 2016).

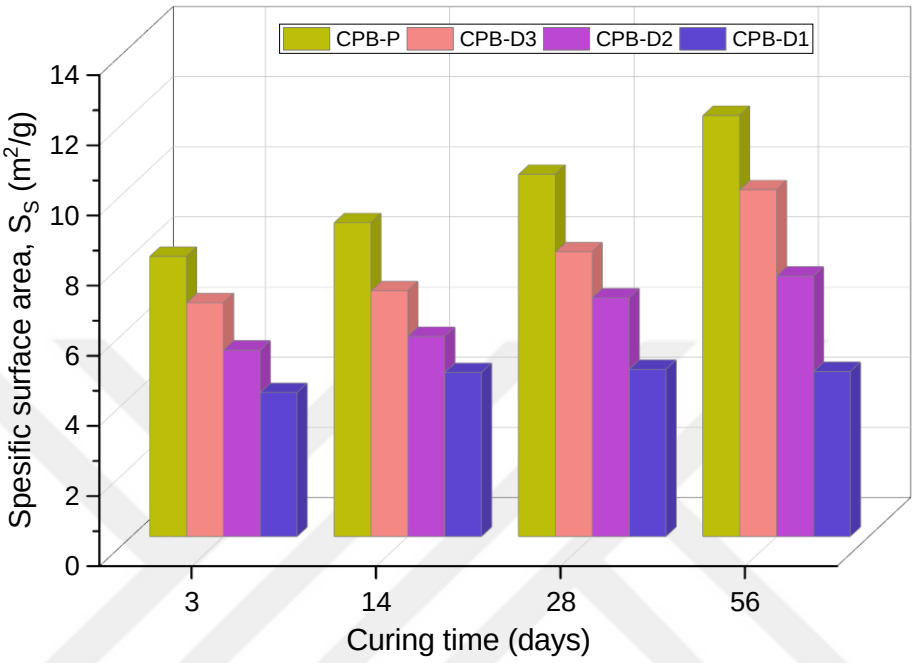


Figure 28. Plots of different fills' specific surfaces with curing age

It is a known fact that coarse-grained fills provide smaller specific surface areas compared to fine-grained ones. As a result of larger Ss values, the amount of surface to be cemented increases. This situation increases the amount of hydration materials that will fill the CPB voids, ensuing in a drop in free water's amount and an increase in filling performance. (Qiu et al., 2020). In addition, with the increase of Ss, the fill's density increases, gaps between the coarse grains in the backfill are filled and a tighter (compact) structure is formed. Consequently, the fill density increases subsidize the performance of fill (Huang et al., 2021a). However, the differences in the surface area of the backfills are sometimes complicated. In other words, backfills with lower Ss values are expected to show higher reactivity, but backfills with higher Ss values show higher reactivity due to their high water holding (Erguler et al., 2014). In addition, the backfill surface area is significantly affected by the oxygen diffusion and oxidation rate. Growing the Ss value causes the medium's acidification by increasing the degree of liberation of detrimental phases like sulfate (Koohestani et al., 2018). Similarly, the

acidification of the environment (lower pH) and the presence of sulfate minerals rise the Ss values of backfilling (Parbhakar-Fox et al., 2013).

3.2.4. Saturation Degree's Evaluation

Figure 28 shows changes in the degree of saturation (Sr) of filling specimens changing with curing age. As cure age increases, the saturation degrees of samples decrease. The reductions in Sr values of CPB-D1, CPB-D2, CPB-D3, and CPB-P (control) specimens that reached 56 days curing age in comparison with 3-day cure age were 16.9%, 19.1%, 26.8%, and 32.9%, respectively. The decrease in the saturation degrees of the samples or the water consumption indicates that the cement hydration process is healthy. Sr is significantly governed by the drainage properties of CPB samples. Six-hole plastic containers used during sample preparation increase the drainage ability of the backfills, thereby reducing the degree of saturation over time. Decreases in Sr values increase the performance and quality of backfills (Libos and Cui, 2020). Water consumption, which occurs because of hydration reactions in backfills, causes great suction forces. These suction forces directly affect the pore structure of the backfills (Xu and Cao, 2018).

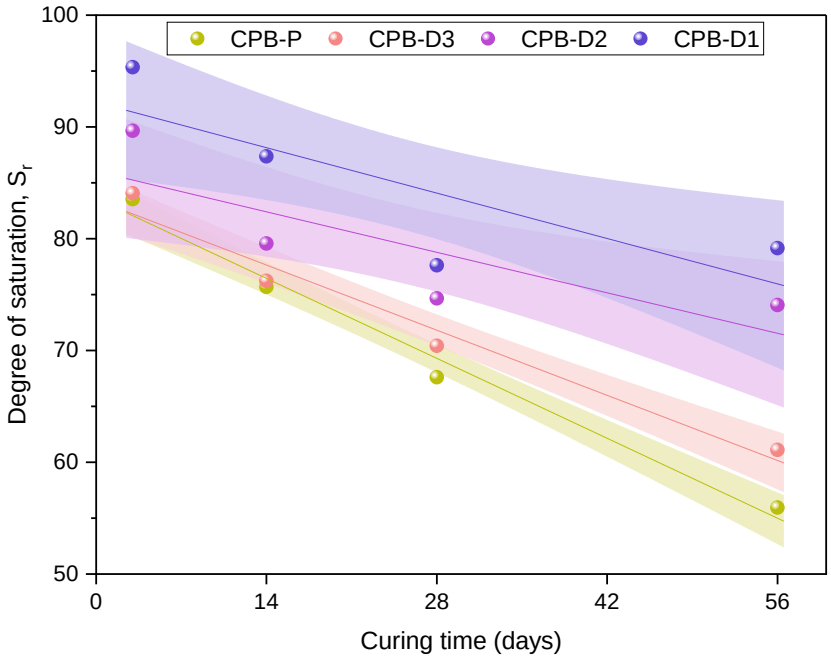


Figure 29. Plots of different fills' saturation degree with curing age

In fact, the rise in absorption force of backfilling strengthens the inter-granular bond, increasing the fracture resistance and strengths (Li et al., 2020a). The Sr values of all CPB samples ranged from 56.1% to 94.9%. In addition, the highest Sr value was viewed in the 3-day cured CPB-D1 specimen, while the lowest Sr value was viewed in the 56-day CPB-P (control) specimen. Saturation degrees of all samples decreased gradually during the first 56 days. However, after 28 days of curing, small increases of 2.01% and 0.91% were observed in the Sr values of the CPB-D1 and CPB-D2 specimens, respectively. Usually, first 28 days were wasted due to free-water hydration reactions in cavities of fillings specimens and the Sr values decreased.

However, the increases in CPB-D1 and CPB-D2 specimens can be explained by the oxidation of acidic dam tailings and damaging hydration products. Especially sulfide minerals (e.g., pyrite and pyrrhotite) mix with the pore waters of the backfills and cause great damage to C-S-H gels. Damage to hydration products leads to the fact that the water in the CPB is not consumed for hydration reactions (Li and Fall, 2016). This is one of the most important reasons that increase the degree of saturation in CPBs. In addition, high Sr values crystallize CPB hydration materials (Yin et al., 2020a). Excess water remaining in the backfills evaporates, increasing the formation of voids. This will eventually give rise to fills' stability and rigidity drops.

3.3. Chemical Analysis of Hardened Fills

Figures 29, 30 show the chemical analysis results of filling specimens created based on the recipe in Table 15. The main chemical minerals of the samples containing dam and process tailings are S/SO_4^{-2} (sulfur/sulfate), Ca (calcium), Si (silicon), K (potassium), Fe (iron), and Al (aluminum). Sulfate (Figure 29a), calcium (Figure 29b), and silicon (Figure 30) concentrations in CPB-LPDT-1 and CPB-LPDT-2 samples containing acidic dam tailings decreased for the first 28 days and then started to increase. The sulfate, calcium, and silicon concentrations of the CPB-LPDT-1 specimen diminished by 5.74%, 4.29%, and 12.2%, respectively, during the first 28 days of curing time. Afterward, 1.28%, 0.51%, and 4.75% increases were observed up to 56 days of curing age. Similarly, the sulfate, calcium, and silicon values of the CPB-LPDT-2 specimen reduced by 4.39%, 6.32%, and 7.71%, respectively, and enlarged by 0.29%, 0.13%, and 0.30%, respectively. The main reason for the changes in these

samples containing acidic tailings can be clarified by the detail that binder increases the alkalinity (pH value) of the CPB medium. This situation starts with the suspension of the calcium mineral (drop in the amount of calcium) until the curing period of 28 days. With the suspension of the Ca mineral, hydration reactions begin, and the pH of the backfill medium rise, neutralizing the acidity caused by pyritic tailings (Yin et al., 2020b). Reduction in sulfate, calcium, and silicon minerals is directly related to neutralization. After 28 days of curing, the pH decrease in the CPB-LPDT-1 and CPB-LPDT-2 specimens increases the amount of sulfate and leads to a weakening in the structure of chemical bonds (Benzaazoua et al., 2006).

In acidic environments (with low pH), the sulfur mineral is found in the creation of sulfate, and the amount of sulfate increases in direct proportion with the decrease in pH in CPB mixtures. In addition, at low pH, sulfide minerals (e.g., pyrite and pyrrhotite) react in filling matrix, increasing the sulfate volume. This situation rises the acidity of fill medium and destabilizes the hydration reactions (Benzaazoua et al., 2008). Additionally, increased acidity/sulfate causes oxidation of CPB hydration products, reducing strengths. This is an indicator of the negative effect of sulfurous compounds such as sulfate on backfills and has been studied in detail in various works (Li and Fall, 2018; Yan et al., 2020b). Sulfate is one of the most destructive composites found in backfills and gives rise to a structural corrosion of filling. Sulfate ions harm the hydration materials, such as C-S-H, and trigger a condition identified as 'sulfate attack' (Tian and Fall, 2021). Sulfate attacks are mostly formed by the response of ettringite crystals, which are created by the effect of sulfate, with calcium aluminates (e.g., C_3A and C_4AF) in the backfill (Fall and Pokharel, 2010). The increased amount of ettringite as a result of the increase in sulfate minerals creates a layer when C_3A reacts with water. This layer prevents the cement hydration reactions in the CPB environment and causes less hydration product and lower absorption formation.

Deterioration of hydration materials is an indication that minerals such as calcium do not join in the reactions of cement hydration (Li et al., 2020b). This situation gives rise to a growth in calcium minerals in the backfill. In addition, sulfate outbreaks are one of the foremost causes of the augmented sulfate and silicon values in backfill samples (Dong et al., 2019a).

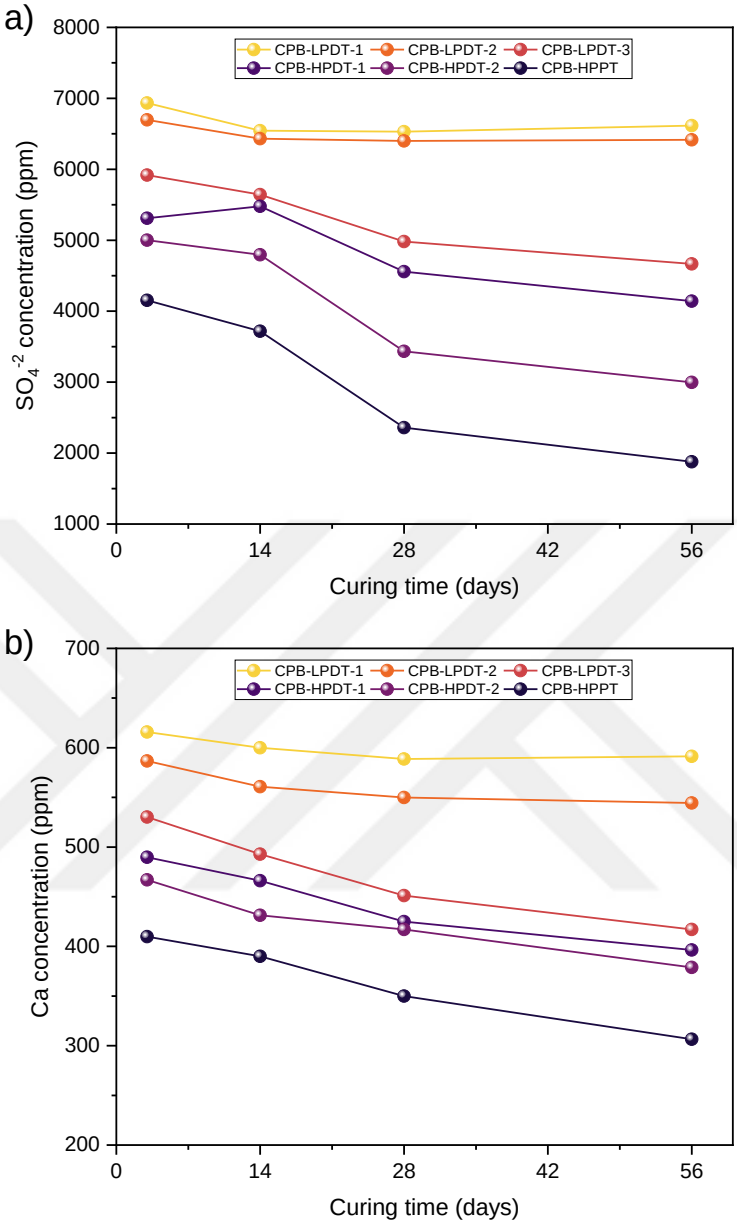


Figure 30. Plots of SO_4^{-2} (a) and Ca (b) values within filling with age

The sulfate, calcium, and silicon values in the CPB-LPDT-3, CPB-HPDT-1, CPB-HPDT-2, and CPB-HPPT specimens decreased in the range of 20.9% to 55.1%, 19.2% to 24.8%, and 15.1% to 17.2%, respectively. The principal reason for these decreases can be better explained by the acidic neutralization (basic environment) caused by the studied tailings. The lowest sulfate, calcium, and silicon values (1884, 312, and 24.3 ppm, respectively) were obtained from the 56-day-old CPB-HPPT sample. The highest values (6963, 622, and 54.1 ppm, respectively) were found in the

3-day CPB-LPDT-1 sample. Additionally, potassium (K) values were between 5.22 and 26.4 ppm, iron (Fe) values were between 1.87 and 3.31 ppm, and aluminum (Al) values were between 0.49 and 0.90 in all CPB samples (Figure 31 and Figure 32).

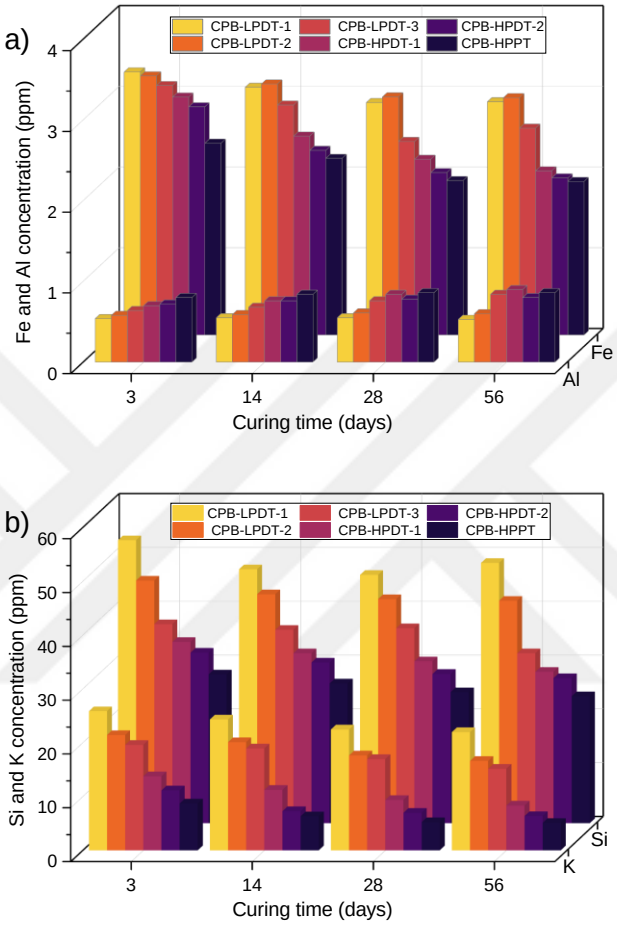


Figure 31. Plots of Fe-Al (a) and K-Si (b) values within filling with age

3.4. Filling Bleed Water's Geochemical Analysis

3.4.1. Evaluation of pH Change of CPB Samples with Additives

Figures 31 and 32 display pH change of the backfill samples covering GBFS, FA, and acidic/basic tailings over time (Table 14). Witness specimens (CPB100@L and CPB100@H) up to 28 days of curing had the highest pH values. Significant reductions were then observed in these samples up to the 56-day curing time. These decreases were determined as 5.83% and 3.24% for CPB100@L and CPB100@H specimens created with acidic/basic tailings, respectively. It is clearly seen that the pH

values of all backfill (with and without additives) containing low pH (acidic) tailings are near or below neutral at an early age (Figure 31 and Figure 32). The pH values of the backfills containing high pH (basic) tailings were generally above 8. This phenomenon seen in CPB samples is since basic tailings ease the hydration of cement. On the contrary, acidic tailings damage the cement hydration products and reduce the filling performance. Portlandite ($Ca(OH)_2$) formed as a result of hydration neutralizes acidification in CPB samples at an early age (up to 28 days). Moreover, the tendency of pH values of CPBs to decrease after 28 days is because sulfuric minerals (e.g., pyrite and chalcopyrite) decrease the alkalinity of the CPB medium by promoting acid production (Al-Moselly et al., 2022).

From Figure 31 and Figure 32, it was observed that elastic modulus EM, which represents fills' stiffness/deformation, progressively augmented at a lessening rate in the CPB100@L and CPB100@H (control) specimens. Nevertheless, akin to stability results in all backfills, EM also reached a maximum after 56-day. These values vary between 0.17 and 0.19 MPa for low/high pH fillers containing 10% GBFS. Similarly, EM values in the backfill samples containing 10% FA were between 0.14 and 0.17. A significant increase in EM values of GBFS and FA additive CPBs was grasped in comparison with control samples after 28 days of curing time. The reason behind this growth is due to the long-term pozzolanic characteristics of GBFS and FA additives. Compared to OPC, these additives (GBFS and FA) help support the hydration process by continuing to fill the voids in the filler medium with hydration products in the long run. The results clearly show that CPB samples lost more strength in low pH (acidic) media than in high pH (basic) media. While supplementary cementitious products such as GBFS and FA, which are employed in place of OPC, subsidized fill's long-term performance, the results obtained from different studies emphasize that these additives reduce the CPB strength (He et al., 2021; Li et al., 2019b). However, some studies indicate that there will be significant decreases in fill's strength over time, depending on the degree of acidic (low pH) environment (Wang et al., 2016; Zhao et al., 2022). Even when sulfate-resistant cement is used, low pH values are not sufficient to increase the backfill strength. Therefore, it is highly recommended to use pozzolanic additives such as GBFS and FA in CPB samples to prevent performance losses as well as to neutralize acidic tailings (Li et al., 2020c).

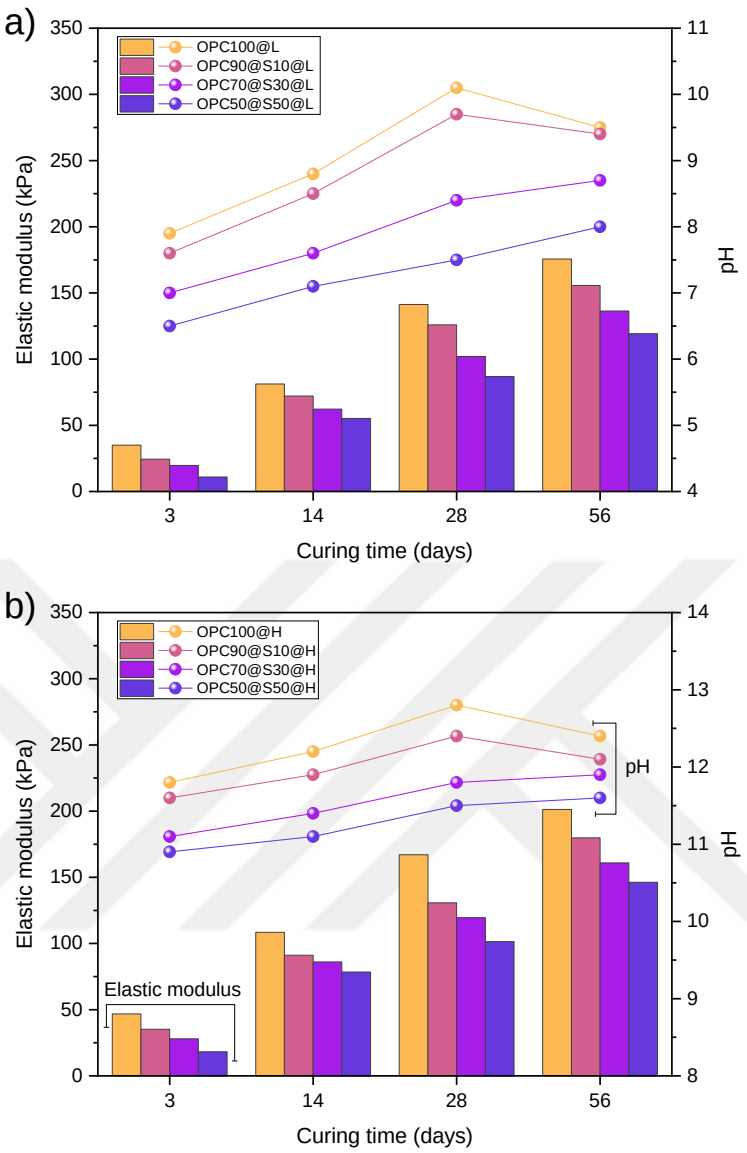


Figure 32. EM/pH in slag-based fills with age: (a) EM @ acidic tailings; (b) pH @ acidic tailings; (c) EM @ basic tailings; (d) pH @ basic tailings

Excess SO_4^{-2} (sulfate) ions in acidic tailings are captivated by C-S-H gels, triggering the formation of growing minerals (e.g., ettringite) that inhibit the hydration reaction. This causes the pores to expand and microcracks to form in the CPB. Acidic tailings used in this study contain more sulfate than basic wastes (5644<3945 mg/L). The low sulfate content of basic tailings reduces the negative effects on the backfills and provides better results. In addition, secondary minerals shaped at low SO_4^{-2} concentrations (≤5000 ppm) lessen the pore size of the fillings and avert O_2 access to cavities (Aldhafeeri and Guz, 2017).

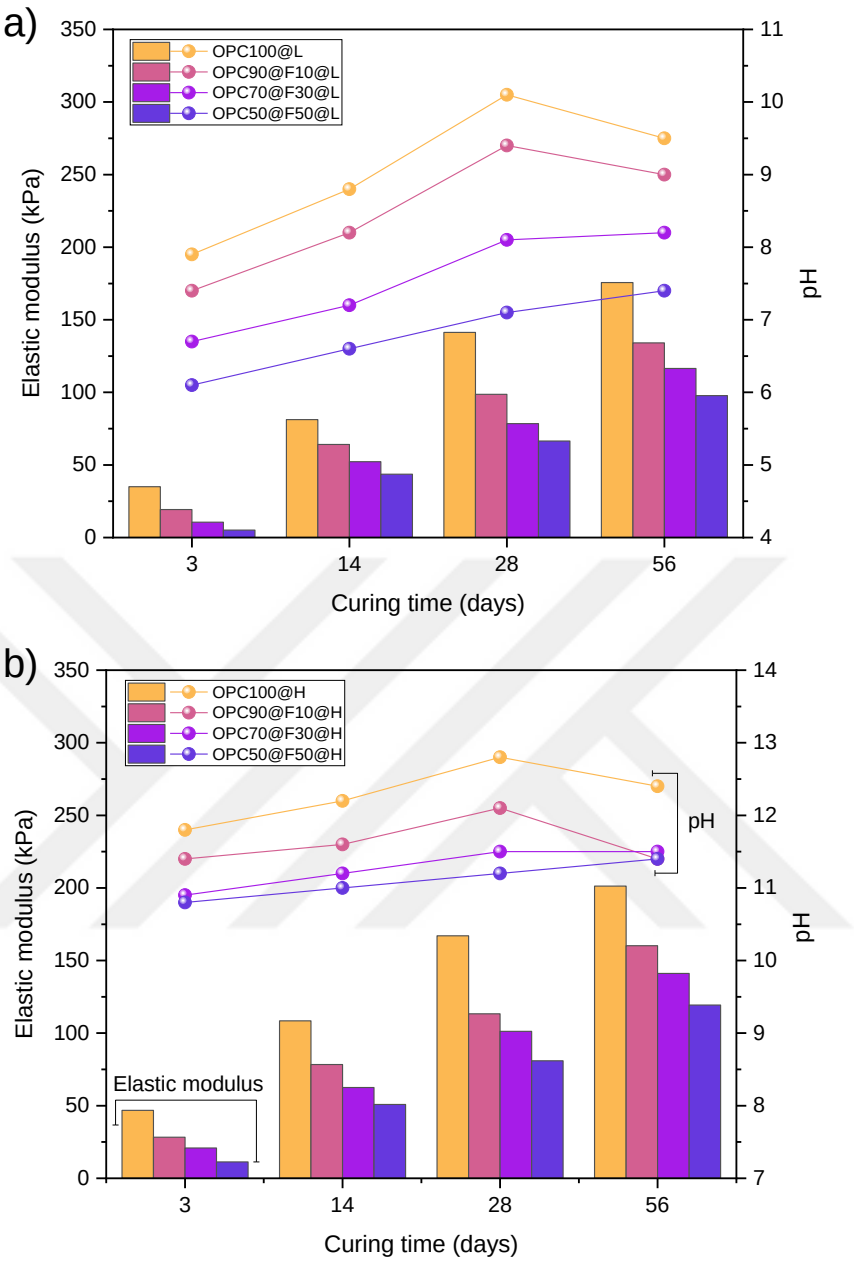


Figure 33. EM/pH in fly ash based fills with age: (a) EM @ acidic tailings; (b) pH @ acidic tailings; (c) EM @ basic tailings; (d) pH @ basic tailings

The main reason behind the poor performance of FA substituted filling specimens can be explicated by the fragmentation of the glass phases through activation of this mineral additive. This phenomenon explains the use of chemicals to activate FA additives (Qiu et al., 2019). The importance of pH values in backfill applications is an indisputable fact because tailings with different characteristics (e.g., chemical) occur during ore processing.

3.4.2. Assessment of pH Change of CPB Containing Dam Tailings

Figure 33 shows the pH variation of CPB samples prepared with dam and process tailings, depending on the curing age. pHs of CPB specimens augmented till the first 14 days of curing. However, after this curing period, serious decreases were experienced especially in the samples prepared with acidic dam tailings. The pH values of all samples increased between 25.1% and 33.9% in the first 14 days. Then, the pH values decreased between 10.5% and 23.1% until the curing period of 56 days. The pH change that occurs within CPB samples depending on the curing time generally develops because of pyrite's oxidation. It is also a function of the interaction between hydraulic cements and mineral tailings (Qi and Fourie, 2019). The binder blended to filling materials tends to raise the pH of the environment due to its high CaO content (Bois et al., 2005; Cihangir et al., 2018). This phenomenon can be explained by the reaction of SO_4^{-2} (sulfate) ions formed by the oxidation of pyrite minerals with $Ca(OH)_2$ (portlandite) to form an excess of gypsum (Li et al., 2021a). In addition, pH alterations in CPB samples (acidic or basic) directly influence the growth of calcite and ettringite crystals.

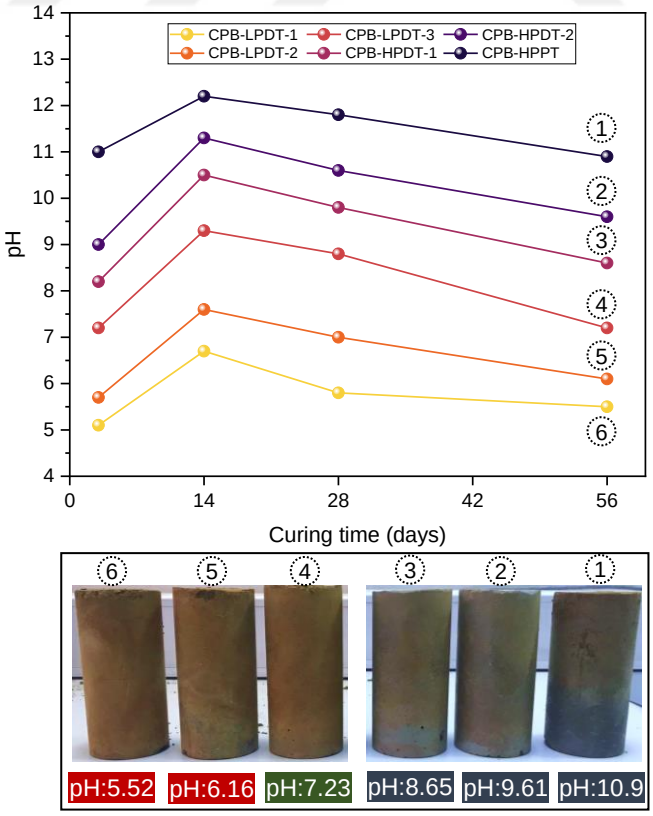


Figure 34. Plots of pH values observed within filling with age

High pH values (>10) promote the creation of an alkaline and/or alkaline environment, creating a favorable medium for the development of CPB hydration products (Galvão et al., 2018). But, low pHs (<10) leads to degradation/dissolution of the hydration materials, resulting in reduced backfill strengths and deterioration of structural integrity (He et al., 2019b). This phenomenon is clearly seen in CPB-LPDT-1 and CPB-LPDT-2 specimens. At the end of the 56 days curing period, the pH drops (5.52 and 6.16, respectively) of the samples led grave stability damages. The pH values of CPB-LPDT-3, CPB-HPDT-1, CPB-HPDT-2, and CPB-HPPT specimens were obtained as 7.23, 8.65, 9.61, and 10.9, respectively, during the 56-day curing period. Furthermore, the uppermost pH was gained from the CPB-HPPT sample in the 14-day curing period (pH: 12.16), while the lowest pH value was obtained from the CPB-LPDT1 sample in the 3-day curing period (pH: 5.52). One can interpret from Figure 33 that filling samples prepared with acidic dam tailings at 56 days have a brownish color because of oxidation. In addition, it is seen that the samples prepared with basic dam and process tailings have a gray color (non-oxidized layer) due to the absence of secondary minerals caused by pyrite oxidation.

3.4.3. Assessment of EC of CPB Containing Dam Tailings

Electrical conductivity (EC) is frequently used to determine the corrosion severity of cementitious materials (e.g., CPB and concrete) and to evaluate hydration reactions. It is also possible to obtain information about the porosity of cementitious materials by means of water permeability and/or ionic diffusion. The electrical conductivity can also be expressed as a ratio that determines the conductivity between the pore phases of the grains. Figure 34 shows the EC results of pore waters in the backfills. Fills' EC values decreased from 6.18% to 13.9% up to the 14-day curing time. Then it increased from 2.48% to 13.3% up to the 56-day curing time. The main reason behind these reductions is the damage of conductive ions in the resolution or the reduction in the total dissolved solids concentration (Canales et al., 2020). In general, excess ion quantity in the solution directly causes an increase in the EC values. However, the solubility of the filler hydration products is related to the number of ions (Li et al., 2021b).

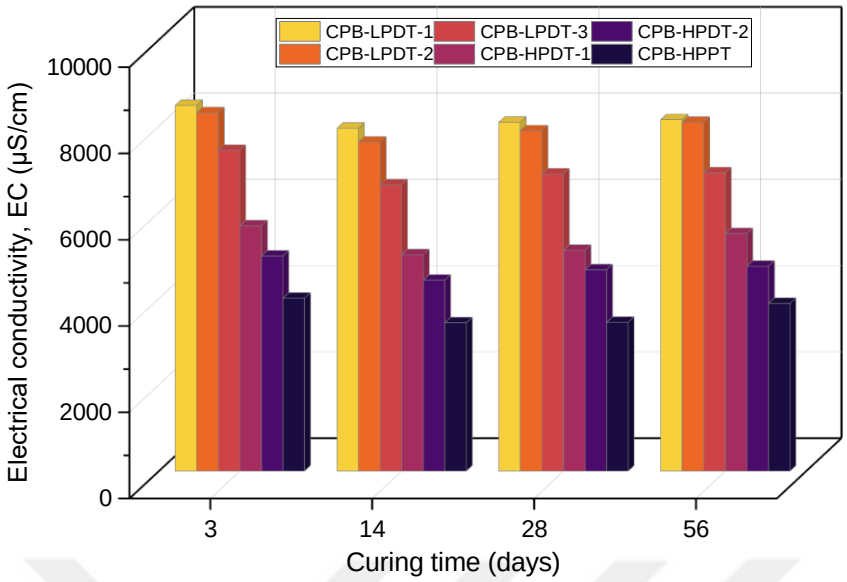


Figure 35. Plots of EC factor within filling with age

Especially in acidic environments (pH<10), the dissolution of hydration products causes an increase in electrical conductivity (Elghali et al., 2019a). Rises in pHs of filling after the initial 14 days decreases the electrical conductivity. This increases the strength of the CPB samples by providing a suitable environment for hydration. But, after the 14-day curing age, pH decreases in CPB medium increasing the electrical conductivity, causing deterioration of the hydration materials, and decreasing the strength values. These phenomena prove that CPB-LPDT-1 and CPB-LPDT-2 specimens with lower pH values achieve higher EC values. The 14-day CPB-HPPT sample reached the lowest EC value (8503 µS/cm), while the 3-day CPB-LPDT-1 sample reached the highest EC value (3455 µS/cm).

3.4.4. Analysis of Redox Potential of CPB Containing Dam Tailings

Eh (Redox potential) gives information about the oxidation and reduction degrees of the chemicals in the CPB. In addition, Eh is a factor that indicates the electron attraction of oxidized/reduced tailings grains relative to hydrogen. Figure 35(a) shows the Eh changes of filling specimens depending on cure age. Eh values of all CPB samples ranged from 0.41V to 0.63V. In addition, Eh in all specimens lessened up to the 14-day curing time but increased after this curing time. Eh values decreased in the range of 3.59-6.62% in the 14-day cure period compared to the 3-day cure period. However, a rise of 6.41-19.4% was observed in the 56-day cure age in

comparison with 14-day curing age. Eh of samples prepared with acidic dam tailings (CPB-LPDT-1, CPB-LPDT-2, and CPB-LPDT-3) were lower than samples prepared with basic tailings (CPB-HPDT-1, CPB-HPDT-2 and CPB-HPTT). In general, Eh is expected to rise in CPB samples as the degree of saturation (Sr) and water content (w) decrease. Furthermore, fills' acidic nature affects Eh values (Qi and Fourie, 2019). Figure 35(b) displays the relation between redox potential and pH. The detachment of minerals or the ion mobility in fill is usually controlled by temperature and hydrogen concentrations (Bussière, 2007; Beya et al., 2019). This highlights the importance of redox potential and pH change on CPB.

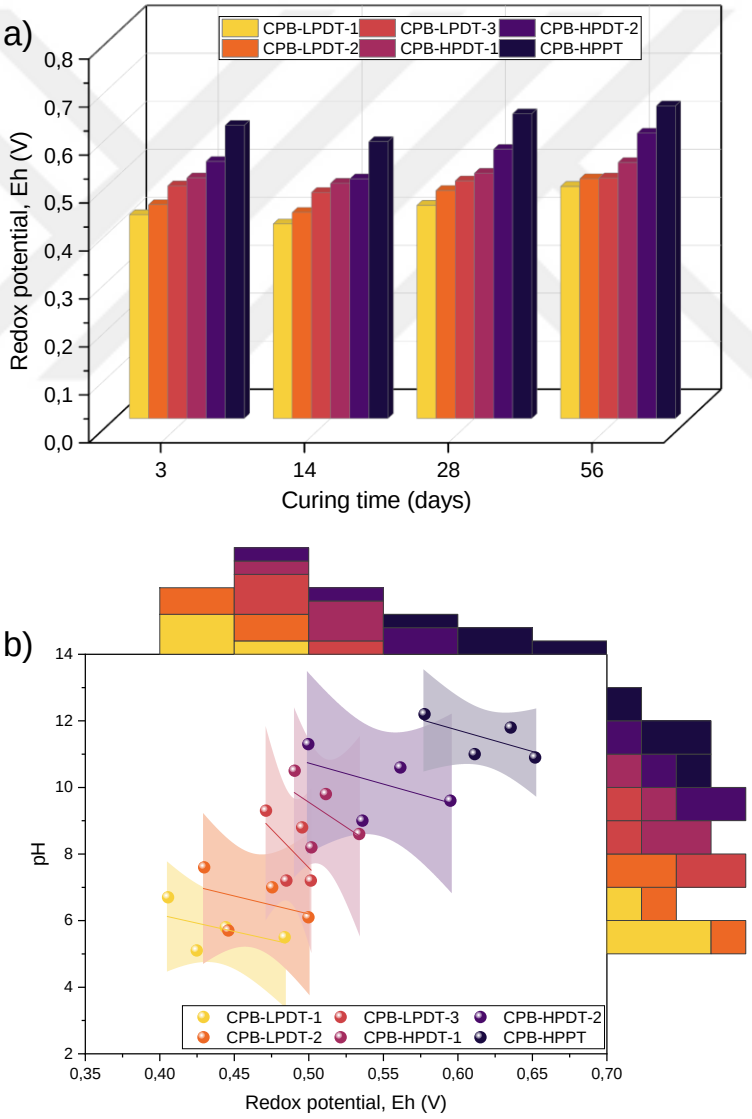


Figure 36. Plots of (a) Eh and (b) pH-Eh factors within filling with age

3.5. Microstructural Results

3.5.1. XRD Results

The quality/performance of cured CPB samples are considerably influenced by characteristics of cement hydration materials and chemical/mineralogical composition (Xiao et al., 2021b). XRD tests were applied to determine the performance and hydration products of paste backfill samples. Figure 36 shows XRD plots of 28-day CPB samples produced using the recipe in Table 14. One can interpret from Figure 36 that the most concentrated volume of hydration materials in CPBs is portlandite. While the portlandite density reached an extreme value of 7340 CPS (counts per sec.) within fill specimens covering low pH tailings, this value was 9450 CPS within fill specimens covering high pH tailings. The central motive for this alteration in portlandite density is that CPBs containing high pH tailings (basic) support the formation of more hydration products owing to their basic nature (Sun et al., 2022). In addition, different hydration materials such as C_3A, C_4AF, C_2S, and C_3S are clearly visible from the XRD charts. But these hydration products were less than portlandite. The volume of hydration products was highest in witness specimens (OPC100@L and OPC100@H) and deepest in FA substituted samples. For instance, density of portlandite at 3°-2θ for the OPC70@S30@L and OPC100@L samples was measured as 5890 and 6810 CPS, respectively. These changes in the peaks decrease due to the hydration reaction, which shows the effect of FA and GBFS additives on CPB (Li et al., 2022). The performance of paste backfills generally depends on the amount of hydration materials (e.g., C-S-H gels). Moreover, the presence of hydration materials within the CPB environment can typically be associated with the development of a basic (high pH) environment (Wang et al., 2020a).

To understand the effect of dam/process tailings on hydration products of CPB, XRD analyses were realized on CPB-HPPT, CPB-LDPT-1, and CPB-HPDT-2 specimens. Figure 37 displays that filling specimens cured at 56-days created large volumes of portlandite (CH or $Ca(OH)_2$), calcite ($CaCO_3$), C_2S/C_3S (calcium silicates), and Et (Ettringite). In addition, the CPB-LPDT-1 (lowest pH) sample achieved lower gypsum values compared to the CPB-HPPT (control) and CPB-HPDT-2 (highest pH) specimens. This phenomenon indicates that the basic medium (higher pH values) has

greater hydration development for filling samples. The excess formation of portlandite minerals in the basic environment supports the formation of gypsum, which accelerates the development of hydration. The formation of gypsum generally affects the strengths positively by supporting the hydration reactions of the backfills. It also contributes to the decrease of void ratio (porosity) and accelerates the fill's setting time. This is consistent with the XRD results of CPB samples prepared with basic (high pH) dam tailings, as could be viewed evidently in Figure 37.

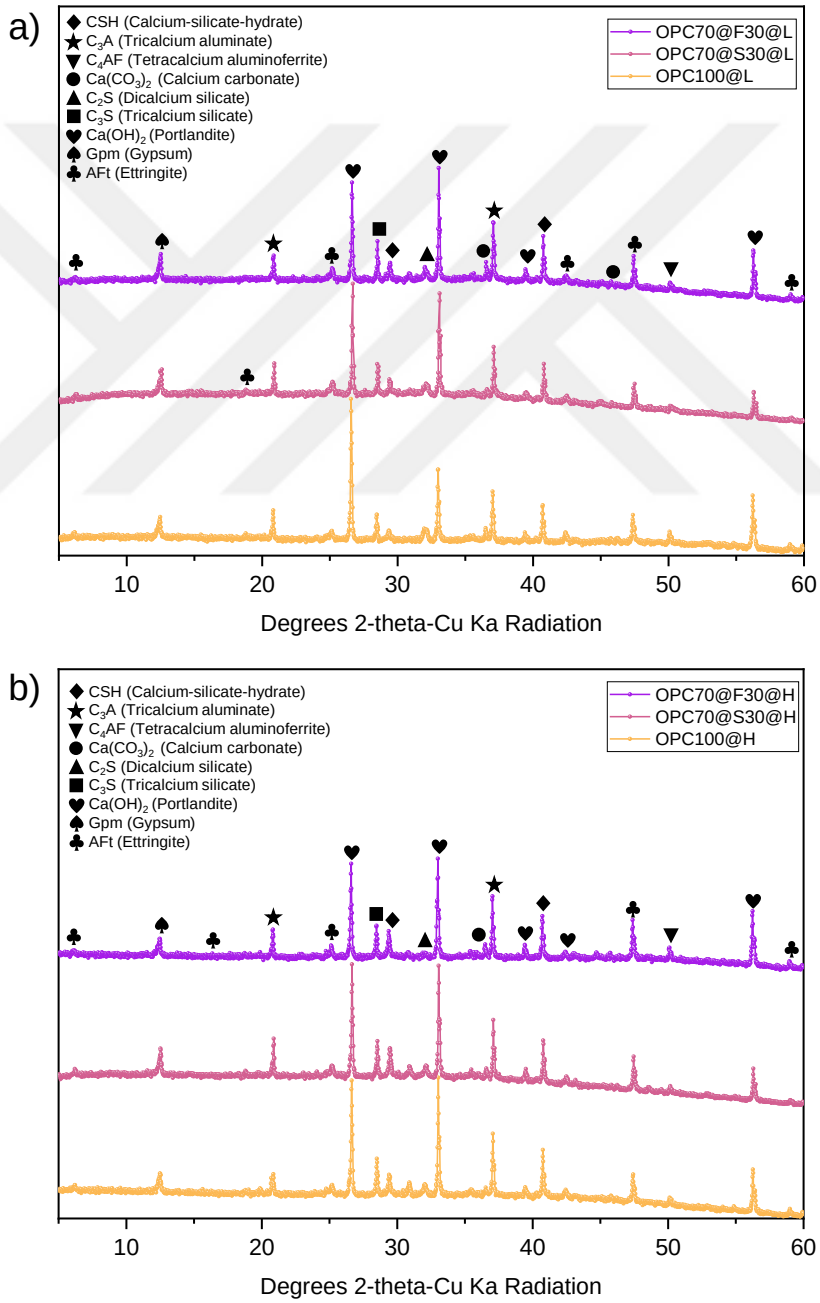


Figure 37. XRD profiles of acidic(a) and basic (b) based fills at 28 days

The relatively small volumes of gypsum/hydration materials created in CPB-LPDT-1 sample compared to other samples show inhibition of hydration. The small amount of gypsum formed because of the acidic (low pH) environment caused by the high sulfate content specifies that the expanded minerals in the backfill samples originated from ettringite. This is in line with earlier works (Aldhafeeri and Fall, 2017; Yan et al., 2020b). Especially in specimen of CPB-LPDT-1 (created with acidic dam tailings), a larger volume of ettringite crystals was found in comparison with others. Ettringite can be take consideration a vital parameter initiating the performance degradation of CPB samples. The presence of expanding minerals such as ettringite in the pores of acidic CPB samples is a direct cause of the formation of microcracks (Xue et al., 2022). In addition, this may cause physical harm to the fill medium by causing solidifying of microstructure. The harm physically rises with falling pH (increasing acidity) values in the CPB matrix.

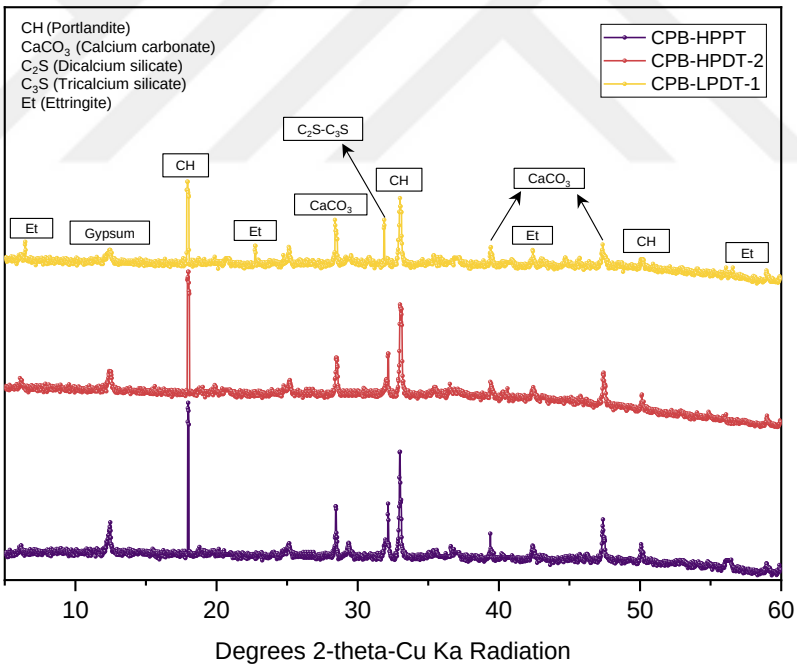


Figure 38. Fill's XRD profiles: (a) CPB-HPPT; (b) CPB-EPDT-2; and (c) CPB-LPDT-1

Dong et al. (2019) stated that low pHs (high sulfates) may damage hydration materials (e.g., C-S-H) formed within paste fill samples, which may cause a decrease in strength values. In addition, absorption of SO_4^{-2} (sulfate) ions by the CSH gels and reaction with calcium aluminates (e.g., C_3A and C_4AF) to form ettringite significantly

affect the backfill performance. Li and Fall (2016) stated that with growing SO_4^{-2} content, the binding of SO_4^{-2} to C-S-H gels occurs sooner and fill's strength falls. Ettringite and portlandite formed in large volumes show that CSH gels shaped within the fill medium give rise to a high amount of SO_4^{-2} absorption. The above-mentioned situation explains why the CPB-LPDT-1 sample has low strength values.

3.5.2. TG/DTG Results

TG/DTG (thermal gravimetric/differential thermal gravimetric) analysis is a method that helps to interpret the hydration products of cementitious materials such as backfill. It is also used to identify products corresponding to thermal degradation of different hydrated phases of cured filling materials. Figure 38 shows the TG/DTG curves of CPBs cured for 28 days with additives (50% substitution rate) and with no additive (control). Witness specimens (OPC100@L and OPC100@H) take greater bulks of hydration materials compared to the GBFS and FA substituted samples. However, samples containing FA had lower volumes of hydration product compared to samples containing GBFS. DTG curves for CPB samples usually exhibit three different peak values relative to the hydration products that degrade at precise heating varieties. Peak one happened at about 100-150°C (Han et al., 2015). This peak is usually caused by dehydration of C-S-H hydrates. In addition, loss of bond waters and dehydration of ettringite affect the formation of this peak. The second peak occurred at approximately 440-560°C. This peak is mainly formed as a result of dehydroxylation of portlandite ($Ca(OH)_2$) minerals. The third peak occurred at about 820-920°C. This peak is linked to the decomposition of $CaCO_3$ (calcite) compounds (Wang et al., 2020a). In general, a significant mass loss peak occurs in the TG/DTG curves of filling specimens between 350 and 650°C owing to the disintegration of hydration products (especially $Ca(OH)_2$) (Aldhafeeri and Fall, 2017). When the losses are examined, the control samples (up to 19.38%) have the highest mass loss. Additionally, the paste backfilling mixtures produced from low or high pH tailings also significantly affected mass losses. The results regarding the hydration products from the TG/DTG curves are supported by the XRD results (Fig. 38).

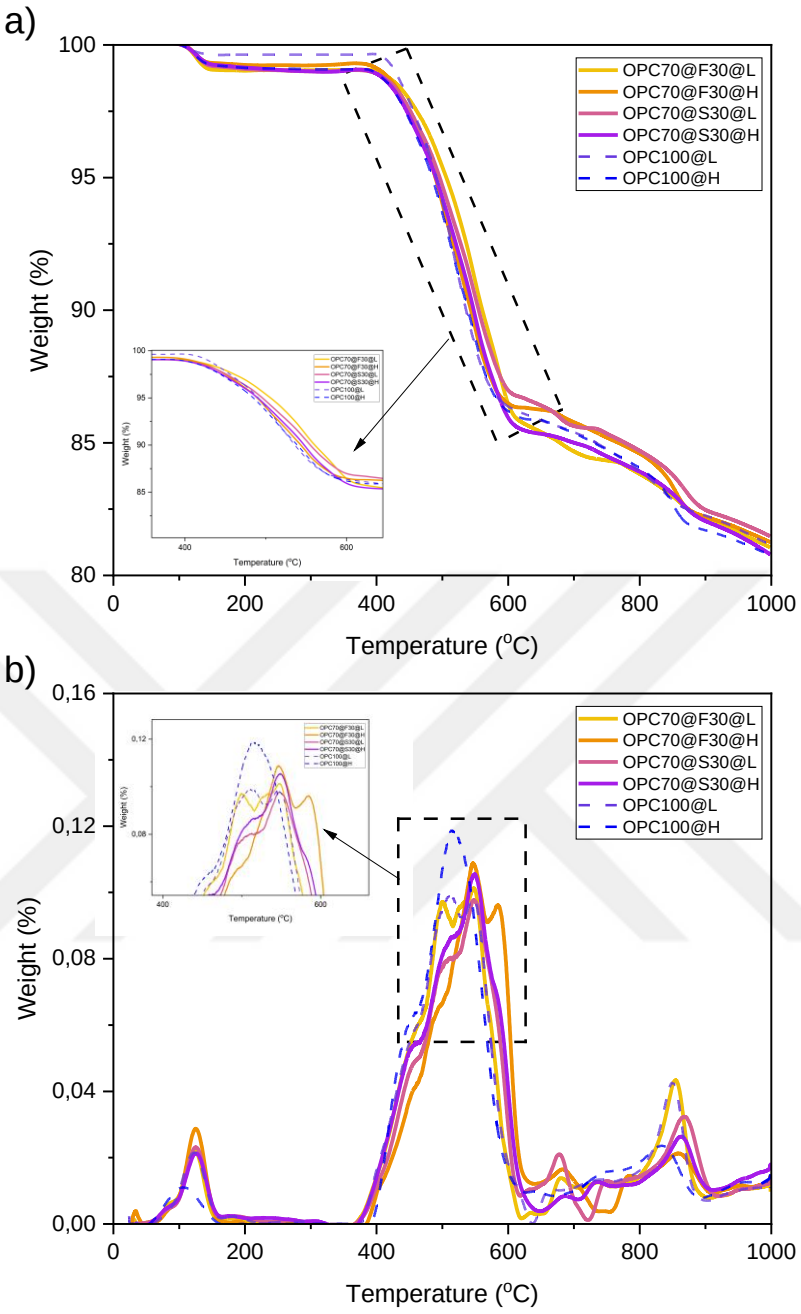


Figure 39. Thermogravimetric analyses TG (a) and DTG (b) of acidic and basic tailings based filling specimens at 28 days

Changes in hydration products of filling specimens created with process/dam wastes and cured for 56 days were investigated with the help of TG/DTG analyses (Figure 39). It is clearly seen that CPB specimen (CPB-LPDT-1) prepared with low pH (acidic) dam tailings possesses a very low volume of hydration products in comparison with others.

However, the CPB sample (CPB-HPPT) prepared using high pH (basic) process tailings had the highest volume of hydration material. In addition, the hydration material volume of CPB-HPDT-2 specimen created with high pH dam tailings is between the CPB-HPPT and CPB-LPDT-1 samples.

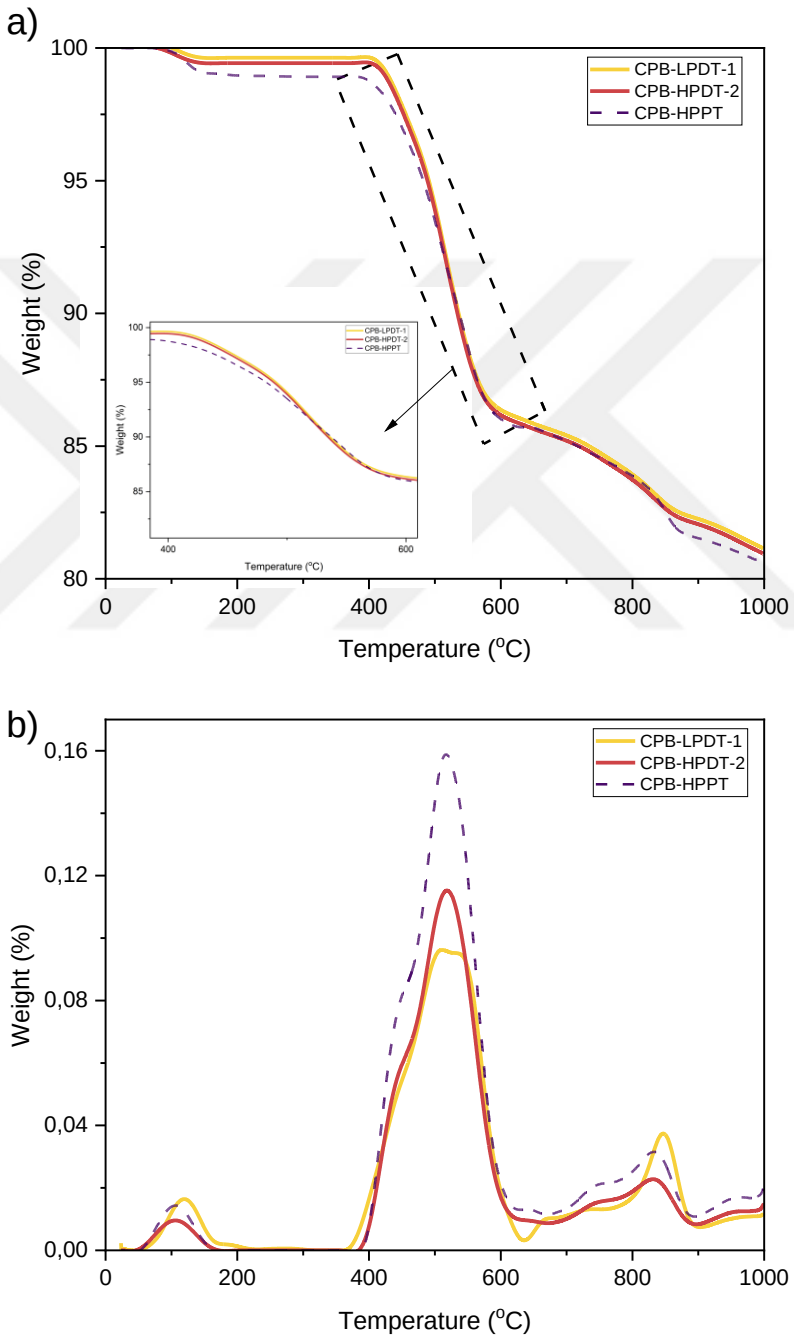


Figure 40. TGA profiles of process and dam tailings based fills at 56 days: (a) CPB-HPPT vs. CPB- HPDT-2; and (b) CPB-HPPT vs. CPB- LPDT-11

DTG curves of CPB samples prepared with the process and dam tailings generally had three endothermic peak values (Figures 39(a) and 39(b)). The peaks that occur are completely related to weight loss and represent the phase transformation of the hydration products. The peak occurring at 40-160°C is closely linked with the dryness of C-S-H and ettringite crystals (Zhang et al., 2021d). In addition, the loss of bond waters is a factor in the formation of this peak. The second peak, which occurs at 350-650°C, usually develops due to the dehydroxylation of $Ca(OH)_2$ (calcium hydroxide or portlandite) (Wang et al., 2020b). The quantity damage (peak) at 800-900°C is due to the disintegration of the mineral $CaCO_3$ (calcite) (Zajac et al., 2020). As the quantity harms in CPB samples are evaluated, the highest mass loss is in the CPB-HPPT sample prepared with process tailings. In addition, the CPB-HPDT-2 sample prepared with basic tailings had less hydration product volume compared to the CPB-HPPT sample and more than the CPB-LPDT-1 sample. These phenomena are an indication that acidic dam tailings damage the hydration products by disrupting the CPB environment. However, acidic wastes significantly affect CPB quality and performance. The interpretations obtained because of the TG/DTG curves were also found to be quite compatible with the XRD results (Figure 37).

3.5.3. MIP Results

Figure 40 shows the pore size distribution (cumulative/incremental) of 28 days cured fills created with 50% substituted additives for OPC (GBFS and FA) and tailings at diverse pH values. A 50% substitution ratio was chosen to better understand the difference between additive and non-additive (control) fill samples. One can interpret from Figure 40 that the chosen proportion of substitution and the use of additives for the backfill mixtures significantly affect the CPB pore distribution.

The n_{tot} (total porosity) values of OPC100@L and OPC100@H (control) samples were 28.5% and 26.8%, respectively. While n_{tot} values for CPB samples containing low pH (acidic) tailings (OPC50@S50@L and OPC50@F50@L) were 35.4% and 41.2%, n_{tot} values were determined as 33.6% and 39.1% for CPB samples containing high pH (basic) tailings (OPC50@S50@H and OPC50@F50@H). In addition, d_{cr} (critical pore size) was determined to range from 1.5 to 2.1 μm in control specimens, although it shifted from 1.7 to 3.2 μm in GBFS and FA substituted CPB

samples. The results show that GBFS and FA additives increase the porosity of the filler samples. In addition, with the addition of additives to the CPB samples, the increased w/c ratio because of the decrease in cement dosage increases the total porosity (Zhou et al., 2022).

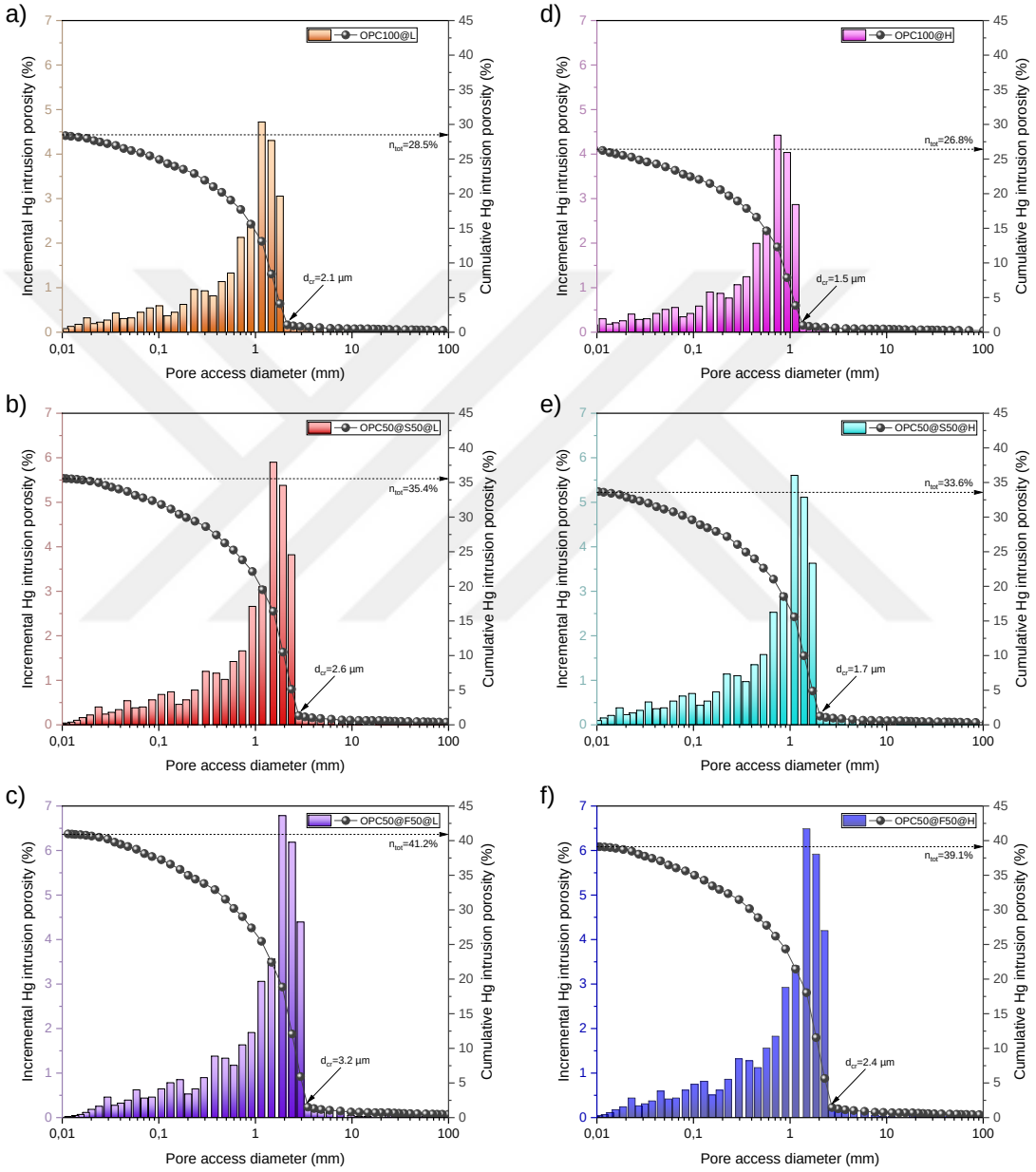


Figure 41. Plots of cumulative/incremental PSD profiles of acidic (a, b, c) and basic (d, e, f) tailings based fillings specimens

Differences in pore distribution between the additives is due to the coarser grain of the fly ash. (Behera et al., 2021). Strength development and permeability are directly

correlated to the number of pores in cement-based mixtures such as CPB. In addition, fills's water content and the creation of hydration products eventually affect the matrix's pore distribution (Huang et al., 2021b; Zhou et al., 2022). As a result of this situation, the hydration materials created within control specimens reduced the porosity and filled the space between the grains. This situation caused the control samples to reach higher strength values when compared to GBFS and FA added backfill samples. The strength results in Figure 20 clearly show the pore distribution effect on fill's quality/performance property.

Generally, cemented products (e.g., CPB/concrete) can be alienated to diverse groups, such as gel, mesopores, and macropores, based on their void ratio. Huang et al. (2017) evaluated the pores of cemented materials in three different ways: air voids (>105 nm), capillary pores (55-105 nm), and mesopores (5-50 nm). When the total porosities of the backfill samples with and without additives are examined within the scope of the study, it is clearly seen that mesopores dominate. Porosity is basically connected to the PSD, chemical reactions, and hydration products of the materials that make up the backfill (e.g., tailings, cement, and additives). The overall porosity increases in direct proportion to the increase in the grain fineness of the tailings in the backfill (Ke et al., 2016). Total porosity is lower in backfill samples prepared with acidic (low pH) tailings compared to backfill samples prepared with basic (high pH) tailings. It also causes the formation of more hydration products, resulting in higher compressive strengths (Yue, 2021). Sulfate attacks are among the parameters that influence fill's quality/performance. Hydration products exposed to sulfate attacks give rise to the creation of ettringite/gypsum expanding minerals. This causes the openings to expand and micro-cracks to form in the CPB (Aldhafeeri and Fall, 2017). This is clearly seen in filling specimens created with FA additive and low pH (acidic) tailings. Poor strengths, high porosity, low CaO concentrations and the incapability to create adequate hydration materials in these samples at early curing times affect the backfill quality significantly (Li et al., 2022).

3.5.4. SEM Results

Figure 41 shows SEM images of 56-day cured GBFS (OPC70@S30@L and OPC70@S30@H) and control (OPC100@L and OPC100@H) specimens owing to

their higher strengths than samples covering FA. Particle and surface images of the samples were examined under ×2000 magnification. From these pictures, cracks, hydration products, and pores of different sizes formed on the surfaces of CPB samples can be clearly seen. When the OPC100@L and OPC100@H specimens are surveyed, one can deduct that filling specimens made with tailings with low pH values (acidic) form fewer hydration products, and the number of voids is higher than the mixtures containing low pH waste (Figure 41(a) and 41(b)). The reason behind this is that pHs of the tailings affect the hydration reaction by changing the alkalinity of the CPB environment (El Mahboub et al., 2022; Li et al., 2020a; Kou et al., Kou et al., 2020; Xue et al., 2019c). This is supported by the differences in strength values found in Figure 20.

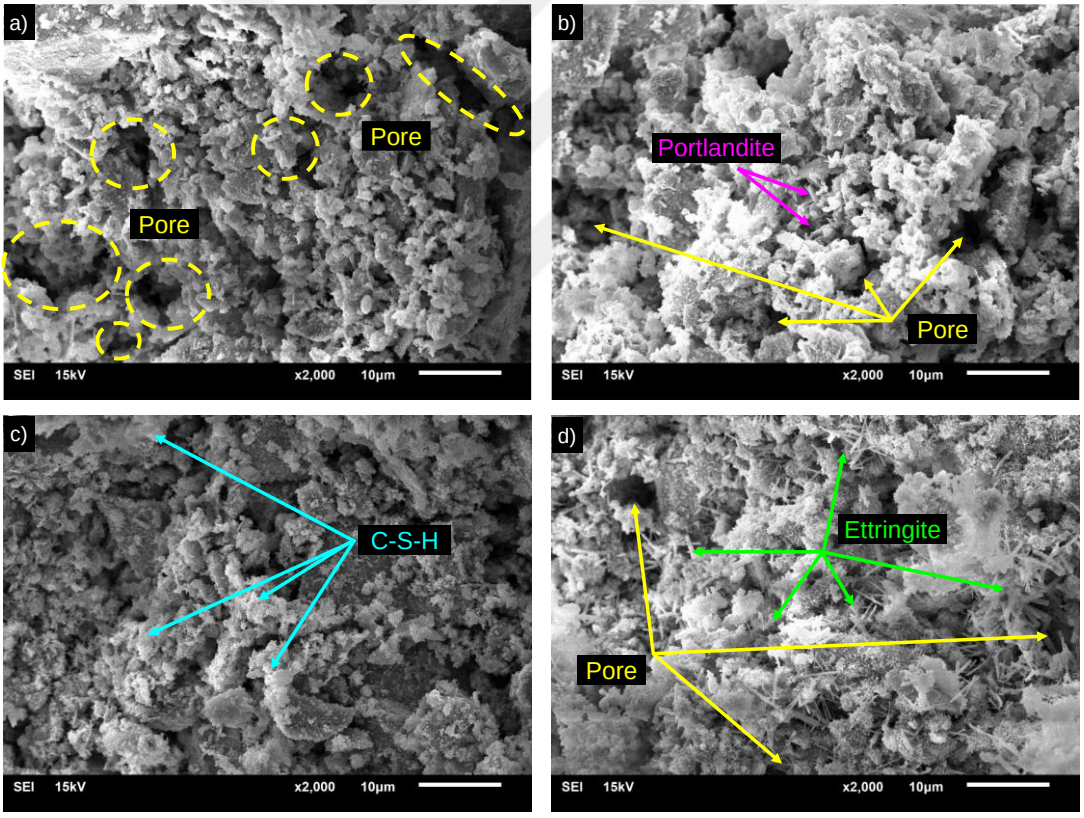


Figure 42. SEM graphs of additive (c, d) and non-additive (a, b) based fills

In GBFS substituted CPB samples (OPC70@S30@L and OPC70@S30@H), one can interpret that additive led to weaker mass formation. This is well in line with MIP/UCS outcomes. From the SEM pictures, it can be said that the acids formed after the curing period of 56 days damage the C-S-H gels and cause ettringite formation by

reacting with $Ca(OH)_2$ (Portlandite) (Guo et al., 2022). The high amount of ettringite observed in Figure 41(d) is thought to be due to the large amount of $Ca(OH)_2$ in this sample. The reason behind this is that pozzolanic additives (e.g., GBFS and FA) have key effects on fills' long-term ageing properties. One can also infer that the outcomes gained from XRD/TGA analyses together with SEM images can provide important information about hydration products.

Figure 42 shows SEM micrographs of CPB-HPPT (control), CPB-LPDT -1 (most acidic), and CPB-HPDT -2 (most basic) samples. Diverse sizes of cracks, pores, and hydration products formed in the cured CPB specimens were envisaged under ×1000 and ×5000 increase. Fewer hydration products and ettringite were observed in sample CPB-LPDT -1 (Fig. 44(c)) compared to samples CPB-HPPT and CPB-HPDT -2 (Figures 42(a) and 42(b)). In addition, in CPB-HPPT and CPB-HPDT-2 specimens made with basic tailings, grains were coated/tightly guaranteed with CSH gels. This directly affects the strengths positively by causing the formation of a solid structure in the backfill specimens. Besides, the basicity of the CPB medium (high pH values) increases alkalinity and positively supports the hydration process (Cao et al., 2019c). For CPB samples prepared with basic tailings, this observation is also compatible with XRD, UCS, and TGA (TG/DTG) results. Many studies support this observation (Li et al., 2019a; Tariq and Yanful, 2013; Cao et al., 2021d).

Figure 42(c) confirms the presence of major volumes of ettringite crystals shaped in the CPB-LPDT-1 (most acidic) sample cured for 56 days. One can infer that cement quantity declines significantly because of the acidity of the CPB environment (Zheng et al., 2021). This can be clarified by the detail that the sulfate absorption that happens through the creation of ettringite crystals in the acidic environment (low pH values) fills the pores of CPB. With the decrease of pH values in the CPB environment, sulfate absorption increases and prevents the formation of gypsum that will fill the pores of the samples. This increases the number of voids in the CPB, promoting poor internal structure and reducing backfill performance. The huge quantity of the space shaped in the CPB-LPDT -1 specimen in Figure 42(c) kindly cares this interpretation (Yilmaz et al., 2020; Wang et al., 2022c). Therefore, as viewed apparently in Figure 21(b), the strengths of 56-day cured CPB-LPDT -1 and CPB-LPDT -2 specimens decrease significantly.

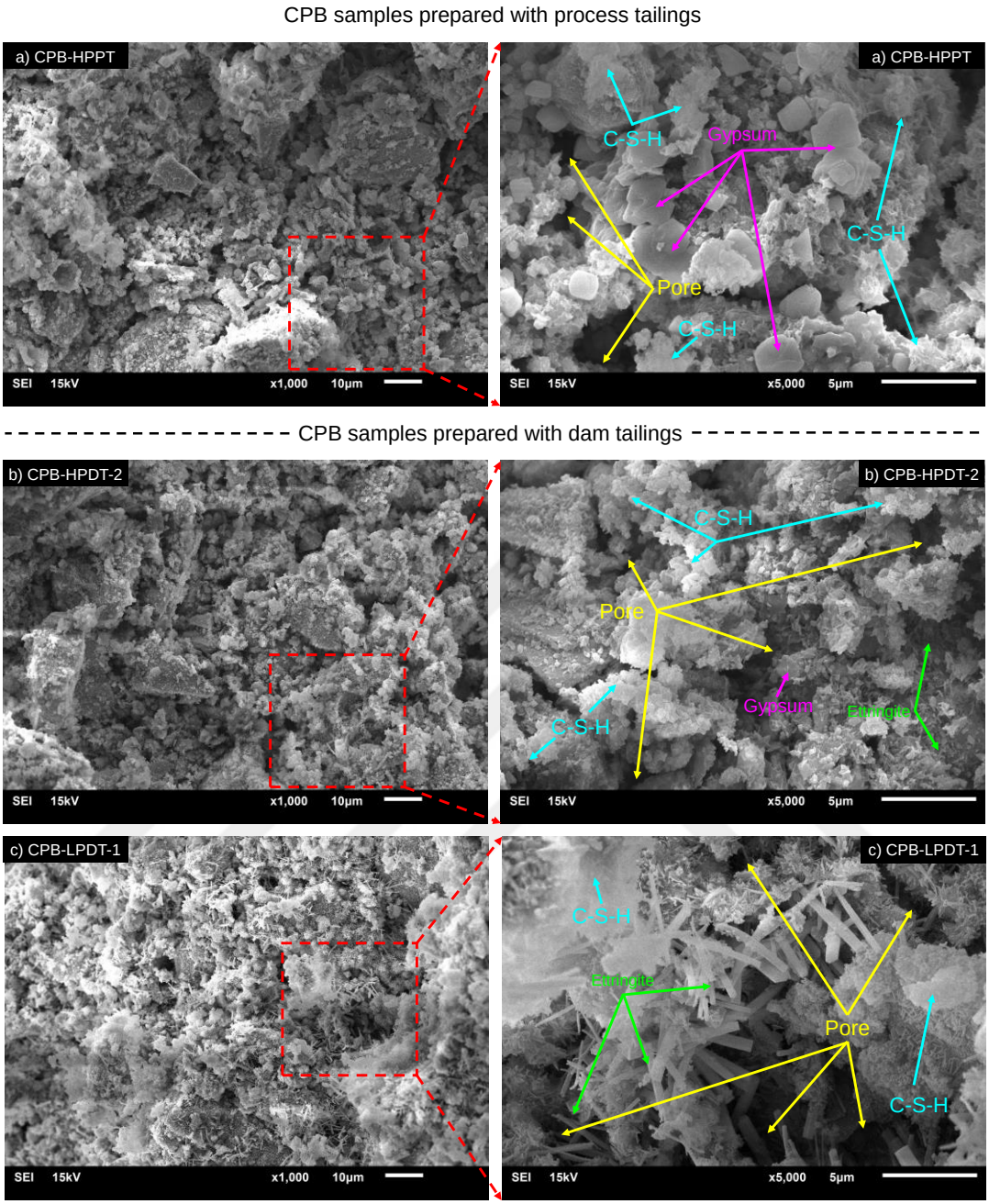


Figure 43. SEM micrographs of process and dam tailings based filling specimens at 56 days: (a) CPB-HPPT, (b) CPB- HPDT-2 and (c) CPB- LPDT-1

4. CONCLUSIONS

4.1. Extended Summary

Mining is very important to national economies, but it produces 6-12 billion of tons of mineral processing tailings annually. Highly reactive sulfide minerals (e.g., pyrite/pyrrhotite) within tailings are oxidized to form SO_4^{-2} (sulfate) by reacting with oxygen and water. This causes heavy metal contaminations, sulfate attacks, acid mine drainage formations over time, causing stern irrevocable destructions to air/water/soil. To lessen these severe ecological impacts of tailings, one of the most chosen practices is to employ CPB. It is frequently used in most modern underground mines in many countries, including Turkey. Reusing the tailings as CPB and filling the underground stations by CPB provide environmental, technical, and operational advantages for the disposal of problematic mining wastes. In addition, it is the preferred method for green and sustainable mining. The key features of this backfill technique are that it eliminates the potential for environmentally harmful sulfur-rich mine tailings (e.g., acid mine drainage and rehabilitation costs). Moreover, it meaningfully reduces the number of tailings generated by supporting the underground stops.

Most of the studies carried out to date have focused on rheological/hydration and pozzolanic/mechanical characteristics of CPB specimens with additives (either mineral or chemical). Mineral additive effect on strength/microstructural properties of CPB specimens which is made of tailings with diverse pHs, is clearly disregarded. In addition, the impacts of tailings treatment are not extensively investigated. Besides, the potential usage of dam tailings having diverse pHs in CPB manufacturing are not sufficiently explored. The ultimate design of CPB specimens for mines is habitually based on the products which are created, cured, and experimented at lab. In particular, the characteristic structure of tailings directly affects the filling structure. Traditional molds underestimate the impact of acidic (low pH) dam and process effluent on filling quality and performance. As a result, finding the appropriate backfill recipes to assess the effects of effluent (dam and process) and mineral additives can help reduce the harmful impact of these mining wastes.

This M.Sc. thesis study focuses on the effect of pyritic process wastes created at diverse pHs and supplementary products, such as GBFS/FA, which are replaced in

changing amounts to filling mixes, on ultimate functions and behavior of filling. Fill mixes containing two different tailings (either acidic or basic) were created with 0%, 10%, 30%, and 50% additive replacement proportions. In addition, employing dam tailings on fill's quality/properties was also experimentally explored. While collecting specimens from diverse dam parts, process tailings were sampled from the filtering unit of a flotation technique used ore dressing facility. Specimens were created by employing a constant binder amount (5% by weight) and different solid contents (72% and 76% by weight). They were then subjected to curing at the periods shifting from 3 days to 56 days. Experiments such as geo-chemical/mechanical/micro-structural and geotechnical tests were realized on filling specimens. The results obtained provided a better understanding of the backfills. This M.Sc. thesis study will help in the design of filling blends in terms of performance, safety, and cost savings. Besides, it will show a path to allow the reduction of environmental impacts caused by tailings.

The thesis is handled in three different stages. In the first step, the quality of the paste backfills containing low (4.9) and high (10.8) pH pyritic tailings was investigated. In addition, significant savings were targeted by using both GBFS and FA additives at different replacement ratios instead of relatively expensive Portland cement (OPC) used within backfilling. It was concluded that the cement hydration is immediately affected by the acidic tailings pH, and thus the performance of the backfill is negatively affected. In the second step, the physico-chemical properties and pore structure of CPB specimens produced from dam tailings were investigated. The results proved that there was a significant decrease in the strength of the backfills produced from sulfur-rich tailings. In addition, deterioration of the physical/chemical and micro-structural characteristics of filling has occurred. In the third stage, the basic strength and geotechnical properties of the fills produced from dam wastes were investigated in detail. As a result, it was noticed that during the early curing period, the cement increases the pH of backfilling, but during the long curing period, the pH of filling can be lowered by dam tailings, which are prone to acid formation and erosion.

4.2. Key Research Highlights

The chief deductions of this M.Sc. thesis study are derived from experimental research/observations on filling specimens created using dam tailings with different

characteristics, process tailings subjected to diverse flotation processes, and industrial waste (e.g., slag/fly ash). Considering the various tests performed (e.g., mechanical and microstructure test) the foremost consequences were as follows:

- The strength values of filling specimens made with low pH (acidic) process tailings and industrial wastes (GBFS and FA) decreased between 10.9% and 32.1% for GBFS substituted specimen and between 15.8% and 32.1% for FA substituted specimen in comparison with witness specimen (OPC100@L). In addition, the strength of the backfills prepared with high pH (basic) tailings decreased between 10.9% and 18.9% for the GBFS substituted sample and between 16.1% and 35.8% for the FA substituted specimen in comparison with witness specimen.
- One can interpret that the differences in the pHs of process tailings significantly affected CPB's strength/microstructure. It subsidizes the creation of additional hydration materials by supporting the hydration environment of high pH (basic) tailings in the fillings. On the other hand, low pH (acidic) tailings cause low reactivity, negatively affecting CPB performance.
- Irrespective of the category of tailings (acidic or basic) used in CPB blends, GBFS additive performed better than FA additive. For both industrial additives used, the highest CPB strength was seen at the 90/10 mixing ratio. Similarly, the lowest strength results were at the 50/50 mix ratio.
- Element analysis indicated that the sulfate, calcium, and silicon concentrations of the CPB -LPDT-1 and CPB-LPDT-2 specimens with acidic dam tailings decreased in the initial 28-days and later started to rise. In CPB-LPDT-3, CPB-HPDT-1, CPB-HPDT-2 and CPB-HPPT specimens, sulfate, calcium, and silicon concentrations decreased between 13.9% and 55.1% until the 56-day curing period, thanks to the neutralization of acidic environment triggered with tailings.
- The pH values of CPB samples containing dam wastes increased until the first 14-day curing period and then decreased. The pH values of the CPB-LPDT-1, CPB-LPDT-2, CPB-LPDT-3, CPB-HPDT-1, CPB-HPDT-2 and CPB-HPPT

specimens augmented by 32.1%, 32.9%, 30.1%, 27.8%, 26.3%, and 11.6%, respectively, at 14 days in comparison with to 3-day curing age.

- Compared with 3-day curing age, the strengths of 28-day cured CPB-LPDT-1 and CPB-LPDT-2 samples increased by 29.7% and 36.2%, respectively. These values then decreased by 20.1% and 13.4%, respectively, up to the 56-day curing time. In addition, strength values of CPB-LPDT-3, CPB-HPDT-1, CPB-HPDT-2, and CPB-HPPT samples increased continuously up to 56 days of curing time.
- When the microstructural analyses of CPB-LPDT -1 (having the most acidic dam tailings) sample was tested, fewer gypsum and hydration products were found compared to the other samples. In addition, CPB samples containing high pH (basic) dam tailings (CPB-HPDT-1, CPB-HPDT-2, and CPB-HPPT) produced fewer ettringite crystals.
- The strength values of all CPB samples (produced based on Table 16), independent of dam and process tailings, increased in the first 28 days, then decreased between 7.1% and 25.9% up to the 56-day curing time.
- When stress-strain behavior of CPBs being cured at 28/56 days was examined, the CPB-P sample had the highest tensile and brittle behavior. CPB-D1 sample had the highest strain and ductile behavior at similar curing times. In addition, the highest E50 value (116 kPa) was in the CPB-P sample, while the lowest E50 value (14 kPa) was in the CPB-D1 sample.
- Compared to 3-day curing age, w (water content) values of all 56-day cured CPB samples decreased in the range of 19.8% to 53.1%. During the similar curing period, e (void ratio) values of all backfills decreased between 2.41% and 24.9%, while Ss (specific surface area) values decreased between 13.9% and 51.1%. In addition, the degree of saturation (Sr) decreased between 15.6% and 34.2%.
- Geotechnical tests display that acidic dam tailings must be used in conjunction with cementitious materials (basic materials) such as CPB to counteract their harmful effects. In addition, it is thought that the harmful effects of dam tailings will be minimized and/or eliminating by using them within CPB specimens and filling them into underground mines.

4.3. Limitations of This Thesis Work

The results showed that industrial waste such as GBFS/FA can be used instead of OPC in the backfill. With the use of these additives in CPB, high strengths like OPC are not obtained. However, it should not be overlooked that it provides many benefits such as minimizing binder prices, wastes' total quantity, and ecological harm. Today, most mining firms aim to use pozzolanic materials (GBFS/FA) within CPB specimens. In addition, this study showed that basic materials such as CPB should be used in under-ground mines as a regional/local support part for falling the destructive effects of dam tailings. The reason behind this is that dam tailings show diverse characteristics under climatic/sedimentation conditions. To reduce the undesirable effects of acidic dam tailings and to make them sustainable, the chemical/geochemical characteristics of tailings should be examined in detail.

One of the restrictions of this M.Sc. study is that it cannot characterize entire dam facility because of a surface dam tailings collection which may reflect wrong results as a limited part of tailings. To healthier scrutinize the impact of tailings, samples should be taken to reflect profounder (sampling through drilling) and broader zones (by increasing the number of samples). In addition, it is more convenient to store the collected samples in airtight and watertight containers so that their properties do not change (e.g., oxidation). Another limitation of this study is that a lab trial is realized by taking samples from process tailings once. In the preparation of flotation tailings samples, it is more appropriate to take samples from different points of the facility and to create composite samples from these samples. Thus, the samples collected can be representative of the entire plant. In upcoming experimental/field works, the usage of diverse mineral/chemical extracts and tailings within backfilling will be explored, paying much more attention to the limitations mentioned above, and expanding their findings with the help of different analyzes and/or tests.

4.4. Upcoming Research Directions

The research existing in this MSc thesis not only delivered an improved caring of mechanical/microstructural characteristics of CPB specimens manufactured by employing dam and process tailings, but also recognized the paths of interest for

additional investigations on techniques or approaches which could be employed in the backfill operation. These interesting paths comprise:

- Additional investigations on hydration development and mechanical properties of CPB specimens made with calcareous sand as a substitute of dam and/or process tailings are needed. Considering that today's tailings have both high economic value and disposal problems (especially acidic tailings), there is a lack in the literature. For example, tailings that have deteriorated in dam over time and have no economic value are not sustainable for mining operations and eventually lead to serious environmental problems such as acids and leachates. Thus, the effect of acidic tailings (dam and process) can be reduced by adding additives such as sand with high CaO value at different substitution rates (e.g., 10%, 20% and 30%) as aggregate to CPB.
- In addition to using the sand as aggregate in backfilling, additional lab works are also needed to use the sand as cement substitutes in backfilling considering the effects of mineral/chemical additives. The results will not only affect by the mechanical microstructure of filling, but also by the physical, chemical, and mineralogical compositions of additives. It will be useful to understand how CPB, which is prepared with different additive types and contents as a function of curing conditions (i.e., time, temperature, and stress), affects the hydration development, pore structure and strength. Thanks to these additives to be used, the backfill's long-term ageing difficulties (e.g., acidification and leaching) can be eliminated or openly reduced. These additives can also save huge amounts of money regarding cement usages in filling for mining companies.
- Alternative testing methods such as NMR (nuclear magnetic resonance) and CT (computer tomography) can be employed to better characterize the backfills and better understand their failure modes under different dynamic events or static loading conditions. In addition, backfill products based on dam/process tailings can be examined, considering different curing conditions (e.g., stress, temperature and curing). In this way, it becomes easier to understand how CPB specimens will behave in the long- and short-term.

REFERENCES

Adiansyah, J. S., Rosano, M., Vink, S., & Keir, G. (2015). A framework for a sustainable approach to mine tailings management: disposal strategies. Journal of cleaner production, 108, 1050-1062.

Ait-Mokhtar, A., Amiri, O., Dumargue, P., & Sammartino, S. (2002). A new model to calculate water permeability of cement-based materials from MIP results. Advance in Concrete Research, 13 (1), 1-7.

Akinyemi, B. A., Alaba, P. A., & Rashedi, A. (2022). Selected performance of alkali-activated mine tailings as cementitious composites: A review. Journal of Building Engineering, 50, 104154.

Akkaya, U. G., Cinku, K., & Yilmaz, E. (2021). Characterization of strength and quality of cemented mine backfill made up of lead-zinc processing tailings. Frontiers in Materials, 383.

Aldhafeeri, Z., & Fall, M. (2017). Sulphate induced changes in the reactivity of cemented tailings backfill. International Journal of Mineral Processing, 166, 13-23.

Aldhafeeri, Z., Fall, M., Pokharel, M., & Pouramini, Z. (2016). Temperature dependence of the reactivity of cemented paste backfill. Applied Geochemistry, 72, 10-19.

Ali, B., Yilmaz, E., Tahir, A., Gamaoun, F., El Ouni, M., & Murtaza Rizvi, S. (2021). The durability of high-strength concrete containing waste Tire steel fiber and coal fly ash. Advances in Materials Science and Engineering, 2021, 7329685.

Al-Moselly, Z., Fall, M., & Haruna, S. (2022). Further insight into the strength development of cemented paste backfill materials containing polycarboxylate ether-based superplasticizer. Journal of Building Engineering, 47, 103859.

Alp, I., Deveci, H., Sungun, Y.H., Yilmaz, A.O., Kesimal, A., & Yilmaz, E. (2009). Pozzolanic characteristics of a natural raw material for use in blended cements. Iranian Journal of Science and Technology, Transaction B, Engineering, 33(4), 291-300.

Amrani, M., Taha, Y., Kchikach, A., Benzaazoua, M., & Hakkou, R. (2019). Valorization of phosphate mine waste rocks as materials for road construction. Minerals, 9(4), 237

Amaratunga, L.M., & Hmidi, N. (1998). Cold-bond agglomeration of gold mill tailings for backfill using gypsum beta-hemihydrate and cement as low cost binders. Canadian Metallurgical Quarterly, 36 (4), 283-288.

Archibald, J.F., Lausch, P., & He, Z.X. (1993). Quality control problems associated with backfill use in mines. CIM Bulletin, 86 (972), 53-57.

Aubertin, M., Bussière, B., & Chapuis, R. (1996). Hydraulic conductivity of homogenized tailings from hard rock mines. Canadian Geotechnical Journal, 33 (3), 470-482.

Bascetin, A., Adiguzel, D., Eker, H., Odabas, E., & Tuylu, S. (2021). Effects of puzzolanic materials in surface paste disposal by pilot-scale tests: observation of physical changes. International Journal of Environmental Science and Technology, 18(4), 949-964.

Behera, S. K., Mishra, D. P., Singh, P., Mishra, K., Mandal, S. K., Ghosh, C. N., Kumar, R., & Mandal, P. K. (2021). Utilization of mill tailings, fly ash and slag as mine paste backfill material: Review and future perspective. Construction and Building Materials, 309, 125120.

Belem, T., & Benzaazoua, M. (2008). Design and application of underground mine paste backfill technology. Geotechnical and Geological Engineering, 26 (2), 147-174.

Belem, T., El Aatar, O., Bussière, B., & Benzaazoua, M. (2016). Gravity-driven 1-D consolidation of cemented paste backfill in 3-m-high columns. Innovative Infrastructure Solutions, 1 (1), 1-12.

Benkendorff, P.N. (2006). Potential of lead/zinc slag for use in cemented mine backfill. Mineral Processing and Extractive Metallurgy: Institution of Mining and Metallurgy Transactions Section C, 115 (3), 171-173.

Benzaazoua, M., Bussière, B., Demers, I., Aubertin, M., Fried, É., & Blier, A. (2008). Integrated mine tailings management by combining environmental desulphurization and cemented paste backfill: Application to mine Doyon, Quebec, Canada. Minerals Engineering, 21(4), 330-340.

Benzaazoua, M., Belem, T., & Yilmaz, E. (2006). Novel lab tool for paste backfill. Canadian Mining Journal, 127(3), 31.

Benzaazoua, M., Fall, M., & Belem, T. (2004). A contribution to understanding the hardening process of cemented pastefill. Minerals Engineering, 17(2), 141-152.

Beya, F.K., Mbonimpa, M., Belem, T., Li, L., Marceau, U., & Kalonji, P. (2019). Mine backfilling in the permafrost, Part I: Numerical prediction of thermal curing conditions within the cemented paste backfill matrix. Minerals 9 (3), 165.

Blissett, R. S., & Rowson, N. A. (2012). A review of the multi-component utilisation of coal fly ash. Fuel, 97, 1-23.

Bois, D., Poirier, P., Benzaazoua, M., Bussière, B., & Kongolo, M. (2005). A feasibility study on the use of desulphurized tailings to control acid mine drainage. CIM Bulletin, 98 (1087), 74-74.

Brackebusch, F.W. (1994). Basics of paste backfill systems. Mining Engineering, 46 (10), 1175-1178.

Bull, A. J., & Fall, M. (2020). Thermally induced changes in metalloid leachability of cemented paste backfill that contains blast furnace slag. Minerals Engineering, 156, 106520.

Bussière, B. (2007). Colloquium 2004: Hydrogeotechnical properties of hard rock tailings from metal mines and emerging geoenvironmental disposal approaches. Canadian Geotechnical Journal, 44 (9), 1019-1052.

Canales, R. M., Kozlovskaya, E., Lunkka, J. P., Guan, H., Banks, E., & Moisio, K. (2020). Geoelectric interpretation of petrophysical and hydrogeological parameters in reclaimed mine tailings areas. Journal of Applied Geophysics, 181, 104139.

Cao, S., Yilmaz, E., Yin, Z., Xue, G.L., Song, W.D., & Sun, L. (2021a). CT scanning of internal crack mechanism and strength behavior of cement-fiber-tailings matrix composites. Cement and Concrete Composites, 116, 103865.

Cao, S., Xue, G.L., Yilmaz, E., & Yin, Z. (2021b). Assessment of rheological and sedimentation characteristics of fresh cemented tailings backfill slurry. International Journal of Mining, Reclamation and Environment, 35(5), 319-335.

Cao, S., Xue, G.L., Yilmaz, E., Yin, Z., & Yang, F. (2021c). Utilizing concrete pillars as an environmental mining practice in underground mines. Journal of Cleaner Production, 278, 123433.

Cao, S., Xue, G.L., Yilmaz, E., & Yin, Z.Y. (2021d). Assessment of rheological and sedimentation characteristics of cemented tailings backfill slurry. International Journal of Mining, Reclamation, and Environment, 35(5), 319-335.

Cao, S., Zheng, D., Yilmaz, E., Yin, Z., Xue, G.L., & Yang, F. (2020). Strength development and microstructure characteristics of artificial concrete pillar considering fiber type and content effects. Construction and Building Materials, 256, 119408.

Cao, S., Yilmaz, E., Song, W., & Xue, G. (2019a). Assessment of acoustic emission and triaxial mechanical properties of rock-cemented tailings matrix composites. Advances in Materials Science and Engineering, 2019, 6742392.

Cao, S., Xue, G.L., & Yilmaz, E. (2019b). Flexural behavior of fiber reinforced cemented tailings backfill under three-point bending. IEEE Access, 7(1), 139317-139328.

Cao, S., Yilmaz, E., & Song, W.D. (2019c). Fiber type effect on strength, toughness and microstructure of early age cemented tailings backfill. Construction and Building Materials, 223, 44-54.

Cao, S., Yilmaz, E., & Song, W.D. (2018). Evaluation of viscosity, strength and microstructural properties of cemented tailings backfill. Minerals, 8(8), 352.

Cao, Z., Shen, L., Zhao, J., Liu, L., Zhong, S., Sun, Y., & Yang, Y. (2016). Toward a better practice for estimating the CO2 emission factors of cement production: An experience from China. Journal of Cleaner Production, 139, 527-539.

Cavusoglu, I., Yilmaz, E., & Yilmaz, A. O. (2021a). Additivity effect on properties of cemented coal fly ash backfill containing water-reducing admixtures. Construction and Building Materials, 267, 121021.

Cavusoglu, I., Yilmaz, E., & Yilmaz, A. O. (2021b). Sodium silicate effect on setting properties, strength behavior and microstructure of cemented coal fly ash backfill. Powder Technology, 384, 17-28.

Cayouette, J. (2003). Optimization of the paste backfill plant at Louvicourt mine. CIM Bulletin, 96 (1075), 51-57.

Chen, Q., Tao, Y., Feng, Y., Zhang, Q., & Liu, Y. (2021). Utilization of modified copper slag activated by Na2SO4 and CaO for unclassified lead/zinc mine tailings based cemented paste backfill. Journal of Environmental Management, 290, 112608.

Chen, S.-M., Wang, W., Yan, R., Wu, A.-W., Wang, Y.-M., & Yilmaz, E. (2022). A joint experiment and discussion for strength characteristics of cemented paste backfill considering curing conditions. Minerals, 12(2), 211.

Chen, T., Lei, C., Yan, B., Li, L. L., Xu, D. M., & Ying, G. G. (2018). Spatial distribution and environmental implications of heavy metals in typical lead (Pb)-zinc (Zn) mine tailings impoundments in Guangdong Province, South China. Environmental Science and Pollution Research, 25(36), 36702-36711.

Chen, X., Shi, X., Zhou, J., Du, X., Chen, Q., & Qiu, X. (2019). Effect of overflow tailings properties on cemented paste backfill. Journal of environmental management, 235, 133-144.

Cheng, H. Y., Wu, S. C., Zhang, X. Q., & Wu, A. X. (2020). Effect of particle gradation characteristics on yield stress of cemented paste backfill. International Journal of Minerals, Metallurgy and Materials, 27(1), 10-17.

Chowdary, M. V. S. S. P., & Asadi, S. S. (2021). Impact of material properties on characteristics of engineered cementitious composite. Materials Today: Proceedings, 42, 325-329.

Cihangir, F., Ercikdi, B., Kesimal, A., Ocak, S., & Akyol, Y. (2018). Effect of sodium-silicate activated slag at different silicate modulus on the strength and microstructural properties of full and coarse sulphidic tailings paste backfill. Construction and Building Materials, 185, 555-566.

Cihangir, F., Ercikdi, B., Kesimal, A., Turan, A., & Deveci, H. (2012). Utilisation of alkali-activated blast furnace slag in paste backfill of high-sulphide mill tailings: effect of binder type and dosage. Minerals Engineering, 30, 33-43.

Clayton, S., Grice, T. G., & Boger, D. V. (2003). Analysis of the slump test for on-site yield stress measurement of mineral suspensions. International Journal of Mineral Processing, 70(1-4), 3-21.

Coussy, S., Benzaazoua, M., Blanc, D., Moszkowicz, P., & Bussière, B. (2011). Arsenic stability in arsenopyrite-rich cemented paste backfills: a leaching test-based assessment. Journal of Hazardous Materials, 185(2-3), 1467-1476.

Consoli, N. C., Rotta, G., & Prietto, P. (2006). Investigation of yielding-compressibility-strength relationship for an artificially cemented soil cured under stress. Géotechnique, 56 (1), 69-72.

Consoli, N. C., Rotta, G., Foppa, D., & Fahey, M. (2007). Mathematical model for compression behaviour of cemented soil cured under stress. Geomechanics and Geoengineering, 2 (4), 269-280.

Cooke, R. (2007). Backfill pipeline distribution systems: Design methodology review. CIM Bulletin, 100 (1103), 1-8 (Paper 20).

Cui, B., Liu, Y., Feng, G., Bai, J., Du, X., Wang, C., & Wang, H. (2020). Experimental study on the effect of fly ash content in cemented paste backfill on its anti-sulfate erosion. International Journal of Green Energy, 17(12), 730-741.

Cui, L., & Fall, M. (2020). Numerical simulation of consolidation behavior of large hydrating fill. International Journal of Concrete Structures and Materials, 14 (23), 1-16.

Cui, L., & Fall, M. (2017). Modeling of pressure on retaining structures for underground fill mass. Tunneling and Underground Space Technology, 69, 94-107.

Cui, L., & Fall, M. (2016). An evolutive elasto-plastic model for cemented paste backfill. Computers and Geotechnics, 71, 19-29.

Cui, L., & Fall, M. (2015). A coupled thermo-hydro-mechano-chemical model for cemented paste backfill. Tunneling and Underground Space Technology, (50) 396-414.

Dai, X., Ren, L., Guo, Z., Yilmaz, E., Fang, K., & Jiang, H. (2022). Strength analysis and optimization of alkali activated slag backfills through response surface methodology. Frontiers in Materials, 9, 844608.

Dashti, J., & Nematzadeh, M. (2020). Compressive and direct tensile behavior of concrete containing Forta-Ferro fiber and calcium aluminate cement subjected to sulfuric acid attack with optimized design. Construction and Building Materials, 253, 118999.

Deschamps, T., Benzaazoua, M., Bussière, B., Aubertin, M., & Belem T. (2008). Microstructural and geochemical evolution of paste tailings in surface storage. Minerals Engineering, 21 (4), 341–353.

Dikonda, R.K., Mbonimpa, M., & Belem, T. (2021). Specific mixing energy of cemented paste backfill, Part II: Influence on the rheological and mechanical properties and practical applications. Minerals 11 (11), 1159.

Dinis, M. D. L., Fiúza, A., Futuro, A., Leite, A., Martins, D., Figueiredo, J., ... & Vila, M. C. (2020). Characterization of a mine legacy site: an approach for environmental management and metals recovery. Environmental Science and Pollution Research, 27(9), 10103-10114.

Dirige, A.P.E., & De Souza, E. (2007). Engineering design of backfill systems in undercut mining. CIM Bulletin, 100 (1103), 1-7 (Paper 23).

Dong, L., Tong, X., Li, X., Zhou, J., Wang, S., & Liu, B. (2019b). Some developments and new insights of environmental problems and deep mining strategy for cleaner production in mines. Journal of Cleaner Production, 210, 1562-1578.

Dong, Q., Liang, B., Jia, L., & Jiang, L. (2019a). Effect of sulfide on the long-term strength of lead-zinc tailings cemented paste backfill. Construction and Building Materials, 200, 436-446.

Drif, B., Taha, Y., Hakkou, R., & Benzaazoua, M. (2021). Integrated valorization of silver mine tailings through silver recovery and ceramic materials production. Minerals Engineering, 170, 107060.

Dudeney, A. W. L., Chan, B. K. C., Bouzalakos, S., & Huisman, J. L. (2013). Management of waste and wastewater from mineral industry processes, especially leaching of sulphide resources: state of the art. International Journal of Mining, Reclamation and Environment, 27(1), 2-37.

Eker, H., & Bascetin, A. (2022). Influence of silica fume on mechanical property of cemented paste backfill. Construction and Building Materials, 317, 126089.

El Mahboub, K., Mbonimpa, M., Belem, T., & Maqsoud, A. (2022). Rheological characterization of cemented paste backfills containing superabsorbent polymers (SAPs). Construction and Building Materials, 317, 125863.

Elghali, A., Benzaazoua, M., Bussière, B., & Bouzahzah, H. (2019). Determination of the available acid-generating potential of waste rock, part II: Waste management involvement. Applied Geochemistry, 100, 316-325.

Ercikdi, B., Yilmaz, T., & Kulekci, G. (2014). Strength and ultrasonic properties of cemented paste backfill. Ultrasonics, 54(1), 195-204.

Erguler, G. K., Erguler, Z. A., Akcakoca, H., & Ucar, A. (2014). The effect of column dimensions and particle size on the results of kinetic column test used for acid mine drainage (AMD) prediction. Minerals Engineering, 55, 18-29.

Ettoumi, M., Jouini, M., Neculita, C. M., Bouhlel, S., Coudert, L., Taha, Y., & Benzaazoua, M. (2021). Characterization of phosphate processing sludge from Tunisian mining basin and its potential valorization in fired bricks making. Journal of Cleaner Production, 284, 124750.

Fahey, M., Helinski, M., & Fourie, A.B. (2009). Some aspects of the mechanics of arching in the paste backfilled stopes. Canadian Geotechnical Journal, 46 (11), 1322-1336.

Falagán, C., Grail, B. M., & Johnson, D. B. (2017). New approaches for extracting and recovering metals from mine tailings. Minerals Engineering, 106, 71-78.

Fall, M., & Pokharel, M. (2010). Coupled effects of sulphate and temperature on the strength development of cemented tailings backfills: Portland cement-paste backfill. Cement and Concrete Composites, 32(10), 819-828.

Fall, M., Belem, T., Samb, S., & Benzaazoua, M. (2007). Experimental characterization of the stress-strain behaviour of cemented paste backfill in compression. Journal of Materials Science, 42(11), 3914-3922.

Fall, M., Benzaazoua, M., & Ouellet, S. (2005). Experimental characterization of the influence of tailings fineness and density on the quality of cemented paste backfill. Minerals Engineering, 18(1), 41-44.

Fang, K., Cui, L., & Fall, M. (2020). A coupled chemo-elastic cohesive zone model for backfill-rock interface. Computers and Geotechnics, 125, 103666.

Fang, K., Fall, M., & Cui, L. (2021). Thermo-chemo-mechanical cohesive zone model for cemented paste backfill-rock interface. Engineering Fracture Mechanics, 244, 107546.

Figueiredo, J., Vila, M. C., Fiúza, A., Góis, J., Futuro, A., Dinis, M. L., & Martins, D. (2019a). A holistic approach in re-mining old tailings deposits for the supply of critical-metals: A Portuguese case study. Minerals, 9(10), 638.

Figueiredo, J., Vila, M. C., Góis, J., Biju, B. P., Futuro, A., Martins, D., & Fiúza, A. (2019b). Bi-level depth assessment of an abandoned tailings dam aiming its reprocessing for recovery of valuable metals. Minerals Engineering, 133, 1-9.

Fontes, W. C., de Carvalho, J. M. F., Andrade, L. C., Segadães, A. M., & Peixoto, R. A. (2019). Assessment of the use potential of iron ore tailings in the manufacture of ceramic tiles: From tailings-dams to “brown porcelain”. Construction and Building Materials, 206, 111-121.

Fourie, A.B., Fahey, H., & Helinski, M. (2007). Using effective stress theory to characterize the behaviour of backfill. CIM Bulletin, 100 (1103), 1-9 (Paper 27).

Fourie, A.B., Helinski, M., & Fahey, M. (2006). Filling the gap – a geomechanics perspective. ACG Newsletter, 26 (5), 1-4.

Galvão, J. L. B., Andrade, H. D., Brigolini, G. J., Peixoto, R. A. F., & Mendes, J. C. (2018). Reuse of iron ore tailings from tailings dams as pigment for sustainable paints. Journal of Cleaner Production, 200, 412-422.

Ghasemi, Y., Emborg, M., & Cwirzen, A. (2019). Exploring the relation between the flow of mortar and specific surface area of its constituents. Construction and Building Materials, 211, 492-501.

Giergiczny, Z. (2019). Fly ash and slag. Cement and Concrete Research, 124, 105826.

Grabinsky, M., Bawden, W., & Thompson, B. (2021). Required plug strength for continuously poured cemented paste backfill in longhole stopes. Mining, 1 (1), 80-99.

Guo, Z., Sun, X., Zhang, X., Qiu, J., Jiang, H., Zhao, Y., ... & Zhang, Q. (2022). Effect of superplasticizer on rheology and thixotropy of superfine-tailings cemented paste backfill: Experiment and modelling. Construction and Building Materials, 316, 125693.

Han, F., Zhang, Z., Wang, D., & Yan, P. (2015). Hydration heat evolution and kinetics of blended cement containing steel slag at different temperatures. Thermochimica Acta, 605, 43-51.

Hane, I., Belem, T., Benzaazoua, M., & Maqsoud, A. (2017). Laboratory characterization of cemented tailings paste containing crushed waste rocks for improved compressive strength development. Geotechnical and Geological Engineering, 35 (2), 645-662.

Haruna, S., & Fall, M. (2020). Time-and temperature-dependent rheological properties of cemented paste backfill that contains superplasticizer. Powder Technology, 360, 731-740.

Hassani, F.P., Ouellet, J., & Hossein, M. (2001). Strength development in underground high-sulphate paste backfill operation. CIM Bulletin, 94 (1050), 57-62.

Hassani, F., Razavi, S.M., & Isagon, I. (2007). A study of physical and mechanical behaviour of gel fill. CIM Bulletin, 100 (1103), 1-7 (Paper 28).

Helinski, M., Fahey, M., & Fourie, A. (2007a). Numerical modelling of cemented paste backfill deposition. Journal of Geotechnical and Geoenvironmental Engineering, 13 (10), 1308-1319.

Helinski, M., Fourie, A.B., Fahey, F., & Ismail, M. (2007b). Assessment of the self-desiccation process in cemented mine backfills. Canadian Geotechnical Journal, 44 (10), 1148-1156.

He, R., Zhang, S., Zhang, X., Zhang, Z., Zhao, Y., & Ding, H. (2021). Copper slag: The leaching behavior of heavy metals and its applicability as a supplementary cementitious material. Journal of Environmental Chemical Engineering, 9(2), 105132.

He, X., Yuhua, Z., Qaidi, S., Isleem, H. F., Zaid, O., Althoey, F., & Ahmad, J. (2022). Mine tailings-based geopolymers: A comprehensive review. Ceramics International.

He, Y., Chen, Q., Qi, C., Zhang, Q., & Xiao, C. (2019). Lithium slag and fly ash-based binder for cemented fine tailings backfill. Journal of Environmental Management, 248, 109282.

He, Y., Zhang, Q., Chen, Q., Bian, J., Qi, C., Kang, Q., & Feng, Y. (2021). Mechanical and environmental characteristics of cemented paste backfill containing lithium slag-blended binder. Construction and Building Materials, 271, 121567.

He, Z., Zhu, X., Wang, J., Mu, M., & Wang, Y. (2019b). Comparison of CO2 emissions from OPC and recycled cement production. Construction and Building Materials, 211, 965-973.

Hossain, M. M., Karim, M. R., Hasan, M., Hossain, M. K., & Zain, M. F. M. (2016). Durability of mortar and concrete made up of pozzolans as a partial replacement of cement: A review. Construction and building materials, 116, 128-140.

Huang, S., Xia, K., & Qiao, L. (2011). Dynamic tests of cemented paste backfill: effects of strain rate, curing time, and cement content on compressive strength. Journal of Materials Science, 46(15), 5165-5170.

Huang, Y., Wang, Q., & Shi, M. (2017). Characteristics and reactivity of ferronickel slag powder. Construction and Building Materials, 156, 773-789.

Huang, Z., Yilmaz, E., & Cao, S. (2021a). Analysis of strength and microstructural characteristics of mine backfills containing fly ash and desulfurized gypsum. Minerals, 11(4), 409.

Huang, Z., Cao, S., & Yilmaz, E. (2021b). Investigation on the flexural strength, failure pattern and microstructural characteristics of combined fibers reinforced cemented tailings backfill. Construction and Building Materials, 300, 124005.

Ighalo, J. O., Kurniawan, S. B., Iwuozor, K. O., Aniagor, C. O., Ajala, O. J., Oba, S. N., Iwuchukwu, F. U., Ahmadi S., & Igwegbe, C. A. (2022). A review of treatment technologies for the mitigation of the toxic environmental effects of acid mine drainage (AMD). Process Safety and Environmental Protection, 157, 37-58.

Jafari, M., & Grabinsky, M. (2021). Effect of hydration on failure surface evolution of low sulfide content cemented paste backfill. International Journal of Rock Mechanics and Mining Sciences, 144, 104749.

Jafari, M., Shahsavari, M., & Grabinsky, M. (2021). Drained triaxial compressive shear response of cemented paste backfill (CPB). Rock Mechanics and Rock Engineering, 54 (6), 3309-3325.

Jafari, M., Shahsavari, M., & Grabinsky, M. (2019). Hydration effects on specific gravity and void ratio of cemented paste backfill. Geotechnical Testing Journal, 43(5), 1300-1316.

Jia, H.W., Yan, B.X., & Yilmaz, E. (2021). A large goaf group treatment by means of mine backfill technology. Advances in Civil Engineering, 2021, 3737145.

Jiang, D., Li, X., Jiang, W., Li, C., Lv, Y., & Zhou, Y. (2020). Effect of tricalcium aluminate and sodium aluminate on thaumasite formation in cement paste. Construction and Building Materials, 259, 119842.

Jiang, H.Q., Han, J., Li, Y., Yilmaz, E., Sun, Q., & Liu, J. (2020a). Relationship between ultrasonic pulse velocity and uniaxial compressive strength for cemented paste backfill with alkali-activated slag. Nondestructive Testing and Evaluation, 35(4), 359-377.

Jiang, H.Q., Fall, M., Yilmaz, E., Yang, L., & Ren, L. (2020b). Effect of mineral admixtures on flow properties of fresh cemented paste backfill: Assessment of time dependency and thixotropy. Powder Technology, 372, 258-266.

Jiang, H.Q., Yi, H., Yilmaz, E., Liu, S., & Qiu, J. (2020c). Ultrasonic evaluation of strength properties of cemented paste backfill: Effects of mineral admixture and curing temperature. Ultrasonics, 100, 105983.

Jiang, H.Q., Fall, M., Li, Y., & Han, J. (2019a). An experimental study on compressive behaviour of cemented rockfill. Construction and Building Materials, 213, 10-19.

Jiang, H.Q., Qi, Z., Yilmaz, E., Han, J., Qiu, J., & Dong, C. (2019b). Effectiveness of alkali-activated slag as alternative binder on workability and early age compressive strength of cemented paste backfills. Construction and Building Materials, 218, 689-700.

Jin, J., Qin, Z., Zuo, S., Feng, J., & Sun, Q. (2022). The role of rheological additives on fresh and hardened properties of cemented paste backfill. Materials, 15(9), 3006.

Kasap, T., Yilmaz, E., Guner, N. U., & Sari, M. (2022a). Recycling dam tailings as cemented mine backfill: Mechanical and geotechnical properties. Advances in Materials Science and Engineering, 2022, 6993068.

Kasap, T., Yilmaz, E., & Sari, M. (2022b) Physico-chemical and micro-structural behavior of cemented mine backfill: Effect of pH in dam tailings. Journal of Environmental Management, 314, 115034.

Ke, X., Zhou, X., Wang, X., Wang, T., Hou, H., & Zhou, M. (2016). Effect of tailings fineness on the pore structure development of cemented paste backfill. Construction and Building Materials, 126, 345-350.

Kesimal, A., Yilmaz, E., Ercikdi, B., Alp, I., & Deveci, H. (2005). Effect of properties of tailings and binder on the short-and long terms strength and stability of cemented paste backfill. Materials Letters, 59(28), 3703-3709.

Kesimal, A., Yilmaz, E., & Ercikdi, B. (2004). Evaluation of paste backfill mixtures consisting of sulphide-rich mill tailings and varying cement contents. Cement and Concrete Research, 34(10), 1817-1822.

Kesimal, A., Yilmaz, E., Ercikdi, B., Alp, I., Yumlu, M., & Ozdemir, B. (2003a) Paste backfill technology in underground mining: A case study. Turkish Journal of Earth Sciences Review, 16 (1), 45-53.

Kesimal, A., Ercikdi, B., & Yilmaz, E. (2003b). The effect of desliming by sedimentation on paste backfill performance. Minerals Engineering, 16 (10) 1009-1011.

Kesimal, A., Yilmaz, E., Ercikdi, B., Alp, I., Yumlu, M., & Ozdemir, B. (2002). Laboratory testing of cemented paste backfill. Madencilik – Scientific Mining Journal, 41 (4), 11-20.

Khudyakov, A. Y., & Vashchenko, S. V. (2020). Analysis of known dependences and the construction of new compaction equations for the fine-fraction materials of the mining and metallurgical complex. Refractories and Industrial Ceramics, 60(6), 618-626.

Kinnunen, P., Ismailov, A., Solismaa, S., Sreenivasan, H., Räisänen, M. L., Levänen, E., & Illikainen, M. (2018). Recycling mine tailings in chemically bonded ceramics–a review. Journal of Cleaner Production, 174, 634-649.

Kiventerä, J., Perumal, P., Yliniemi, J., & Illikainen, M. (2020). Mine tailings as a raw material in alkali activation: A review. International Journal of Minerals, Metallurgy and Materials, 27(8), 1009-1020.

Koohestani, B., Mokhtari, P., Yilmaz, E., Mahdipour, F., & Darban, A. K. (2021). Geopolymerization mechanism of binder-free mine tailings by sodium silicate. Construction and Building Materials, 268, 121217.

Koohestani, B., Darban, A.K., Mokhtari, P., Darezereshki, E., Yilmaz, E., & Yilmaz, E. (2020). Influence of hydrofluoric acid leaching and roasting on mineralogical phase transformation of pyrite in sulfidic mine tailings. Minerals, 10(6), 513.

Koohestani, B., Darban, A. K., Darezereshki, E., Mokhtari, P., Yilmaz, E., & Yilmaz, E. (2018). The influence of sodium and sulfate ions on total solidification and encapsulation potential of iron-rich acid mine drainage in silica gel. Journal of Environmental Chemical Engineering, 6(2), 3520-3527.

Kou, Y., Jiang, H., Ren, L., Yilmaz, E., & Li, Y. (2020). Rheological properties of cemented paste backfill with alkali-activated slag. Minerals, 10(3), 288.

Koupouli, N.J.F., Belem, T., Rivard, P., & Effenguet, H. (2016). Direct shear tests on cemented paste backfill-rock wall and cemented paste backfill-backfill interfaces. Journal of Rock Mechanics and Geotechnical Engineering, 8 (4), 472-479.

Krishna, R.S., Shaikh, F., Mishra, J., Lazorenko, G., & Kasprzhitskii, A. (2021). Mine tailings-based geopolymers: Properties, applications and industrial prospects. Ceramics International, 47 (1), 17826-17843.

Kulekci, G., Ercikdi, B., & Aliyazicioglu, S. (2016). Effect of waste brick as mineral admixture on the mechanical performance of cemented paste backfill. IOP Conference Series: Earth and Environmental Science, 44(4), 042039.

le Roux, K., Bawden, W.F., & Grabinsky, M.W. (2005). Field properties of cemented paste backfill at the Golden Giant mine. Mining Technology, 114 (2), 65-80.

Li, H., Wu, A., & Wang, H. (2019a). Evaluation of short-term strength development of cemented backfill with varying sulphide contents and the use of additives. Journal of Environmental Management, 239, 279-286.

Li, J., Cao, S., Yilmaz, E., & Liu, Y. (2022). Compressive fatigue behavior and failure evolution of additive fiber-reinforced cemented tailings composites. International Journal of Minerals, Metallurgy and Materials, 29(2), 345-355.

Li, J., Cao, S., & Yilmaz, E. (2021a). Characterization of macro mechanical properties and microstructures of cement-based composites prepared from fly ash, gypsum and steel slag. Minerals, 12(1), 6.

Li, J., Yilmaz, E., & Cao, S. (2021b). Influence of industrial solid waste as filling material on mechanical and microstructural characteristics of cementitious backfills. Construction and Building Materials, 299, 124288.

Li, J., Yilmaz, E., & Cao, S. (2020). Influence of solid content, cement/tailings ratio, and curing time on rheology and strength of cemented tailings backfill. Minerals, 10(10), 922.

Li, J., Zhang, S., Wang, Q., Ni, W., Li, K., Fu, P., & Li, Z. (2020). Feasibility of using fly ash-slag-based binder for mine backfilling and its associated leaching risks. Journal of Hazardous Materials, 400, 123191.

Li, Q., Zhang, L., Gao, X., & Zhang, J. (2020c). Effect of pulverized fuel ash, ground granulated blast-furnace slag and CO2 curing on performance of magnesium oxysulfate cement. Construction and Building Materials, 230, 116990.

Li, W., & Fall, M. (2018). Strength and self-desiccation of slag-cemented paste backfill at early ages: Link to initial sulphate concentration. Cement and Concrete Composites, 89, 160-168.

Li, W., & Fall, M. (2016). Sulphate effect on the early age strength and self-desiccation of cemented paste backfill. Construction and Building Materials, 106, 296-304.

Li, W., Sun, Y., Xin, M., Bian, R., Wang, H., Wang, Y. N., & Zhang, D. (2020d). Municipal solid waste incineration fly ash exposed to carbonation and acid rain corrosion scenarios: Release behavior, environmental risk, and dissolution mechanism of toxic metals. Science of the Total Environment, 744, 140857.

Li, Y., Min, X., Ke, Y., Fei, J., Liu, D., & Tang, C. (2019). Immobilization potential and immobilization mechanism of arsenic in cemented paste backfill. Minerals Engineering, 138, 101-107.

Libos, I. L. S., & Cui, L. (2020). Effects of curing time, cement content, and saturation state on mode-I fracture toughness of cemented paste backfill. Engineering Fracture Mechanics, 235, 107174.

Libos, I., Cui, L., & Liu, X. (2021). Effect of curing temperature on time-dependent shear behavior and properties of polypropylene fiber-reinforced cemented paste backfill. Construction and Building Materials, 311, 125302.

Lindsay, M. B., Moncur, M. C., Bain, J. G., Jambor, J. L., Ptacek, C. J., & Blowes, D. W. (2015). Geochemical and mineralogical aspects of sulfide mine tailings. Applied Geochemistry, 57, 157-177.

Liu, L., Xin, J., Qi, C.C., Jia, H., & Song, K. I. (2020). Experimental investigation of mechanical, hydration, microstructure and electrical properties of cemented paste backfill. Construction and Building Materials, 263, 120137.

Liu, L., Zhu, C., Qi, C.C., Zhang, B., & Song, K. I. (2019a). A microstructural hydration model for cemented paste backfill considering internal sulfate attacks. Construction and Building Materials, 211, 99-108.

Liu, L., Fang, Z., Qi, C.C., Zhang, B., Guo, L., & Song, K. I. (2019b). Numerical study on the pipe flow characteristics of the cemented paste backfill slurry considering hydration effects. Powder Technology, 343, 454-464.

Liu, S. G., & Fall, M. (2022). Fresh and hardened properties of cemented paste backfill: Links to mixing time. Construction and Building Materials, 324, 126688.

Lu, H., Qi, C.C., Li, C., Gan, D., Du, Y., & Li, S. (2020). A light barricade for tailings recycling as cemented paste backfill. Journal of Cleaner Production, 247, 119388.

Lu, H., Qi, C.C., Chen, Q., Gan, D., Xue, Z., & Hu, Y. (2018). A new procedure for recycling waste tailings as cemented paste backfill to underground stopes and open pits. Journal of Cleaner Production, 188, 601-612.

Ma, D., Kong, S., Li, Z., Zhang, Q., Wang, Z., & Zhou, Z. (2021). Effect of wetting-drying cycle on hydraulic and mechanical properties of cemented paste backfill of the recycled solid wastes. Chemosphere, 282, 131163.

Mangane, M. B. C., Argane, R., Trauchessec, R., Lecomte, A., & Benzaazoua, M. (2018). Influence of superplasticizers on mechanical properties and workability of cemented paste backfill. Minerals Engineering, 116, 3-14.

Mbonimpa, M., Kwizera, P., & Belem, T. (2019). Mine backfilling in the permafrost, part II: effect of declining curing temperature on the short-term unconfined compressive strength of cemented paste backfills. Minerals 9 (3), 172.

McLean, J., & Cui, L. (2021). Multiscale geomechanical behavior of fiber-reinforced cementitious composites under cyclic loading conditions-A review. Frontiers in Materials, 8, 759126.

Menzel, K., Barros, L., García, A., Ruby-Figueroa, R., & Estay, H. (2021). Metal sulfide precipitation coupled with membrane filtration process for recovering copper from acid mine drainage. Separation and Purification Technology, 270, 118721.

Mohammed, A.M.O., Hossein, M., & Hassani, F.P. (2002). Hydromechanical evaluation of stabilized mine tailings. International Journal of Environmental Geology, 41 (7), 749-759.

Nasharuddin, R., Luo, G., Robinson, N., Fourie, A., Johns, M.L., & Fridjonsson, E.O. (2021). Understanding the microstructural evolution of hypersaline cemented paste backfill with low-field NMR relaxation. Cement and Concrete Research, 147, 106516.

Nasir, O., & Fall, M. (2010). Coupling binder hydration, temperature and compressive strength development of underground cemented paste backfill at early ages. Tunnelling and Underground Space Technology, 25(1), 9-20.

Niroshan, N., Sivakugan, N., & Veenstra, R. L. (2018). Flow characteristics of cemented paste backfill. Geotechnical and Geological Engineering, 36(4), 2261-2272.

Orejarena, L., & Fall, M. (2010). The use of artificial neural networks to predict the effect of sulphate attack on the strength of cemented paste backfill. Bulletin of Engineering Geology and the Environment, 69(4), 659-670.

Ouattara, D., Belem, T., Mbonimpa, M., & Yahia, A. (2018). Effect of superplasticizers on the consistency and unconfined compressive strength of cemented paste backfills. Construction and Building Materials, 181, 59-72.

Ouellet, S., Bussière, B., Aubertin, M., & Benzaazoua, M. (2007). Microstructural evolution of cemented paste backfill: Mercury intrusion porosimetry test results. Cement and Concrete Research, 37(12), 1654-1665.

Ouffa, N., Trauchessec, R., Benzaazoua, M., Lecomte, A., & Belem, T. (2022). A methodological approach applied to elaborate alkali-activated binders for mine paste backfills. Cement and Concrete Composites, 127, 104381.

Ouyang, J., Liu, Z., Zhang, L., Wang, Y., & Zhou, L. (2020). Analysis of influencing factors of heavy metals pollution in farmland-rice system around a uranium tailings dam. Process Safety and Environmental Protection, 139, 124-132.

Pan, A., Jafari, M., Guo, L., & Grabinsky, M. (2021). Hybrid failure of cemented paste backfill. Minerals, 11 (10), 1141.

Panchal, S., Deb, D., & Sreenivas, T. (2018). Variability in rheology of cemented paste backfill with hydration age, binder and superplasticizer dosages. Advanced Powder Technology, 29(9), 2211-2220.

Parbhakar-Fox, A., Lottermoser, B., & Bradshaw, D. (2013). Evaluating waste rock mineralogy and microtexture during kinetic testing for improved acid rock drainage prediction. Minerals Engineering, 52, 111-124.

Park, I., Tabelin, C. B., Jeon, S., Li, X., Seno, K., Ito, M., & Hiroyoshi, N. (2019). A review of recent strategies for acid mine drainage prevention and mine tailings recycling. Chemosphere, 219, 588-606.

Pirapakaran, K., & Sivakugan, N. (2007). A laboratory model to study arching within a hydraulic fill stope. Geotechnical Testing Journal, 30(6), 496-503.

Pokharel, M., & Fall, M. (2013). Combined influence of sulphate and temperature on the saturated hydraulic conductivity of hardened cemented paste backfill. Cement and Concrete Composites, 38, 21-28.

Qi, C.C., & Fourie, A. (2019). Cemented paste backfill for mineral tailings management: Review and future perspectives. Minerals Engineering, 144, 106025.

Qi, C.C., Chen, Q.S., Fourie, A., Tang, X.L., Zhang, Q.L., Dong, X.J., & Feng, Y. (2019). Constitutive modelling of cemented paste backfill: A data-mining approach. Construction and Building Materials, 197, 262-270.

Qi, C.C, Fourie, A., & Chen, Q.S. (2018a) Neural network and particle swarm optimization for predicting the unconfined compressive strength of cemented paste backfill. Construction and Building Materials, 159, 473-478.

Qi, C., Chen, Q., Fourie, A., Zhao, J., & Zhang, Q. (2018b). Pressure drop in pipe flow of cemented paste backfill: Experimental and modeling study. Powder Technology, 333, 9-18.

Qi, C.C., Fourie, A., Chen, Q., & Zhang, Q. (2018c). A strength prediction model using artificial intelligence for recycling waste tailings as cemented paste backfill. Journal of Cleaner Production, 183, 566-578.

Qiao, D., Wang, G., Li, X., Wang, S., & Zhao, Y. (2020). Pollution, sources and environmental risk assessment of heavy metals in the surface AMD water, sediments and surface soils around unexploited Rona Cu deposit, Tibet, China. Chemosphere, 248, 125988.

Qin, J., Zheng, J., & Li, L. (2021). Experimental study of the shrinkage behavior of cemented paste backfill. Journal of Rock Mechanics and Geotechnical Engineering, 13(3), 545-554.

Qin, S.W., Cao, S., & Yilmaz, E. (2022). Employing U-shaped 3D printed polymer to improve flexural properties of cementitious tailings backfills. Construction and Building Materials, 320, 126296.

Qin, S.W., Cao, S., Yilmaz, E., & Li, J.J. (2021). Influence of types and shapes of 3D printed polymeric lattice on ductility performance of cementitious backfill composites. Construction and Building Materials, 307, 124973.

Qiu, J., Guo, Z., Yang, L., Jiang, H., & Zhao, Y. (2020). Effect of tailings fineness on flow, strength, ultrasonic and microstructure characteristics of cemented paste backfill. Construction and Building Materials, 263, 120645.

Qiu, J., Zhao, Y., Xing, J., & Sun, X. (2019). Fly ash/blast furnace slag-based geopolymer as a potential binder for mine backfilling: effect of binder type and activator concentration. Advances in Materials Science and Engineering, 2019.

Rankine, K.J., Sivakugan, N., & Cowling, R.M. (2006). Emplaced geotechnical characteristics of hydraulic fills in a number of Australian mines. Geotechnical and Geological Engineering, 24 (1), 1-14.

Rezaie, B., & Anderson, A. (2020). Sustainable resolutions for environmental threat of the acid mine drainage. Science of the Total Environment, 717, 137211.

Robinson, N., Nasharuddin, R., Luo, G., Fourie, A., Fridjonsson, E.O., & Johns, M.L. (2021). Pore structure evolution of cemented paste backfill observed with two-dimensional NMR relaxation correlation measurements. Industrial and Engineering Chemistry Research, 60 (36), 13253-64.

Saedi, A., Jamshidi-Zanjani, A., & Darban, A. K. (2021). A review of additives used in the cemented paste tailings: Environmental aspects and application. Journal of Environmental Management, 289, 112501.

Sari, M., Yilmaz, E., Kasap, T., & Guner, N. U. (2022). Strength and microstructure evolution in cemented mine backfill with low and high pH pyritic tailings: Effect of mineral admixtures. Construction and Building Materials, 328, 127109.

Siddique, S., & Jang, J. G. (2020). Assessment of molybdenum mine tailings as filler in cement mortar. Journal of Building Engineering, 31, 101322.

Simonsen, A. M. T., Solismaa, S., Hansen, H. K., & Jensen, P. E. (2020). Evaluation of mine tailings' potential as supplementary cementitious materials based on chemical, mineralogical and physical characteristics. Waste Management, 102, 710-721.

Simms, P., & Grabinsky, M. (2009). Direct measurement of matric suction in triaxial tests on early-age cemented paste backfill. Canadian Geotechnical Journal, 46 (1), 93-101.

Singh, P. K., Roy, M. P., Paswan, R. K., Dubey, R. K., & Drebenstedt, C. (2015). Blast vibration effects in an underground mine caused by open-pit mining. International Journal of Rock Mechanics and Mining Sciences, 80, 79-88.

Sivakugan, N., Veenstra, R., & Naguleswaran, N. (2015). Underground mine backfilling in Australia using paste fills and hydraulic fills. International Journal of Geosynthetics and Ground Engineering, 1(2), 1-7.

Sivakugan, N., Rankine, K., Lovisa, J., & Hall, W. (2013). Flow rate computations in hydraulic fill mine stopes. Indian Geotechnical Journal, 43(3), 195-202.

Skrzypkowski, K. (2021). 3d numerical modelling of the application of cemented paste backfill on displacements around strip excavations. Energies, 14(22), 7750.

Stone, D. (2007). Factors that affect cemented rock fill quality in Nevada mines. CIM Bulletin, 100 (1103), 1-6 (Paper 24).

Sun, X., Liu, J., Qiu, J., Wu, P., & Zhao, Y. (2022). Alkali activation of blast furnace slag using a carbonate-calcium carbide residue alkaline mixture to prepare cemented paste backfill. Construction and Building Materials, 320, 126234.

Sun, X., Zhao, Y., Tian, Y., Wu, P., Guo, Z., Qiu, J., Xing, J., & Xiaowei, G. (2021). Modification of high-volume fly ash cement with metakaolin for its utilization in cemented paste backfill: The effects of metakaolin content and particle size. Powder Technology, 393, 539-549.

Tariq, A., & Yanful, E. K. (2013). A review of binders used in cemented paste tailings for underground and surface disposal practices. Journal of environmental management, 131, 138-149.

Thompson, B.D., Bawden, W.F., & Grabinsky, M.W. (2012). In situ measurements of cemented paste backfill at the Cayeli Mine. Canadian Geotechnical Journal, 49 (7), 755-772.

Tian, X., & Fall, M. (2021). Non-isothermal evolution of mechanical properties, pore structure and self-desiccation of cemented paste backfill. Construction and Building Materials, 297, 123657.

Toubri, Y., Plante, B., Demers, I., & Fillion, M. (2022). Probing cleaner production opportunities of the Lac Tio pyrite-enriched tailings generated to alleviate sulfur dioxide emissions. Journal of Cleaner Production, 357, 132027.

Tuylu S., Bascetin A., & Adiguzel, D. (2019). The effects of cement on some physical and chemical behavior for surface paste disposal method. Journal of Environmental Management, 231, 33-40.

Ustabas, I., Erdogdu, S., Omur, I., & Yilmaz, E. (2021). Pozzolanic effect on the hydration heat of cements incorporating fly ash, obsidian, and slag additives. Advances in Civil Engineering, 2021.

Wang, A., Cao, S., & Yilmaz, E. (2022a). Effect of height to diameter ratio on dynamic characteristics of cemented tailings backfills with fiber reinforcement through impact loading. Construction and Building Materials, 322, 126448.

Wang, A., Cao, S., & Yilmaz, E. (2022b). Influence of types and contents of nano cellulose materials as reinforcement on stability performance of cementitious tailings backfill. Construction and Building Materials, 344, 128179.

Wang, L., Guo, F., Lin, Y., Yang, H., & Tang, S. W. (2020). Comparison between the effects of phosphorous slag and fly ash on the CSH structure, long-term hydration heat and volume deformation of cement-based materials. Construction and Building Materials, 250, 118807.

Wang, L., Li, Y., Wang, H., Cui, X., Wang, X., Lu, A., & Gan, D. (2017). Weathering behavior and metal mobility of tailings under an extremely arid climate at Jinchuan Cu-Ni sulfide deposit, Western China. Journal of Geochemical Exploration, 173, 1-12.

Wang, S. F., Sun, L. C., Huang, L. Q., Li, X. B., Ying, S. H. I., Yao, J. R., & Du, S. L. (2019). Non-explosive mining and waste utilization for achieving green mining in underground hard rock mine in China. Transactions of Nonferrous Metals Society of China, 29(9), 1914-1928.

Wang, Y., Cao, Y., Cui, L., Si, Z., & Wang, H. (2020). Effect of external sulfate attack on the mechanical behavior of cemented paste backfill. Construction and Building Materials, 263, 120968.

Wang, Y., Fall, M., & Wu, A. (2016). Initial temperature-dependence of strength development and self-desiccation in cemented paste backfill that contains sodium silicate. Cement and Concrete Composites, 67, 101-110.

Wang, Z., Wang, Y., Cui, L., Bi, C., & Wu, A. (2022c). Insight into the isothermal multiphysics processes in cemented paste backfill: Effect of curing time and cement-to-tailings ratio. Construction and Building Materials, 325, 126739.

Wu, A., Wang, Y., Wang, H., Yin, S., & Miao, X. (2015). Coupled effects of cement type and water quality on the properties of cemented paste backfill. International Journal of Mineral Processing, 143, 65-71.

Wu, A., Wang, Y., Zhou, B., & Shen, J. (2016). Effect of initial backfill temperature on the deformation behavior of early age cemented paste backfill that contains sodium silicate. Advances in Materials Science and Engineering, 2016.

Wu, J., Feng, M., Xu, J., Qiu, P., Wang, Y., & Han, G. (2018). Particle size distribution of cemented rockfill effects on strata stability in filling mining. Minerals, 8(9), 407.

Xiao, B., Fall, M., & Roshani, A. (2021a). Towards understanding the rheological properties of Slag-Cemented paste backfill. International Journal of Mining, Reclamation and Environment, 35(4), 268-290.

Xiao, B., Wen, Z., Miao, S., & Gao, Q. (2021b). Utilization of steel slag for cemented tailings backfill: Hydration, strength, pore structure, and cost analysis. Case Studies in Construction Materials, 15, e00621.

Xiaolong, Z., Shiyu, Z., Hui, L., & Yingliang, Z. (2021). Disposal of mine tailings via geopolymerization. Journal of Cleaner Production, 284, 124756.

Xiapeng, P., Fall, M., & Haruna, S. (2019). Sulphate induced changes of rheological properties of cemented paste backfill. Minerals Engineering, 141, 105849.

Xiu, Z., Wang, S., Ji, Y., Wang, F., & Ren, F. (2022). Experimental study on the triaxial mechanical behaviors of the cemented paste backfill: effect of curing time, drainage conditions and curing temperature. Journal of Environmental Management, 301, 113828.

Xu, W., & Cao, P. (2018). Fracture behaviour of cemented tailing backfill with pre-existing crack and thermal treatment under three-point bending loading: Experimental studies and particle flow code simulation. Engineering Fracture Mechanics, 195, 129-141.

Xue, G.L., & Yilmaz, E. (2022). Strength, acoustic, and fractal behavior of fiber reinforced cemented tailings backfill subjected to triaxial compression loads. Construction and Building Materials, 338, 127667.

Xue, G.L., Yilmaz, E., Feng, G., & Cao, S. (2022). Analysis of tensile mechanical characteristics of fibre reinforced backfill through splitting tensile and three-point bending tests. International Journal of Mining, Reclamation and Environment, 36(3), 218-234.

Xue, G.L., Yilmaz, E., Feng, G., & Cao, S. (2021a). Bending behavior and failure mode of cemented tailings backfill composites incorporating different fibers for sustainable construction. Construction and Building Materials, 289, 123163.

Xue, G.L., Yilmaz, E., Feng, G., Cao, S., & Sun, L.J. (2021b). Reinforcement effect of polypropylene fiber on dynamic properties of cemented tailings backfill under SHPB impact loading. Construction and Building Materials, 279, 122417.

Xue, G.L., Yilmaz, E., Song, W., & Cao, S. (2020). Fiber length effect on strength properties of polypropylene fiber reinforced cemented tailings backfill

specimens with different sizes. Construction and Building Materials, 241, 118113.

Xue, G.L., Yilmaz, E., Song, W.D., & Cao, S. (2019a). Analysis of internal structure behavior of fiber reinforced cement-tailings matrix composites through X-ray computed tomography. Composites Part B: Engineering, 175, 107090.

Xue, G.L., Yilmaz, E., Song, W.D., & Cao, S. (2019b). Mechanical, flexural and microstructural properties of cement-tailings matrix composites: Effects of fiber type and dosage. Composites Part B: Engineering, 172, 131-142.

Xue, G.L., Yilmaz, E., Song, W.D., & Yilmaz, E. (2019c). Influence of fiber reinforcement on mechanical behavior and microstructural properties of cemented tailings backfill. Construction and Building Materials, 213, 275-285.

Xue, G.L., Yilmaz, E., Song, W., & Cao, S. (2018). Compressive strength characteristics of cemented tailings backfill with alkali-activated slag. Applied Sciences, 8(9), 1537.

Yan, B., Ren, F., Cai, M., & Qiao, C. (2019). Influence of new hydrophobic agent on the mechanical properties of modified cemented paste backfill. Journal of Materials Research and Technology, 8(6), 5716-5727.

Yan, B.X., Jia, H., Yilmaz, E., Lai, X., Shan, P., & Hou, C. (2022a). Numerical study on microscale and macroscale strength behaviors of hardening cemented paste backfill. Construction and Building Materials, 321, 126327.

Yan, B.X., Jia, H.W., Yilmaz, E., Lai, X.P., Shan, P.F., & Hou, C. (2022b). Numerical investigation of creeping rockmass interaction with hardening and shrinking cemented paste backfill. Construction and Building Materials, 340, 127639.

Yan, B.X., Lai, X., Jia, H., Yilmaz, E., & Hou, C. (2021). A solution to the time-dependent stress distribution in suborbicular backfilled stope interaction with creeping rock. Advances in Civil Engineering, 2021.

Yan, B.X., & Yilmaz, E. (2020a). Analytical solution for stress distribution in cementitious backfills considering stope inclinations. Recep Tayyip Erdoğan University Journal of Science and Engineering, 1 (2), 26-33.

Yan, B.X., Zhu, W., Hou, C., Yilmaz, E., & Saadat, M. (2020b). Characterization of early age behavior of cemented paste backfill through the magnitude and frequency spectrum of ultrasonic P-wave. Construction and Building Materials, 249, 118733.

Yang, L., Wang, H., Wu, A., Li, H., Bruno, T. A., Zhou, X., & Wang, X. (2020a). Effect of mixing time on hydration kinetics and mechanical property of cemented paste backfill. Construction and Building Materials, 247, 118516.

Yang, L., Xu, W.B., Yilmaz, E., Wang, Q., & Qiu, J. (2020b). A combined experimental and numerical study on the triaxial and dynamic compression behavior of cemented tailings backfill. Engineering Structures, 219, 110957.

Yang, L., Yilmaz, E., Li, J., Liu, H., & Jiang, H.Q. (2018). Effect of superplasticizer type and dosage on fluidity and strength behavior of cemented tailings backfill with different solid contents. Construction and Building Materials, 187, 290-298.

Yang, Y., Zhao, T., Jiao, H., Wang, Y., & Li, H. (2020). Potential effect of porosity evolution of cemented paste backfill on selective solidification of heavy metal ions. International Journal of Environmental Research and Public Health, 17(3), 814.

Yang, Y., Wei, Z., Fourie, A., Chen, Y., Zheng, B., Wang, W., & Zhuang, S. (2019). Particle shape analysis of tailings using digital image processing. Environmental Science and Pollution Research, 26(25), 26397-26403.

Yao, G., Zang, H., Wang, J., Wu, P., Qiu, J., & Lyu, X. (2019). Effect of mechanical activation on the pozzolanic activity of muscovite. Clays and Clay Minerals, 67(3), 209-216.

Yazici, S., & Arel, H.S. (2012). Effects of fly ash fineness on the mechanical properties of concrete. Sadhana, 37(3), 389-403.

Yi, X. W., Ma, G. W., & Fourie, A. (2015). Compressive behaviour of fibre-reinforced cemented paste backfill. Geotextiles and Geomembranes, 43(3), 207-215.

Yilmaz, E. (2018). Stope depth effect on field behaviour and performance of cemented paste backfills. International Journal of Mining, Reclamation and Environment, 32(4), 273-296.

Yilmaz, E. (2011). Advances in reducing large volumes of environmentally harmful mine waste rocks and tailings. Mineral Resources Management, 27, 89-112.

Yilmaz, E., & Yilmaz, E. (2018). Sustainability and tailings management in the mining industry: Paste technology. Mugla Journal of Science and Technology, 4 (1), 16-26.

Yilmaz, E., Cao, S., & Wu, D. (2022). Advances in design and implementation of cementitious backfills. Frontiers in Materials, 9, 964111.

Yilmaz, E., Belem, T., & Benzaazoua, M. (2015a). Specimen size effect on strength behavior of cemented paste backfills subjected to different placement conditions. Engineering Geology, 185, 52-62.

Yilmaz, E., Belem, T., Bussière, B., Mbonimpa, M., & Benzaazoua, M. (2015b). Curing time effect on consolidation behaviour of cemented paste backfill containing different cement types and contents. Construction and Building Materials, 75, 99-111.

Yilmaz, E., Belem, T., & Benzaazoua, M. (2014a). Effects of curing and stress conditions on hydromechanical, geotechnical and geochemical properties of cemented paste backfill. Engineering Geology, 168, 23-37.

Yilmaz, E., Benzaazoua, M., Bussière, B., & Pouliot, S. (2014b). Influence of disposal configurations on hydrogeological behaviour of sulphidic paste tailings: A field experimental study. International Journal of Mineral Processing, 131, 12-25.

Yilmaz, E., Belem, T., & Benzaazoua, M. (2013). Study of physico-chemical and mechanical characteristics of consoli-dated and unconsolidated cemented paste backfills. Mineral Resources Management, 29(1), 81-100.

Yilmaz, E., Belem, T., & Benzaazoua, M. (2012). One-dimensional consolidation parameters of cemented paste backfills. Mineral Resources Management, 28(4), 29-45.

Yilmaz, E., Belem, T., Benzaazoua, M., Kesimal, A., Ercikdi, B., & Cihangir, F. (2011a). Use of high-density paste backfill for safe disposal of copper/zinc mine tailings. Mineral Resources Management, 27(3), 81-94.

Yilmaz, E., Belem, T., Bussiere, B., & Benzaazoua, M. (2011b). Relationships between microstructural properties and compressive strength of consolidated and unconsolidated cemented paste backfill. Cement and Concrete Composites, 33(6), 351-362.

Yilmaz, E., Belem, T., Benzaazoua, M., & Bussière, B. (2010). Assessment of the modified CUAPS apparatus to estimate in situ properties of cemented paste backfill. Geotechnical Testing Journal, 33(5), 351-362.

Yilmaz, E., Benzaazoua, M., Belem, T., & Bussière, B. (2009). Effect of curing under pressure on compressive strength development of cemented paste backfill. Minerals Engineering, 22(9-10), 772-785.

Yilmaz, E., Belem, T., Benzaazoua, M., Kesimal, A., & Ercikdi, B. (2007). Evaluation of the strength properties of deslimed tailings paste backfill. The International Journal of Mineral Resources Engineering, 12 (2), 129-144.

Yilmaz, E., Kesimal, A., & Ercikdi, B. (2004). Evaluation of acid producing sulfidic mine tailings as a paste backfill. Turkish Journal of Earth Sciences Review, 17 (1), 11-19.

Yilmaz, E., Kesimal, A., & Ercikdi, B. (2003). The factors affecting the strength and stability of paste backfill. Yerbilimleri – Bulletin for Earth Sciences, 28 (2), 155-169.

Yilmaz, T., Ercikdi, B., & Cihangir, F. (2020). Evaluation of the neutralization performances of the industrial waste products (IWPs) in sulphide-rich environment of cemented paste backfill. Journal of Environmental Management, 258, 110037.

Yin, S., Shao, Y., Wu, A., Wang, H., Liu, X., & Wang, Y. (2020a). A systematic review of paste technology in metal mines for cleaner production in China. Journal of Cleaner Production, 247, 119590.

Yin, S., Shao, Y., Wu, A., Wang, Z., & Yang, L. (2020b). Assessment of expansion and strength properties of sulfidic cemented paste backfill cored from deep underground stopes. Construction and Building Materials, 230, 116983.

Yin, S., Wu, A., Hu, K., Wang, Y., & Zhang, Y. (2012). The effect of solid components on the rheological and mechanical properties of cemented paste backfill. Minerals Engineering, 35, 61-66.

Yue, C. (2021). Low-carbon binders produced from waste glass and low-purity metakaolin for cemented paste backfill. Construction and Building Materials, 312, 125443.

Yumlu, M., & Guresci, M. (2007). Paste backfill bulkhead failures and pressure monitoring at Cayeli Mine. CIM Bulletin, 100 (1103), 1-10 (Paper 22).

Zajac, M., Skocek, J., Durdzinski, P., Bullerjahn, F., Skibsted, J., & Haha, M. B. (2020). Effect of carbonated cement paste on composite cement hydration and performance. Cement and Concrete Research, 134, 106090.

Zhang, H., Cao, S., & Yilmaz, E. (2022). Influence of 3D-printed polymer structures on dynamic splitting and crack propagation behavior of cementitious tailings backfill. Construction and Building Materials, 343, 128137.

Zhang, Q. L., Li, Y. T., Chen, Q. S., Liu, Y. K., Feng, Y., & Wang, D. L. (2021). Effects of temperatures and pH values on rheological properties of cemented paste backfill. Journal of Central South University, 28(6), 1707-1723.

Zhang, S., Ren, F., Zhao, Y., Qiu, J., & Guo, Z. (2021a). The effect of stone waste on the properties of cemented paste backfill using alkali-activated slag as binder. Construction and Building Materials, 283, 122686.

Zhang, S., Zhao, Y., Ding, H., Qiu, J., & Guo, Z. (2021b). Recycling flue gas desulfurisation gypsum and phosphogypsum for cemented paste backfill and its acid resistance. Construction and Building Materials, 275, 122170.

Zhang, W., Long, J., Wei, Z., & Alakangas, L. (2016). Vertical distribution and historical loss estimation of heavy metals in an abandoned tailings pond at HTM copper mine, northeastern China. Environmental Earth Sciences, 75(22), 1-13.

Zhang, X. L., Kou, J., Sun, C. B., Zhang, R. Y., Su, M., & Li, S. F. (2021). Mineralogical characterization of copper sulfide tailings using automated mineral liberation analysis: A case study of the Chambishi Copper Mine tailings. International Journal of Minerals, Metallurgy and Materials, 28(6), 944-955.

Zhao, D. (2021). Reactive MgO-modified slag-based binders for cemented paste backfill and potential heavy-metal leaching behavior. Construction and Building Materials, 298, 123894.

Zhao, Y., Qiu, J., Wu, P., Guo, Z., Zhang, S., & Sun, X. (2022). Preparing a binder for cemented paste backfill using low-aluminum slag and hazardous oil shale residue and the heavy metals immobilization effects. Powder Technology, 399, 117167.

Zhao, Y., Taheri, A., Karakus, M., Chen, Z., & Deng, A. (2020). Effects of water content, water type and temperature on the rheological behaviour of slag-cement and fly ash-cement paste backfill. International Journal of Mining Science and Technology, 30(3), 271-278.

Zheng, J., Tang, Y., & Feng, H. (2021). Utilization of low-alkalinity binders in cemented paste backfill from sulphide-rich mine tailings. Construction and Building Materials, 290, 123221.

Zheng, J., Zhu, Y., & Zhao, Z. (2016). Utilization of limestone powder and water-reducing admixture in cemented paste backfill of coarse copper mine tailings. Construction and Building materials, 124, 31-36.

Zheng, J., Sun, X., Guo, L., Zhang, S., & Chen, J. (2019). Strength and hydration products of cemented paste backfill from sulphide-rich tailings using reactive MgO-activated slag as a binder. Construction and Building Materials, 203, 111-119.

Zhengfu, B., Inyang, H., Daniels, J., Frank, O., & Struthers, S. (2010). Environmental issues from coal mining and their solutions. Mining Science and Technology, 20(2), 215-223.

Zhou, N., Dong, C., Zhang, J., Meng, G., & Cheng, Q. (2021). Influences of mine water on the properties of construction and demolition waste-based cemented paste backfill. Construction and Building Materials, 313, 125492.

Zhou, N., Zhang, J., Ouyang, S., Deng, X., Dong, C., & Du, E. (2020). Feasibility study and performance optimization of sand-based cemented paste backfill materials. Journal of Cleaner Production, 259, 120798.

Zhou, Y., Fall, M., & Haruna, S. (2022). Flow ability of cemented paste backfill with chloride-free antifreeze additives in sub-zero environments. Cement and Concrete Composites, 126, 104359.

APPENDIX

LIST OF PAPERS

Peer-reviewed journal papers:

1. **Kasap, T.**, Yilmaz, E., & Sari, M. (2022). Physico-chemical and micro-structural behavior of cemented mine backfill: Effect of pH in dam tailings. Journal of Environmental Management, 314, 115034. SCIE Journal Impact Factor: 8.910, Category Quartile: Q1.
2. **Kasap, T.**, Yilmaz, E., Guner, N.U., & Sari, M. (2022). Recycling dam tailings as cemented mine backfill: Mechanical and geotechnical properties. Advances in Materials Science and Engineering, 2022, 6993068. SCIE Journal Impact Factor: 2.098, Category Quartile: Q3.
3. Sari, M., Yilmaz, E., **Kasap, T.**, & Guner, N.U. (2022). Strength and micro-structure evolution in cemented mine backfill with low and high pH pyritic tailings: Effect of mineral admixtures. Construction and Building Materials, 328, 127109. SCIE Journal Impact Factor:7.693, Category Quartile: Q1.

Peer-reviewed conference papers:

1. **Kasap T.**, Yilmaz E., Guner N. U., & Sari M. (2021). pH effect of tailings on physico-chemical and mechanical properties of cemented paste backfill. 4th International Conference on Opencast Mining Technology and Sustainability ICOMS 2021, Singrauli, India, 13 - 14 December 2021, 4, 36-41.
2. Sari M., Yilmaz E., **Kasap T.**, & Guner N. U. (2021). Slag effect on properties of cemented paste backfill containing pyritic tailings at different pH values. 4th International Conference on Opencast Mining Technology and Sustainability ICOMS 2021, Singrauli, India, 13 - 14 December 2021, 4, 32-35.

The author's contribution to the above papers was:

1. Conceptualization, investigation, approach, writing-original draft preparation.
2. Examination, experimental techniques, validation, co-writing-original draft.
3. Study, methodology, research, visualization, writing, reviewing and editing.